Master's thesis

NTNU
Norwegian University of Science and Technology
Faculty of Natural Sciences
Department of Biology

Martin Berggren Nilsen

Behavioural Responses of Nauplii and Copepodids of *Caligus elongatus* (Crustacea: Copepoda: Caligidae) to Light Stimuli of Different Wavebands, Intensities, and Pulsations

Master's thesis in Natural Science with Teacher Education
Supervisor: Cecilie Miljeteig
Co-supervisor: Anna Solvang Båtnes, Maja Hatlebakk
June 2024

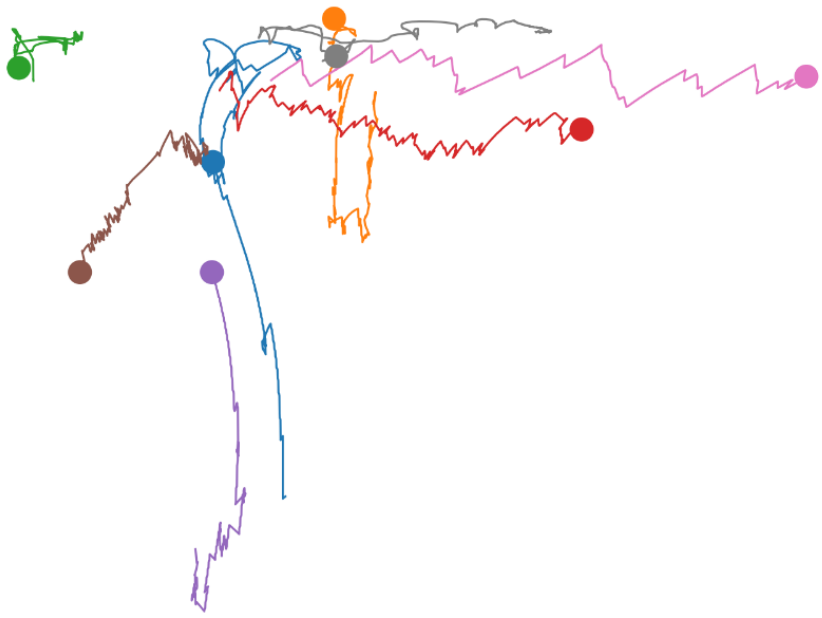

NTNU
Norwegian University of Science and Technology

NTNU
Taskforce Salmon Lice

Martin Berggren Nilsen

Behavioural Responses of Nauplii and Copepodids of *Caligus elongatus* (Crustacea: Copepoda: Caligidae) to Light Stimuli of Different Wavebands, Intensities, and Pulsations

Master's thesis in Natural Science with Teacher Education
Supervisor: Cecilie Miljeteig
Co-supervisor: Anna Solvang Båtnes, Maja Hatlebakk
June 2024

Norwegian University of Science and Technology
Faculty of Natural Sciences
Department of Biology

NTNU
Norwegian University of
Science and Technology

Abstract

Caligus elongatus von Nordmann, 1832 is an ectoparasitic copepod observed on over 80 fish species from various families. Among the hosts are the farmed Atlantic salmon (*Salmo salar*), where *C. elongatus* consumes mucus, epidermis, blood, and epithelial cells. The host can experience adverse side effects from the attachment of the parasite, including itching, petechial bleeding, open wounds, and osmotic shock due to skin lesions. Understanding environmental cues is critical to comprehending the host-finding mechanisms of *C. elongatus*. Furthermore, environmental factors, such as the influence of light on its migration pattern, might be essential in understanding the spread and infection rates of *C. elongatus* and other sea lice. This thesis aimed to examine the response of nauplius and copepodid larvae of *C. elongatus* to light stimuli of different wavebands, pulsations, and intensities in laboratory conditions. The thesis provides insights into the species' response behaviours to light in the early stages of development, a topic that has yet to be extensively explored.

To investigate light responses, a total of 108 experiments, divided equally between nauplii and copepodites, were conducted within 18 different light treatments. Each light treatment consisted of a combination of one waveband (red, green, or blue), one intensity (high or low), and one pulsation (constant light, 0.5 sec on: 3 sec off, 2 sec on: 3 sec off). The light was exhibited from a lightbox positioned directly above a 25×8×3 cm (inside measurements) aquarium filled with water to 16 cm height. A camera taking 120 images per second provided detailed documentation of the behaviour of larvae in the 30 second of dark conditions and the following 90 second of light conditions in each experiment. The images were processed using the Python library OpenCV, and position coordinates for each moving object across every frame were obtained. This ensured the detailed analysis of light responses as provided in this thesis.

The main findings were that neither nauplii nor copepodid showed a positive response in the direction of the light source after the onset of light. These results do not support previous studies reporting larvae of *C. elongatus* as positively phototactic. The main proposed explanations for the absence of positive phototaxis in this thesis was 1) the influence of temperature, 2) genetic differences, and 3) low irradiance levels and light combinations not stimulating the larvae's natural environment. High-intensity light led to a descent in the water column compared to low-intensity light for both development stages. The proposed explanation was avoidance behaviour to avoid predation (for nauplii) and potentially harmful radiation. In addition, the temperature was proposed to be an influencing factor to this observation. The maximum speed among all nauplii (67.82 mm/s) was higher than the maximum speed among all copepodids (55.83 mm/s). However, the average maximum speed was higher among copepodids than nauplii. Among copepodids, pulsating light led to significantly higher maximum speed. The proposed explanation for this was that pulsating light resembles schools of fish swimming by, explaining the higher speed as a part of the host-finding mechanism.

The results of this thesis reveal that more research is needed on the phototaxis of *C. elongatus* larvae and highlights the need for further research to fully understand the implications of light stimuli on their behaviours.

Sammendrag

Caligus elongatus von Nordmann, 1832 er en ektoparasittisk kopepode observert på over 80 fiskearter fra et bredt spekter av familier. Atlantiske laksen (*Salmo salar*) er en av vertene, der *C. elongatus* spiser slim, epidermis, blod og epitelceller. Det gir verten ulike negative følger, inkludert kløe, petekkier (punktblødninger), åpne sår og osmotisk sjokk på grunn av hudlesjoner. Kjennskap til miljøsignaler er avgjørende for å forstå mekanismene *C. elongatus* har for å finne en vert. Videre kan miljøfaktorer, som lysets påvirkning på migrasjonsmønstret dens, være avgjørende for å forstå spredningen og infeksjonsratene til *C. elongatus* og andre sjølus. Denne oppgaven tok sikte på å undersøke responsen til nauplius- og kopepoditt-larver av *C. elongatus* på lysstimuli av forskjellige bølgebånd, pulseringer og intensiteter i laboratorieforhold. Oppgaven gir innsikt i artens responsatferd på lys i de tidlige stadiene av utviklingen, et emne som enda ikke har blitt grundig utforsket.

For å undersøke lysresponser ble totalt 108 eksperimenter, fordelt likt mellom nauplier og kopepoditter, utført innenfor 18 forskjellige lysbehandlinger. Hver lysbehandling besto av en kombinasjon av ett bølgebånd (rødt, grønt eller blått), en intensitet (høy eller lav) og en pulsering (konstant lys, 0,5 sek på:3 sek av, 2 sek på:3 sek av). Lyset ble sendt fra en lysboks plassert rett over et 25×8×3 cm (innvendige mål) akvarium fylt med vann opptil 16 cm. Et kamera som tok 120 bilder per sekund ga detaljert dokumentasjon av atferden til larver i de 30 sekundene med mørkeperiode og de påfølgende 90 sekundene med lysforhold i hvert eksperiment. Bildene ble behandlet ved hjelp av Python-biblioteket OpenCV, og posisjonskoordinater for hvert bevegelige objekt over hvert bilde ble hentet ut. Dette sikret den detaljerte analysen av lysrespons som er presentert i denne masteroppgaven.

Et av hovedfunnene var at verken nauplier eller kopepoditter viste positiv respons i retning av lyskilden i det lyset ble skrudd på. Disse resultatene støtter ikke tidligere studier som har rapportert larver av *C. elongatus* som positivt fototaktiske. De viktigste foreslåtte forklaringene på fraværet av positiv fototaksis i denne oppgaven er 1) påvirkning av temperatur, 2) genetiske forskjeller, og 3) lave irradiansnivåer og lyskombinasjoner som ikke stimulerer larvenes naturlige miljø. Høyintensitetslys førte til en nedstigning i vannsøylen sammenlignet med lavintensitetslys for begge utviklingstrinn. Den foreslåtte forklaringen var unngåelsesatferd for å unngå predasjon (for nauplier) og potensielt skadelig stråling. I tillegg ble temperaturen foreslått å være en påvirkningsfaktor for denne observasjonen. Maksimal hastighet blant alle nauplier (67,82 mm/s) var høyere enn maksimalhastigheten blant alle kopepoditter (55,83 mm/s). Imidlertid var gjennomsnittlig maksimalhastighet høyere blant kopepoditter enn blant nauplier. Blant kopepodittene førte pulserende lys til betydelig høyere maksimalhastighet. Den foreslåtte forklaringen på dette var at pulserende lys kan ligne fiskestimer som svømmer forbi, som kan stimulere kopepodittene til å svømme raskere for større sannsynlighet til å treffe på en vert i vannkolonnen.

Resultatene av denne oppgaven viser at det er behov for mer forskning på fototaksisen til nauplier og kopepottider av *C. elongatus* og understreker behovet for ytterligere forskning for å fullt ut forstå implikasjonene av lysstimuli på atferden deres.

Preface

This master's thesis was written at the Norwegian University of Science and Technology (NTNU) at the Center of Fisheries and Aquaculture (SeaLab) as part of the research and development project Taskforce Salmon Lice. This thesis was written as the final part of my master's degree in natural science with teacher education. My main subjects were biology, with a specialisation in marine biology and aquaculture. The scope of the thesis is 30 ECTC Credits.

Acknowledgements
First, I would like to thank my supervisor, Cecilie Miljeteig, and co-supervisors, Anna Solvang Båtnes and Maja Hatlebakk. Your feedback has been constructive and highly appreciated. I am thankful for the time you have invested to help me through the process. The final product would never have been the same without your guidance.
Secondly, I want to thank the Institute of Biology at NTNU who have sent me on extraordinary field trips on land and sea during the last five years. These experiences have enriched my academic journey and deepened my understanding of the field of biology. Last, but not least, I am tanking my master's student colleagues, Karoline Eilertsen and Asmita Aryal. The last semester has been a learning journey, and I am grateful for your companionship.

Sustainability and relevance of profession
Sustainable development has never been more important. UN Goal number 17 is "Partnerships for the Goals." The collaboration and proximity to the aquaculture industry that Taskforce Salmon Lice has established is a prime example of how this can be done. The Norwegian University of Science and Technology's (NTNU) slogan is "Knowledge for a better world." Scientific communication is highly relevant to making the world better through knowledge. From a teacher's or an academic's perspective, communicating in an inspiring and explainable way should always be considered important. Scientific results and discoveries must be communicated to industries, politicians, organisations, random people in the street, and not least, to children and young people in school. Working on this master's thesis, I have improved my scientific communication skills.

Martin Berggren Nilsen
Trondheim, Norway
June 18, 2024

Table of contents

List of Figures

List of Tables

Abbreviations

B	Light at the blue part of the spectrum
Copepodid (plural copepodids)	The third development stage of Caligus elongatus
E	Irradiance
E_{PAR}	Irradiance integrated over PAR
FLP	First Light Period
G	Light at the green part of the spectrum
H	High-Intensity Light
L	Low-Intensity Light
Larvae	Nauplius stages + Copepodid stage
Nauplius (plural nauplii)	First and second stage of the development
NI	Nauplius II – First development stage
NII	Nauplius II – Second development stage
PAR	Photosynthetically active radiation
NOK	Norwegian krone - national currency of Norway
P0	Constant light
P1	Pulsating light: 0.5 sec on:3 sec off
P2	Pulsating light: 2 sec on:3 sec off
R	Light at the red part of the spectrum
Salmon Lice	*Lepeophtheirus salmonis*
Sea Lice	Louse of the Caligidae family
TLP	Total Light Period

1 Introduction

1.1 Parasitic Sea lice in Norwegian aquaculture

The Norwegian aquaculture industry is deemed significant for the country's economic future, particularly in terms of jobs, innovation, and capital (Meld. St. 16 (2014–2015), s. 8). In 2022, a total of 1 564 948 tonnes of salmon produced in Norway, valued at ~ 102 billion NOK, were slaughtered and sold (The Norwegian Directorate of Fisheries, 2023a). Meanwhile, the sector is facing challenges, such as parasitic sea lice (Copepoda: Caligidae). Parasitic sea lice became a challenge in Norwegian aquaculture already in the 1960s short time after the emergence of cage culture (Pike & Wadesworth, 1999; Costello, 1993). With a total biomass of 450 million Atlantic salmon (*Salmo salar* Linnaeus, 1758) in Norwegian open-net pens by the end of 2022, parasitic sea lice have many potential hosts, providing good conditions for their abundance (Torrissen *et al*., 2013; Grefsrud *et al*., 2023).

Lepeophtheirus salmonis Krøyer, 1838 and *Caligus elongatus* von Nordmann, 1832 are the two species of parasitic sea lice that are causing the most considerable economic impact and ecological influence (Pike & Wadesworth, 1999; Costello, 2006). Fallowing has little to no effect on its abundance (Revie *et al*., 2002), and its injury potential is substantial, especially in large abundance on individual fish. Among potential consequences are physiological stress responses, osmotic shock due to skin lesions, and secondary diseases (Gravil, 1996; Revie *et al*., 2002). Not only farmed fish suffer these consequences. Sea lice are a significant threat to the already vulnerable stock of wild Atlantic salmon, estimated to be 458,000 individuals in 2022 (Norwegian Scientific Advisory Committee for Atlantic Salmon, 2023).

Many resources are employed to prevent, monitor, and limit sea lice abundance (Iversen *et al*., 2017). From 2012 to 2017, the number of operations linked to preventing and controlling sea lice in Norwegian salmon farms increased by 40% (Overton *et al.*, 2018). In the Norwegian Fish Health Report from 2023, farmers reported that *L. salmonis* and *C. elongatus* are often threatened simultaneously by the same delousing strategy (Sommerset *et al.*, 2024). Both medical treatments (chemotherapeutics) and mechanical delousing methods are being used, each with their advantages and disadvantages (Overton *et al.*, 2018, Barrett *et al.*, 2020). However, a shift from medical to non-medical treatments is apparent, favouring methods such as mechanical treatments, as well as preventive barrier technologies (Overton *et al.*, 2018; Barrett *et al.*, 2020).

Non-medical delousing methods, such as thermal delousing systems, freshwater treatment, and other mechanical technologies like flushing and brushing, have proven effective in removing lice but are also stressful for the fish (Overton *et al.*, 2018). Another method is introducing lumpfish and wrasse species to the nets to eat lice off the fish (Overton *et al.*, 2018). In 2022, ~ 33 million cleaner fish were used in Norwegian aquaculture of salmon and rainbow trout (The Norwegian Directorate of Fisheries, 2023b). Moreover, preventive methods can be effective and have several advantages over treatment-focused methods (Barrett *et al.*, 2020). Lice skirts, snorkel cages, and submerged cages are examples of preventive barrier technologies that help prevent the lice from finding fish (Barrett *et al.*, 2020). However, despite several available methods and decades of sea lice research, lice abundance remains significant (Barrett *et al.*, 2020). Additionally, delousing treatments induce side effects such as stress, higher mortality, and

reduced growth (Overton *et al.*, 2018). In 2022, wounds, gill problems and bacterial diseases led to a record high of dead farmed salmon in the marine phase (Sommerset *et al.*, 2023), where sea lice and delousing processes where among the reasons. Thus, the ecological and economic impacts of the abundance of sea lice in Norwegian aquaculture persist.

1.2 Parasitic Copepods (Crustacea: Copepoda)

Copepoda is a crustacean class, currently including > 14 500 validated species (Walter and Boxshall, 2024). Copepoda is a highly diverse class with substantial variations in adaptations and ecology, inhabiting a wide range of marine and terrestrial ecosystems, including harsh environments such as glacial meltwaters and hot springs (Piasecki *et al.*, 2023; Steck et al., 2023). No other multicellular animal group outperforms their abundance (Humes, 1994). Many of them are keystone species vital for the marine food web with their contribution as secondary producers (Bron *et al.*, 2011). In addition, their migration patterns play an essential role in the biological carbon pump through an active vertical flux (Frangoulis et al., 2005).

Some copepods are free-living, others symbiotic parasites (Bron *et al.*, 2011). Parasites are organisms that utilise host species as habitats and food sources. Their life depends on a symbiotic relationship known as parasitism, wherein the parasite exclusively derives a beneficial outcome while the host undergoes some form of negative influence. Most of the crustacean parasites belong to the Copepoda within the order Siphonostomatoida, but they are also documented in other classes (e.g., Malacostraca: Isopoda and Ichtyostraca: Branchiura) (Pike & Wadesworth, 1999). Recent data indicates that around 2,400 species of copepoda are symbiotic ectoparasites on fish (Piasecki *et al.*, 2023). The probability of that number being larger is high, as much remains undiscovered.

As with copepods in general, parasites are a natural and important part of the ecosystem and adapted to various environments. For example, *L. salmonis* is a stenohaline copepod thriving in high-salinity sea water (Torrissen *et al.*, 2013), explaining why freshwater treatments are effective in removing them. In fact, sea trout has several times been documented going back up into freshwater rivers after salmon lice infections to recover (Thorstad & Finstad, 2018). In addition, the distribution of the parasitic copepods varies. *L. salmonis* are distributed in the Northern Hemisphere (Torrissen *et al.*, 2013). *C. elongatus* was previously believed to inhabit the Southern Hemisphere as well (Pike & Wadsworth, 1999), but it might be restricted to the North Atlantic as records of it in Australia and New Zeeland might have been *Caligus chiastos*, and not *C. elongatus* (Hayward *et al.*, 2008; Hemmingsen *et al.*, 2020).

1.2.1 Caligidae: *Caligus* spp

Caligidae is a family of the class Copepoda within the order Siphonostomatoida. Siphonostomatoida exclusively includes parasitic families, wherein Caligidae is the most speciose (Maran *et al.*, 2016; Walter & Boxshall, 2024). Currently, 506 accepted species, including *L. salmonis* and *C. elongatus*, belong to the family Caligidae (Walter & Boxshall, 2024). One trait differing Caligidae from other siphnostomatoids, is their less extent of sexual dimorphism (Piasecki *et al.*, 2023). Many species of Caligidae have large, free-swimming adults of both sexes, whereas other siphnostomatoids usually have dwarf males with limited possibility to move around in the water column after attaching to a host

(Piasecki *et al.*, 2023). Conversely, among many Caligidae, both sexes are able to change hosts, increasing their pathogenic potential (Piasecki *et al.*, 2023).

Adapting to and overcoming the immune system of different host species is energetically demanding. Hence, some parasites, including *L. salmonis*, are host-specific and are classified as specialists with restrictions to salmonids (Hemmingsen, 2020). Conversely, species in the genus *Caligus* spp. are generalists and can parasitise different fish species (Hemmingsen, 2020). *C. elongatus* is recognised as the primary concern among the 276 valid species of *Caligus* spp. and is also the most numerous of these in North Atlantic waters (Boxaspen, 2006; Hemmingsen et al., 2020; Piasecki *et al.*, 2023; Walter and Boxshall, 2024). *C. elongatus* has been observed on more than 80 fish species from a wide variety of families, including sea trout (*Salmo trutta*), lumpfish (*Cyclopterus lumpus*) and herring (*Clupea harengus*) (Kabata, 1979; Pike & Wadsworth, 1999; Heuch *et al.*, 2007).

C. elongatus consumes mucus, epidermis, blood, and epithelial cells and is classified as an ectoparasite because of its nature of sitting on the outside of the host species (Brandal et al., 1976; MacKinnon, 1993; Heuch *et al.*, 1995; Øines *et al.*, 2016). The host species can experience side effects, including itching and open wounds (Costello, 2016). *C. elongatus* is rarely registered to make large wounds, but petechial bleeding is commonly witnessed (Heuch & Schram, 1999). Another consequence is that the fish become stressed, a condition associated with an increased likelihood of obtaining secondary diseases (Costello, 1993). Moreover, petechial bleeding and open wounds caused by the parasite negatively affect the osmoregulation of the fish, potentially causing osmotic shock due to skin lesions (Gravil, 1996). In second turn, this affects the growth and fecundity of the host fish (Boxaspen, 2006), giving consequences for not only the farmers in the aquaculture industry in terms of less growth, but also for wild fish stocks. Furthermore, *C. elongatus* tends to leave its host when disturbed (Pike & Wadsworth, 1999). This increased the risk of diseases being transferred from one fish to another.

1.3 Life cycle and generation time of *C. elongatus*

C. elongatus has its entire life cycle in water and is categorised as a direct parasite because it only requires one host to fulfil it. The females hold fertilised eggs in one or two egg strings (Gravil, 1996; Heuch & Schram, 1999). Gravil (1996) found each egg string to contain 34.06 (SD 24.81) eggs. While the male dies after mating, the female survives and can lay eggs multiple times (Piasecki & MacKinnon, 1995). The eggs hatch, releasing the larvae to water as nauplius I (Piasecki, 1996; Heuch & Schram, 1999). Following nauplius I is nauplius II. Subsequently follows the copepodid stage, four chalimus stages (chalimus I-IV), and an adult stage (Fig. 1.1).

Moulting is a natural process in all crustaceans. Moults occur between the development stages, giving a total of seven moults between the eight development stages in *C. elongatus* (Hartnoll, 2001; Piasecki & MacKinnon, 1995). During the development from nauplius I to nauplius II, the larva's cuticle, consisting of chitin and lime, is replaced by a new one. As nauplii II develops into the infectious copepodid stage through a new moult, the egg yolk soon becomes depleted, leaving the copepodid to live on the last parts of its endogenous lipid reserves (Torrissen *et al.*, 2013). Hence, as an obligate parasite, the copepodid of *C. elongatus* depends on finding a host to fulfil its lifecycle.

All three larvae stages, nauplius I, nauplius II, and copepodid, are free-swimming (Piasecki, 1996). Copepodid is the infective stage where the sea lice attach to a host with the help of frontal filaments. The frontal filaments start developing during the last phase

of the copepodid stage, facilitating further development and firm attachment to the fish during the following four chalimus stages (nonmotile) (Piasecki *et al.*, 2023). However, it should be noted that free-living chalimus stages of Caligidae species have been registered in plankton samples adjacent to aquaculture facilities (Maran *et al.*, 2016). Differences in sex usually first visible at Chalimus III-stage (Piasecki *et al.*, 2023). During the last stage, adult, *C. elongatus* becomes mobile and moves around on the host or onto other fish (Piasecki, 1996; Piasecki & MacKinnon, 1995). Mating occurs by mobile males approaching mobile adult females, also mobile, or in late chalimus stage when still attached to the host (MacKinnon & Piasecki, 1992). Spermatophores from the male are transferred to the genopores of the female (MacKinnon & Piasecki, 1992).

It universally applies to almost all crustaceans that increased temperature increases growth (Hartnoll, 2001). The generation time of parasitic lice depends on the water temperature and will accelerate when the water temperature increases (Bjørn & Finstad, 1998; Costello, 2006). Research done on *C. elongatus* shows that the duration of the nauplius I stage is negative correlated with temperature, ranging from 36.9 h at 5°C to 16.6 h at 15°C (Pike et al., 1993). The nauplius II stage showed a similar pattern, lasting 159.1, 68.1, and 41.1 hours in water at temperatures of 5, 10, and 15°C, respectively (Pike et al, 1993). The moulting process from Nauplius II to copepodid lasted under one hour (reported as < 1h) at 10°C (Pike *et al.*, 1993). It takes approximately 38 day-degrees for a newly hatched egg to become a copepodid (Piasecki & MacKinnon, 1995). Hogans & Trudeau (1989a) found a complete life cycle to take about five weeks at 10-12°C. At a temperature of 10°C (±1°C), Piasecki & MacKinnon (1995) recorded a minimum generation time of 43.3 days (just over six weeks). Both generation durations were obtained in laboratory conditions.

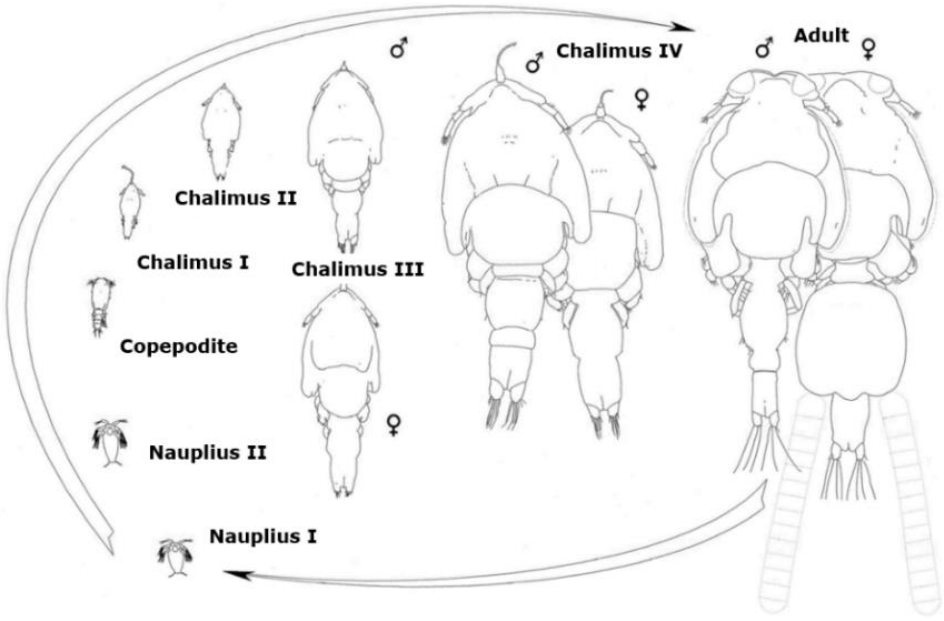

Figure 1.1: *Life cycle of* C. elongatus *including all development stages. Differences in sex usually first visible at Chalimus III-stage, hence only included as of this stage. Modified figure from Piasecki et al. (2023). License: CC-BY-4.0.*

1.4 Morphology at larvae stages of *C. elongatus*

The larvae stages of *C. elongatus* include nauplius I, nauplius II and copepodid, all having different morphological traits (Fig. 1.2). After hatching, nauplius I gradually obtain an elongated shape (Piasecki, 1996). Pike *et al*. (1993) found the size to change in what is referred to as an early-, mid-, and late- stage within nauplius I, changing from 404 µm (SD 3 µm) via 444 µm (SD 3 µm) to 448 µm (SD 1 µm, n=20-24), respectively. They are planktonic but can move with the help of three pairs of external appendages (Pike *et al.*, 1993). The appendages consist of brush-like structures called setae (Pike *et al.*, 1993). In addition, dot-shaped eyes with red pigment are visible at the nauplius I stage (Pike *et al.*, 1993). At the posterior of the larva, two unsegmented, thread-shaped (filiform) structures work as balancers (Kabata, 1972; Pike *et al.,* 1993). The yolk is visible posteriorly as a sizeable, contrasted area (Pike *et al.*, 1993).

Nauplius II has a slimmer and more elongated body than nauplius I (Piasecki, 1996). In an early to mid-stage within nauplius II, the larvae measure 504 µm (SD 3 µm). In the later part of Nauplius II, a length of 550 µm (SD 3 µm, n=20-24) was documented (Pike et al., 1993). The pigmentation is quite similar to the pigmentation in nauplius I but is more patched and divided into three pairs of visible spots with red carmine pigment (Schram, 2004). As in nauplius I, three pairs of appendages are visible, allowing larvae in the nauplius stages to propel themselves around in the water column (Pike *et al.*, 1993). Compared to the nauplius I stage, the amount of yolk has decreased.

The larva is even more elongated in the copepodid stage, giving an efficient hydrodynamic shape (Piasecki, 1996). The copepodid measures 757 µm (SD 5 µm) (Pike *et al.*, 1993). In this stage, thoracic legs are developed, which is one of the developments differentiating them from the previous nauplius stages (Pike et al., 1993; Piasecki, 1996). These legs, by Piasecki & MacKinnon (1995) referred to as "swimming legs", make them faster and more mobile than the previous nauplius stages (Pike *et al.,* 1993). Grasping appendages with strong claws have developed, providing temporary attachment (Piasecki & Mackinnon, 1995). The frontal filaments become visible in slightly older copepodids (Piasecki & Mackinnon, 1993). When attached to a host, these filaments are extruded before providing firm attachment as the copepodids develop into chalimus I (Piasecki & Mackinnon, 1995; Piasecki, 1996).

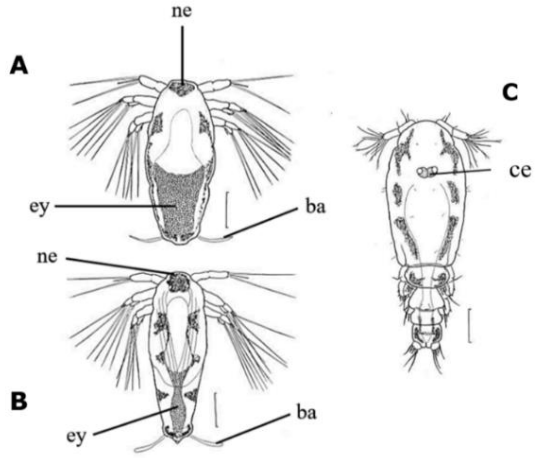

Figure 1.2: *Morphology at early development stages of* C. elongatus*: (A) nauplius I, (B) nauplius II, and (C) copepodid. Abbreviations: ne, nauplius eyes; ey, egg yolk; ba, balancers; ce: copepodid eyes. All scale bars: 100 µm. Modified Figure from Schram (2004). Figure annotations based on Pike et al. (1993).*

1.5 The eye structure in larvae of *C. elongatus*

The larvae must have a vision or sensory system registering differences between dark and light conditions to respond to light stimuli. As displayed in more detail in section 1.6, the properties of light display significant differences between marine and terrestrial habitats. The variations in scattering, absorption, transmission, and reflection of light at various depths and in different underwater environments have led to an extensive range of diverse eye structures and complex visual systems among marine crustaceans (Cronin, 1986; Lythgoe, 1988; Cronin & Jinks, 2001). Steck *et al.* (2023, p. 223) reviewed the field of copepod vision and stated that «copepods are often highly visual creatures with eyes that are an evolutionary playground of diversity.»

The frontal eyes (in earlier research called nauplius eye or cup eyes) of species belonging to the subclass Copepoda have three eyes that appear joined together (Elofsson, 2006). The term "three-parite eye" describes this structure (Elofsson, 2006). Two are paired, and "lateral frontal eyes" are used for these (Fig. 1.3). The unpaired eye is called the "ventral frontal eye" (Elofsson, 2006). MacKinnon (1993) studied the eye structure of *C. elongatus*, in which this three-parite eye was referred to as "paired eyes with a triangular lensless third eye located below and between the two main eyes" (MacKinnon, 1993, p. 793). In copepods, this three-parite eye has three pigment cups (Elofsson, 2006). MacKinnon (1993) found each of the paired lateral frontal eyes to contain such a pigment cup, which consisted of six sensory cells (photoreceptors). In addition, MacKinnon (1993, p. 797) also found the ventral frontal eye, referred to as the "triangular area lying between and below the two eyes," to have at least two of these photoreceptors. In many copepods, the ventral frontal eye consists of nine sensory cells (Elofsson, 2006), suggesting that there could also be more than two for *C. elongatus*.

MacKinnon (1993) proposed that the third eye in *C. elongatus* contains photosensitive structures with a distinct ability to perceive light ventrally. It was also suggested that the eyes of copepodids of *C. elongatus* may have the capacity to sense some directionality of the light source. Moreover, the eye structure of the copepodid of *C. elongatus* appeared to be adapted to perceive light from all directions, even at very low intensities (MacKinnon, 1993).

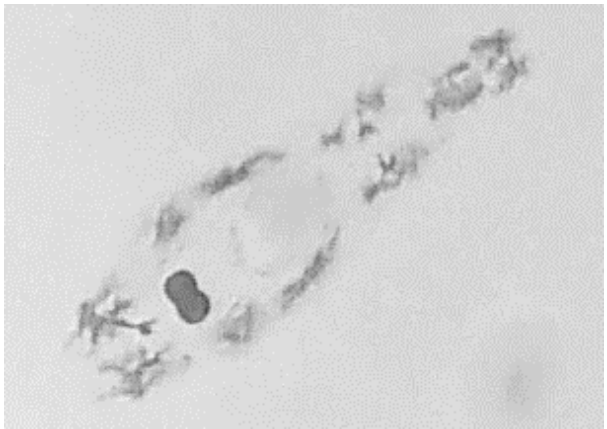

Figure 1.3: *The paired eyes of the copepodid of* C. elongatus *are clearly visible in light microsocope as darker dots (Figure not true to size). Photo taken by Martin Berggren Nilsen.*

1.6 Light as an abiotic factor influencing behaviour and distribution

Light is the essential driver of photosynthesis. Consequently, it is central to the ocean's primary production (Clarke, 1971). In addition, light is a decisive causal factor for the vertical movement of zooplankton (Forward, 1976; Ringelberg, 1999). Vertical migration patterns are well-studied in freshwater and marine waters (Bandara *et al.*, 2021). Different migration patterns have been observed, and the distance can range from a few meters to several hundred meters vertically in the water column (Cottier *et al.*, 2006; Lampert, 1989; Ringelberg, 1999). Distinct types of vertical migration patterns are described more closely in section 1.6.3. Phototaxis is believed to be a fundamental mechanism that enables such vertical movement light-based migration patterns (Ringelberg, 1999). This is detailed further in 1.6.4. When determining behavioural responses to light, the wavelength, intensity, and duration of the light are essential parameters to consider. These factors determine the amount of light available for vision (Menzel, 1979; Land & Nilsson, 2012). The properties of light are described more closely in the following section.

1.6.1 Properties of light

Light is electromagnetic radiation consisting of particles called photons (Jonasz & Fournier, 2007). Photons are characterised by their specific wavelengths (λ) and energy (E). The photons' varying interaction, distribution, and dynamics produce light of different wavelengths (Jonasz & Fournier, 2007). For the human eye, we usually consider visible light to include wavelengths from around 400 to 700 nm (Land & Nilsson, 2012). On this spectrum, we have light of different colours, ranging from violet (380-450 nm) to red (620-750 nm); within, we also find the colours green (495-570 nm) and blue (450-496) (Young et al. 2015, p. 1077). White light includes all visible wavelengths (Young et al. 2015, p. 1077). Obtaining light with a single wavelength is impossible (Young et al. 2015, p. 1077). Hence, when "red," "green," or "blue" light are used in this thesis, it refers to a larger part of the spectrum within the wavelength range of these colours.

The energy of one photon is given by $E = hc/\lambda$. Hence, the energy a photon carries is dependent on the wavelength (λ). Together with standardised numbers given by Planck's constant (h) and the speed of light (c), the energy of one photon can be calculated (Honsberg & Bowden, 2019). As derived from this formula, light of shorter wavelengths carries more energy. Hence, blue, and green light consists of photons carrying more energy than red light (Honsberg & Bowden, 2019). This fact becomes important in understanding why green and blue light reached deeper into the aquatic environment than red light, which is detailed further in the following sections.

1.6.2 Light within the ocean: reflection, absorption, and irradiance

Solar radiation travels through the Earth's atmosphere. Here, light is scattered by the smaller air molecules (Kirk, 2011). Dust and clouds also contribute to light scattering (Kirk, 2011). The light must first come through the air-water interface to penetrate the water column. Depending on the wind, a given amount of light is reflected into the atmosphere (Kirk, 2011). The sun's elevation plays a crucial role in the significance of the wind, where lower elevations contribute to significantly less reflection back into the atmosphere compared to high elevations (Kirk, 2011). However, most light are transmitted through the air-water interface and penetrates down into the water column (Clarke, 1971). The photons entering the water column will soon be absorbed at one point or another. This can be by photosynthetic biota, particulate matter, or by molecules in the water itself, such as oxygen

(Kirk, 2011). Dissolved organic matter (DOM) is one of several optical components that absorb light and is essential for how deeply the light penetrates the water column (Jonasz & Fournier, 2007). Before photons are absorbed, they often become scattered, making them move in a "zig-zag path" (Klark, 2011, s. 98). This makes the photon move for a longer distance before reaching the same depth compared to if it were to move without such scattering. The chemical components in sea water, local variations in the concentration of particulate matter, and phytoplankton are among the factors that contribute to such scattering of photons (Jonasz & Fournier, 2007).

The light-absorbing and the light-scattering components absorb and scatter light of different wavelengths. In the ocean, colours of shorter wavelengths are more apparent due to the high light absorptions at the red part of the spectrum (Menzel, 1979). Red light of longer wavelengths with low-energy photons are rapidly absorbed by the water itself (Stomp, 2008). In comparison, blue and green light carrying more energy are less rapidly absorbed and reflected, reaching deeper into the water column. This is also why the ocean often appears blue, as the photons representing light on the blue (and green) part of the spectrum are less absorbed (Klark, 2011). However, even colours of shorter wavelengths are rapidly absorbed in the ocean. For every 70 meters in the most transparent ocean water, blue light is reduced by a factor of 10 (Land & Nilsson, 2012). In addition, light from the blue part of the spectrum is rapidly absorbed by organic material, making turbid waters, such as inland waters, sometimes appear green (Stomp, 2008; Klark, 2011). When enough organic material is in the water, sometimes the red part of the spectrum reaches deepest, making the water appear red (Stomp, 2008).

Irradiance, E, is a property of the underwater light field most frequently and readily quantified (Klark, 2011). It measures how much light is available in the underwater environment, in simpler terms, the light intensity, and it is essential for understanding the radiation transfer in water (Klark, 2011). Irradiance often has the unit photons m^{-2} s^{-1} nm^{-1}, but is sometimes reported as Wm^{-2}, or mol photons m^{-2} s^{-1} nm^{-1}. By finding the energy of each photon as described in section 1.6.2, it is possible to change between these units.

There are two different forms of irradiance: downwards irradiance (E_d) and upward irradiance (E_u) (Klark, 2011). The downward irradiance decreases with depth, based on absorption and reflection rates, which differ based on the properties of the given aquatic medium (Klark, 2011). When light is reflected, some of it is reflected against the water surface, contributing to the upward irradiance (Klark, 2011). Often, it is valuable to know the irradiance over the whole spectrum of photosynthetically active radiation (PAR), denoted $E_{PAR,}$ generally considered to range from 400 to 700 nm (Klark, 2011). This is obtained by integrating the irradiance over the whole spectrum, thereby providing the total E from all wavebands visible at the given measurement time.

Given the less absorption of light of shorter wavelengths in open sea environments, many open sea marine crustaceans have λ_{max}, the maximal wavelength sensitivity, at 460 – 480 nm (Menzel, 1979). The eyes of many other animals (e.g., fish and arthropods) can also perceive light in the ultraviolet range from 320 to 400 nm (Land & Nilsson, 2012). Within the animal's maximum wavelength sensitivity, many exhibit what Menzel (1979) refers to as a "wavelength-specific behaviour pattern," in which they will exhibit different sets of behavioural patterns concerning different wavelengths of light. Such wavelength-specific behaviour patterns are advantageous for several reasons, where predator avoidance (in

terms of positioning in areas with fewer predators), recognition of conspecific animals (e.g., hosts), and movement against areas richer in nutrients are among some of these benefits (Menzel, 1979). Furthermore, light contributes to the vertical migrations of numerous copepod species and other zooplankton, which are detailed further in the following subsection.

1.6.3 Vertical migration patterns affected by light

Many marine and freshwater copepods and various other zooplankton move based on light variations between day and night (Lampert, 1989; Hays *et al.,* 1994). For many species, the normal is a higher population density in the upper layer of the water column at night and vice versa during the day. This phenomenon has been named diel vertical migration (DVM) (Lampert, 1989; Aarseth & Schram, 1999). Meanwhile, some species engage in reverse diurnal migration and are attracted to the light of specific wavebands. For these species, the population density is highest in the upper water layers during the day and in deeper water at night (Bandara *et al.,* 2021). Seasonal migrations that extend longer have also been documented (Bandara *et al.,* 2021). In addition, several other diurnal migration variants have been described, including twilight diurnal migration, which describes an upward movement immediately after sunset, followed by a downward movement at midnight (Bandara *et al.*, 2021). The polar night has also demonstrated its influence on migration, where the moonlight and northern lights (Aurora Borealis) influence the plankton's movement (Båtnes *et al.,* 2015). Båtnes *et al.* (2015) estimate that Calanus spp. can respond to light from the moon and the northern lights down to 120-170 meters and 80-120 meters, respectively. There has been a suggestion that plankton in polar regions observe light with wavebands below the limit of human vision (Berge *et al.,* 2009).

Studies point to both proximal and ultimate explanations for plankton's diurnal migration, and researchers have proposed several potential explanatory models. The most pronounced relative change in light intensity occurs at sunrise and sunset, and this change is believed to be a proximal explanation for initiating migration (Cottier *et al.,* 2006; Ringelberg, 1999; Aarseth & Schram, 1999). Observing that many species have a reverse migration cycle than their predators, avoiding predation, especially from planktivorous fish, has been put forward as one of the most central ultimate reasons (Lampert, 1989; Ringelberg, 1999; Hays, 2003). Both field and experimental evidence support this predator-evasion hypothesis (Hays *et al.,* 1994).

Vertical migration patterns must not be misinterpreted as fully synchronous movements. Asynchronous and distinct movements occur (Bandara *et al.*, 2021; Cottier *et al.*, 2006). Laboratory conditions have described behavioural responses to relative rates of irradiance, many of which are like the observed swimming patterns during DVM (Cohen & Forward, 2002). One of the mechanisms behind vertical migration is phototaxis, which is detailed further in the following section.

1.6.4 The significance of phototaxis in the context of vertical migration

Phototaxis is the "positive or negative displacement along a light gradient or vector." (Jékely, 2009, p. 2795). Organisms can be negatively or positively phototactic. Organisms moving towards light are said to be positive phototactic. Conversely, those moving away are negatively phototactic (Jékely, 2009). Some can perceive the light's direction, allowing them to orient themselves along the vector in three dimensions; others cannot (Jékely, 2009). Phototaxis is often tightly controlled as unregulated positive phototaxis would have

put the organism at risk through potentially damaging UV radiation in the upper part of the water column (Jékely, 2009). Hence, many organisms exhibit positive phototaxis to a given threshold of intensity before descending (negative phototaxis) when the light intensity becomes too high (Jékely, 2009). Many marine invertebrates in the early stages of development, i.e., non-feeding larvae stages, are positive phototactic. The hypothesis is that this increases the dispersal of the larva (Jékely, 2009).

1.7 Host Finding Mechanism

Positive phototaxis, as described above, has been documented among parasites of Caligidae. In *L. salmonis*, host-finding mechanisms include positive phototaxis (visual sensory input), positive semiotaxis (chemical sensory input), and positive rheotaxis (mechanical sensory input) (Torrissen *et al.,* 2013; Bailey *et al.,* 2006). For example, in the case of positive semiotaxis, researcher have found that semiochemicals act as an attractant on *L. salmonis* through significant directional moving activity against odours from hosts (Bailey et al., 2006). However, no such positive directional movement was observed when exposed to odours from a non-host: turbot (*Scophthalmus maximus*) (Bailey et al., 2006). Heuch *et al.*, (1995) found copepodids of *L. salmonis* to exhibit positive phototaxis in 6 m deep enclosures in the ocean, hypothesising a cross-over effect due to the reverse pattern observed in its host (Atlantic salmon). Regarding copepodids of *C. elongatus*, Hogans and Trudeau (1989b) and MacKinnon (1993) found nauplii and copepodids to be positive phototactic, moving in the direction of the light. When testing positive semiotaxis in *C. elongatus*, Hogans and Trudeau (1989b) found that copepodids within 10 centimetres of the host fish (*S. Salar*) directly swam to the fish. Furthermore, Piasecki and MacKinnon (1995) observed negative rheotaxis in copepodids, avoiding a pipette sucking in water.

Despite some knowledge about the behavioural and host-finding mechanisms among caligid parasites, more remains undiscovered. To develop models that can estimate spread and infection rates, Costello (2006) argues for the need for more data on the larval behaviour of Caligus spp. Studying the behaviour of nauplii and copepodids of *C. elongatus* when exposed to different wavebands, intensities, and light pulsations will contribute to this. Examining the response of the nauplii and copepodids of *C. elongatus* to different light stimuli will provide knowledge about the species' response behaviours to light in early stages of development. It can also help estimate their aggregation in the sea concerning light conditions. The results may also be relevant for the aquaculture industry, which uses light and diverse types of installations in cage cultures. Furthermore, it provides a basis for studying other abiotic factors. By knowing how larvae of *C. elongatus* respond to different light conditions, it will be easier to consider light as an influencing factor in an experimental context.

1.8 Research aims

The primary goal of this thesis is to investigate behavioural responses to light stimuli in nauplii and copepodids of *C. elongatus* in controlled laboratory conditions, aiming to investigate the following:

1. **Differences in vertical positioning in response to light**

a) Are there differences in the average vertical positioning between light and dark conditions?
b) Which factors, and combinations of factors (waveband, intensity, and pulsing), help predict their response to light in terms of vertical positioning?

2. **Differences in average and maximum speed in response to light**

a) What are the average and maximum speeds obtained in dark- and light conditions?
b) Which factors and combinations of factors affect average and maximum speed in light conditions?

In addition, investigations of general behaviour, such as movement patterns and activity levels in light conditions, are analysed and discussed.

2 Methods and Materials

2.1 Collection of egg strings, hatchery, and incubation of larvae

All experiments were conducted in March 2024 at NTNU Centre of Fisheries and Aquaculture (NTNU Sealab) in Trondheim, Norway. Sea lice can only produce egg strings while attached to a host fish. Hence, using fish as experimental animals was necessary to ensure a continuous supply of lice. Atlantic salmon, kept in 380-litres tanks, was used as host to produce sea lice (*Caligus elongatus)*. The fish were checked daily for wounds and abnormal behaviour per protocol to ensure the welfare of the fish. Temperature, oxygen, and water flow levels in the tanks were controlled daily together with daily feedings. Approved animal experiment permit, allowing hold of fish infested with sea lice, was given by The Norwegian Food Safety Authority (FOTS ID 29582).

Before collecting egg strings, the fish were sedated with 5 mg/L metomidate hydrochloride (Aquacalm.vet) and 0,25 mL/L benzokain (Benzoak.vet). Adult female lice of *C. elongatus (2. and 3. Generation culture, CeSørøya, Origin in Production Area 12)* with egg strings were removed from the fish, and the egg string was carefully removed from the louse with the help of tweezers (Dumont #7 Forceps, Dumostar). After removing the egg string, the female lice were put back on the fish, allowing the possibility of producing new egg strings and ensuring the continuity of the lice culture.

After being picked off the lice, all egg strings were placed in numbered incubator tubes (modified 50 mL Centrifuge Tubes, VWR) in a hatchery for incubation. The hatchery consisted of 8 rows with 16 incubator tubes in each row (Fig. 2.1). All of them were numbered according to row name (A-H) and column number (1-16). The incubator tubes are modified fine mesh (150 µm) plankton net at both ends to ensure flow-through. The plankton net at the bottom is welded on, while the net at the top is fastened by screwing the top lid ring onto the tube. To know the age of the larvae, the eggs were checked daily for hatching. When hatching was registered in the incubator tube, the hatching date was noted, and the remaining egg strings moved to a new incubator tube. This ensured that hatched larvae were kept in the same tubes according to their hatching dates.

The hatchery (Fig. 2.1) received water from NTNU Sealabs seawater intake (Trondheimfjorden) and was built as a flow-through system with water filtering, allowing continuous flowing of seawater through each individual incubator tube (Furberg, 2022). The climate regulated room containing the hatchery had a light-dark cycle of 24:0 h. A digital thermometer (Lab Thermometer IP65) was placed next to the hatchery with the sensor in the water, constantly measuring the water temperature. The temperature of the hatchery water was modified by adjusting the water input level by using a valve on the input pipe above the hatchery. When turning the flow level down, the water stayed longer in the hatchery as the water was changed out by overflowing an outlet hole on the top side of one of the hatchery walls. Consequently, slowing down the input water made the water stay in the hatchery longer, letting the climate-regulated room with a higher temperature warm up the hatchery water to a greater extent. This was done to keep the temperature in the hatchery at 10 degrees.

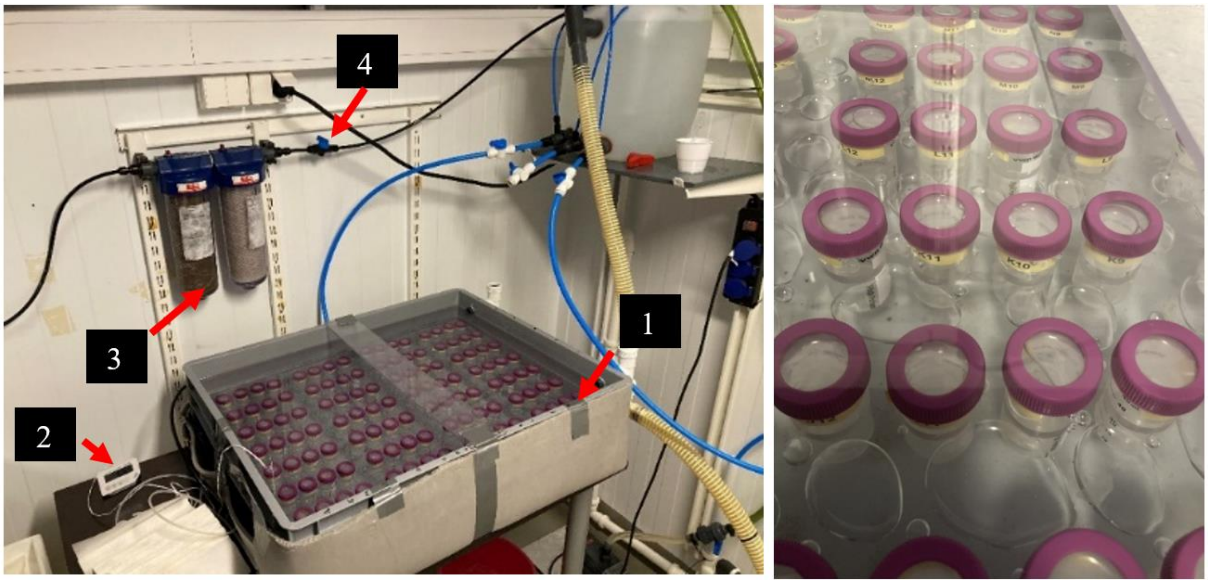

Figure 2.1: *Left: (1) Hatchery used to incubate egg strings of* C. elongatus *with (2) digital thermometer continuously measuring the water temperature, (3) water filtering system, and (4) valve for adjustments of input water and temperature regulation. Right: Numbered incubator tubes housing the egg strings.*

2.2 Experimental setup

2.2.1 Aquarium, camera, and lightbox setup

A 25×8×3 cm (inside measurements) aquarium made of 4 mm soda-lime glass and food and drinking-water approved silicon (Illbruck GS202) were used in all experiments (Fig 2.2). To ensure stability, the aquarium was glued to the outer edge (to reduce reflections) of a 20×10 cm 6 mm glass bottom plate. The aquarium was placed on a black mat, which in turn was taped to a stable table-top inside the climate room where the experiments were conducted. To ensure that the aquarium was always placed in the same position under the light and at the same distance from the camera, taped corners were made on the mat into which the aquarium could be placed. With the help of a taped mark at the side of the aquarium 16 cm up from the aquarium bottom, an equal amount of water (0.384 litres) was used each time. The aquarium was placed inside a stand (Fig 2.2) with a black plastic sheet attached around it. A lightbox was fastened to the stand above the aquarium, ensuring that the light stimulus was oriented directly above the water surface. The shell of this lightbox was customised and 3D-printed by Stephen Grant at NTNU and works as a container for a light plate consisting of 64 LEDs in an 8x8 matrix (NeoPixel NeoMatrix 8x8 RGBW LED Matrix, Adafruit). The light plate was connected to a development board (Uno Rev 3, Arduino), which made it possible to control and program the light with the desired light treatments. The development board was attached to a HDMI cable via a USB-cable, which, in turn, was attached to a computer outside the climate room. The light was programmed using the Arduino software and changed by basic coding between experiments to get the desired light setting. The distance from the light plate to the top of the aquarium was measured to be 4 cm, giving 13 cm from the light to the water surface.

A camera (ORX-10GS-51S5M-C, Teledyne FLIR, Canada) with a lens (TAMRON M112FM16, 1/1.2 18 mm F/2.0 C, Tamron, Japan) was positioned 46 cm from the front side of the aquarium on a tripod (PNY 751492623078, PNY). The camera was connected to the

computer outside the climate room, making it possible to start and stop it outside the room. For this, Spinview (Teledyne FLIR, version 3.1.0.79) were used. All experiments were photographed at 120 fps (frames per second), giving a minimum of 14400 images over a minimum of 2 minutes of imaging. The manual process of turning on the light from the computer after 30 seconds of imaging in dark conditions induced minor differences in when the light got turned on, sometimes leading to a longer imaging time. Hence, the frame number at which the light was turned on had to be found manually afterward. To be able to find it, a piece of aluminium foil was attached over the aquarium's long side and down the aquarium's inside. The aluminium foil gave a reflection when the light turned on, which otherwise would be hard to detect with the experimental setup mentioned here, especially in low intensities.

Two near-infrared lamps (*845 nm, Eneo, Germany)* were placed on each side of the aquarium. Infrared-sensitive video cameras can record infrared light without affecting the organisms studied (Bandara *et al.*, 2021). Baylor (1959) presented a method for observing small crustaceans of a certain transparency using infrared light and video recording (Bandara *et al.*, 2021). It made it possible to study organisms in total darkness and when exposed to different wavebands and intensities of white light (Baylor, 1959). Similarly, in this experiment, infrared lamps were used to light up the larvae in dark conditions, making it possible for the camera to see and focus on them. The lamps are the same as those used by Miljeteig et al. (2014), which mounted the lamps in adjustable stands for adjustment and steady placement on flat surfaces. To better cover the whole aquarium, the lamps were placed laying sideways with the adjustable stands bent over (Fig. 2.2). The lamps were covered with the same visible light absorption filters as described in Vatn (2019): LEE Filters #87C Infrared Polyester Filter, 0 %, absorption up to 800 nm.

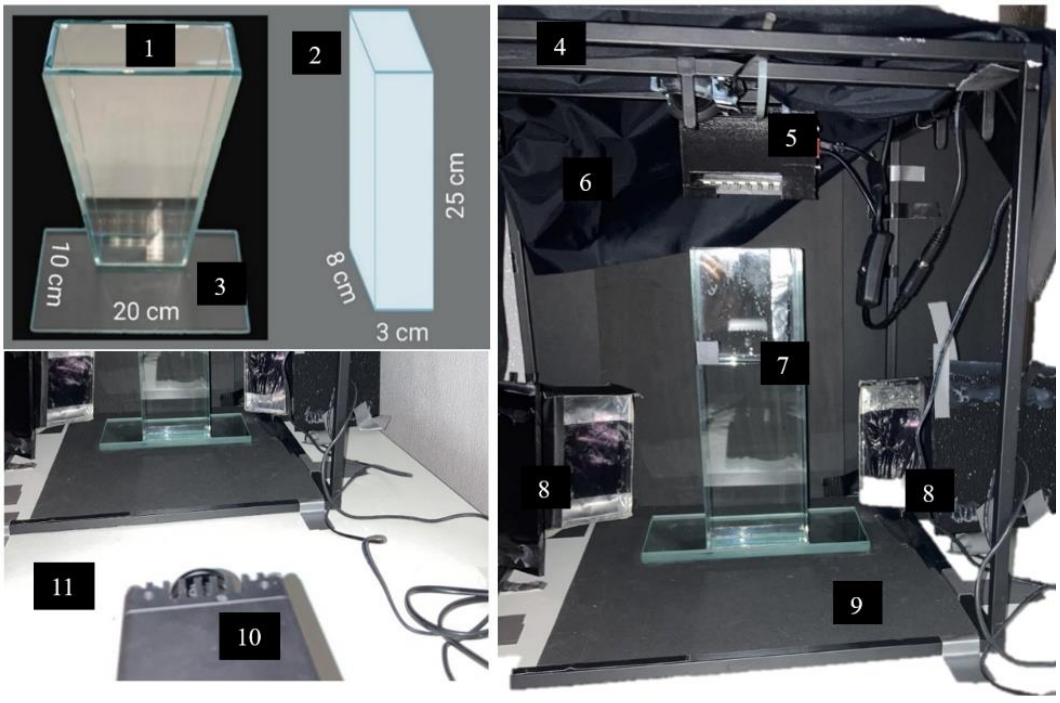

Figure 2.2: *(A) The (1) aquarium with given (2) inner dimensions mounted on a (3) glass bottom plate. (B) A (4) stand is holding the (5) light box and a (6) black plastic sheet covering the (7) aquarium and the two (8) near-infrared lamps. A (9) black mat with taped marked holds the aquarium in position. (B) The (10) camera placed on a tripod on a (11) desktop table is positioned 46 cm away from the aquarium.*

2.2.2 Dark climate room

All experiments were carried out in a dark climate room. All sources of light pollution were removed by taping over them to avoid influence from light sources other than the LEDs placed directly above the aquarium. The room kept the water used in the experiments at 12.2°C (± 0.2°C). The water was tapped from the hatchery into a 10-liter plastic tank and placed in the dark climate room at least one day in advance. This was done to acclimatise the water to the temperature of the dark climate room. Hence, the water temperature did not change significantly as the experiments were carried out.

2.2.3 Light stimulus

The light plate consisting of 64 LEDs in an 8x8 matrix was coded in Arduino IDE (Version 2.2.1, Arduino) to give light conditions of different wavebands, intensities, and pulsations. The LEDs were coded to light up with blue light (emission peak: 462 nm, width at half max: 21 nm), green light (emission peak: 519 nm, width at half max: 31 nm), and red light (emission peak: 637 nm, width at half max: 18 nm) (Fig. 2.3). Different numbers of LEDs and different brightness settings were used in high and low-intensity light. Two rows of 8 diodes each were used for high-intensity green and red light. One row was used for blue light. Brightness was set to 10 for all three colours. For low intensity, two diodes were used for green and red light, while one diode was used for blue. Here, brightness was set to 1. In addition to waveband and intensity, each of the experiments was conducted at a specific level of pulsation: P0 representing constant light; P1 having 0.5 sec on 3 sec off; and P2 having 2 sec on 3 sec off. A hyperspectral light sensor (µSPEC, In-situ marine optics) equipped with a planar irradiance sensor was used to measure the maximum irradiance ($\mu W/cm^2$), and the E_{PAR} (wm^{-2}). The measurements of the irradiance were done by Maja Hatlebakk. Table 2.1 presents the obtained E_{PAR} for each waveband at both intensity levels. Values are given in both wm^{-2}, μWcm^{-2} and µmol photons $m^{-2}s^{-1}$. Note that the values for low intensities of light were too close to the limit of what the hyperspectral light sensor was able to measure. Hence, the E_{PAR} for the low intensities is not based on measurements but calculated based on its associated high-intensity irradiance. As high-intensity was set 80 times higher than low-intensity light, the low-intensity irradiance was found by dividing the measured high-intensity irradiance by 80.

2.3 Experimental procedure

2.3.1 Number of experiments, replicates, and batches

A total of 108 experiments were conducted divided equally between nauplii and copepodids. Each replicate included 18 single experiments, giving all possible combinations from a total of three different wavebands (R, Red; G, Green; B, Blue), three different pulsations (P0, constant light; P1, 0.5 sec on 3 sec off; P2, 2 sec on 3 sec off) and two different intensities (H, High; L, Low) (Table 2.1). An overview of the 18 different light treatments is presented in Table 2.2. A total of 3 replicates were done for both nauplii and copepodids, giving a total number of 54 experiments for both nauplii and copepodids. After nine successive experiments, the 15 individuals used in each experiment were replaced to prevent overexposure. That is, each replicate consisted of two batches of new larvae. The order and composition of wavebands, pulsations, and intensities were randomised within each replicate by a randomisation script made in R (Version 4.1.1, RStudio). The randomisations of experiments are detailed in Appendix A.

Table 2.1: *Measurement of E_{PAR} for low- and high-intensity light of each waveband. Three different units of measurement are given.*

Light treatment	E_{PAR} (wm^{-2})	E_{PAR} (μWcm^{-2})	E_{PAR} ($\mu mol\ photons\ m^{-2}s^{-1}$)
Red Low	0.00045	0.0451	2.1×10^{-3}
Red High	0.0361	3.61	1.7×10^{-1}
Green Low	0.00050	0.0499	2.3×10^{-3}
Green High	0.0399	3.99	1.8×10^{-1}
Blue Low	0.00039	0.0391	1.8×10^{-3}
Blue High	0.0313	3.13	1.4×10^{-1}

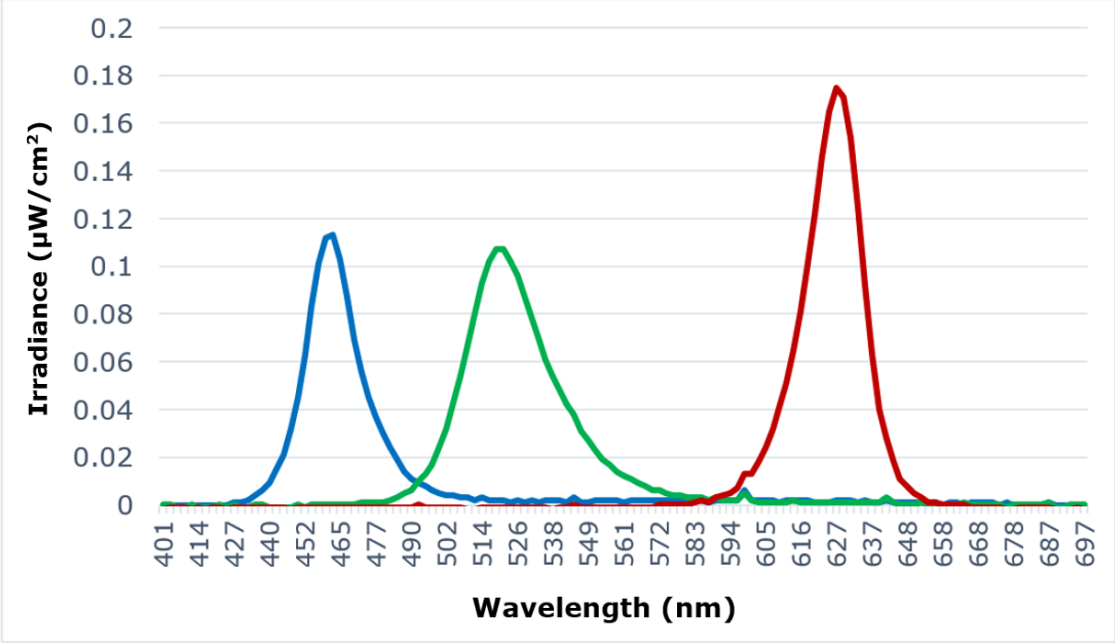

Figure 2.3*: Irradiance ($\mu W/cm^2$) for each of the wavebands used in the experiment. Full width at half maximum equals 21 nm, 31 nm, and 18 nm for blue, green, and red light, respectively. Emission peak at 462 nm for blue, 519 nm for green and 637 for red.*

2.3.2 Step-by-step experimental procedure

Incubator tubes containing hatched larvae were taken out of the hatchery and immediately placed in a cup filled with water from the hatchery. To ensure the usage of only living individuals, the hatchery tubes were left standing for at least one minute before the lice that were actively swimming were taken out with a plastic pipette and placed in a weighing boat. After counting to ensure the correct number of lice per experiment, 15 individuals were transported to the climate room.

The time it takes from nauplii to develop into copepodids depends on the water temperature in the hatchery. Although the larvae are distributed in tubes according to hatching date, it is not given that all are at the same place in their development. This is especially the case in the transition between the various stages, e.g., between nauplius II and the copepodid stage. To ensure that only nauplii stage larvae were used in the nauplii experiments and *vice versa* for the copepodid stage, the weighing boat containing 15 lice was checked under a stereo microscope to ensure that the lice were at the desired developmental stage (Fig. 2.4). The microscope light was kept to a minimum to prevent excessive light exposure before the start of the experiment.

Table 2.2: *Overview of the 18 light treatments of different combinations of waveband (3 levels), intensity (2 levels) and pulsation (3 levels).*

	Low (L)			*High (H)*		
	Constant (P0)	*0.5 sec on, 3 sec off (P1)*	*2 sec on, 3 sec off (P2)*	*Constant (P0)*	*0.5 sec on, 3 sec off (P1)*	*2 sec on, 3 sec off (P2)*
Red (R)	R-L-P0	R-L-P1	R-L-P2	R-H-P0	R-H-P1	R-H-P2
Green (G)	G-L-P0	G-L-P1	G-L-P2	G-H-P0	G-H-P1	G-H-P2
Blue (B)	B-L-P0	B-L-P1	B-L-P2	B-H-P0	B-H-P1	B-H-P2

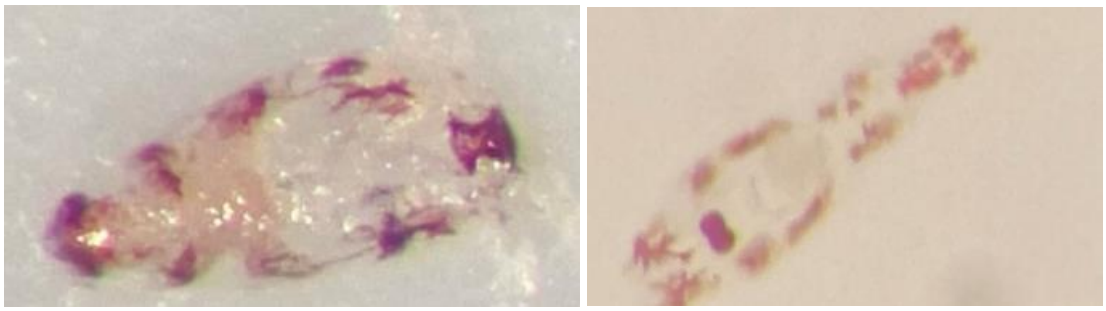

Figure 2.4: *The morphological difference observed between nauplii and copepodids when placed under the microscope. Left: Nauplius II stage. Right: Copepodid stage. Note: Figure not to be used as a size comparison. Photos by Martin Berggren Nilsen.*

The larvae were transferred from the weighing boat to the aquarium using a plastic pipette. An acclimatisation time of 15 minutes was given before the start of the experiment to minimise potential impacts on the larvae's behaviour caused by the transportation and the light-dark cycle of 24:0 h in the hatchery. After an acclimatisation time of 15 minutes, the image acquisition was started manually from the computer outside. The given light setting was turned on after 30 seconds and left running until the given light setting had been on for 90 seconds, resulting in a total image acquisition time of 2 minutes in 120 fps. Images were directly stored into pre-named folders assigned to each experiment on the computer and transferred to hard drives for safer storage (Portable SSD T7 Shield USB 3.2 1TB, Samsung). Following this, the image acquisition was manually stopped. A subsequent acclimatisation period of 8 minutes was given to the larvae to minimise potential impacts from the previous light treatment in the following experiment. During the acclimatisation period, the camera was directed to a new image folder, and the next light treatment was coded. This process was repeated nine times per batch, before the larvae were replaced.

After each batch, the aquarium was emptied in the sink outside the climate room and rinsed. Cold water was used to prevent the glass from heating up. The aquarium was brought back to the climate room, where it stood without water for at least 15 minutes to get back to the temperature of the climate room. Then, it was filled with seawater from the plastic tank. The Aquarium was placed in correct position using taped marked areas and the aluminium foil piece was fasted and adjusted. These adjustments ensured extra time between every batch, giving any temperature difference between the aquarium and the climate room time to equalise. Preparations were performed before preparing a new batch of lice to minimize the heating of water.

2.4 Image analysis

Manually registering the movement of every individual on video footage is time-consuming. Hence, software that automates this process has been created and used in several studies to study the behavioural response of crustaceans (Bandara et al., 2021). As a part of this master thesis, two scripts were developed to process, detect, track and finally, give output of the movement of larvae in terms of xy-coordinates across all photos, in each experiment. The Open-Source Computer Vision Library (OpenCV) (version 4.9.0, OpenCV Team, https://opencv.org/) were used in the making of scripts in Python (version 3.10.11). AI (ChatGPT, Version 3.5, Open AI) was used as a supportive tool in putting together the framework and in suggestions functions from the OpenCV library. In addition, some functions (GaussianBlur and findCountur) were used after inspiration from pseudocodes provided in Bjørnstad & Solstad (2019). The next section discusses the usefulness, but also the importance of awareness, when using artificial intelligence solutions when making scripts for use in research. Following is a brief introduction to OpenCV, and thereafter, pseudocodes explaining the basic logic and algorithms behind the scripts that are used in this thesis.

2.4.1 Artificial Intelligence (AI) as a Supportive Tool

Artificial Intelligence (AI) has become an integrated part of many industries, helping solve complex problems more efficiently than previously possible. AI has also become a valuable tool in biological research, where it has been applied in several fields, such as medicine, gene editing, and host-pathogen interactions (Bhardwaj *et al.*, 2022). Because of AI, numerous possibilities have been opened for the academic community and scientific researchers (Bhardwaj *et al.*, 2022). Hassoun *et al*. (2021) state, "The time for AI in biology has arrived." Among the applications of AI is the development of hardware and software appropriate for biological applications (Bhardwaj *et al.*, 2022). What would have taken years to conduct can be done in less time with the help of AI (Hassoun *et al.*, 2021; Bhardwaj *et al.*, 2022).

Although AI is a robust and efficient tool, it is essential to use it correctly. Among several limitations are limited computational output capability (Hassoun *et al.*, 2021). Hence, transparency is essential when outsourcing tasks to AI involving limited amount of human participation (Hassoun *et al.*, 2021). As a tool leaning on a huge amount of data, it can make mistakes in several ways. Researchers should be aware of issues with the AI services they use (Hassoun *et al.*, 2021). For example, letting AI make a script without understanding the logic and functions behind it would, in the worst case, lead to incorrect results with computational errors that do not reflect actual results. The usage of AI in academic research is a powerful tool, but awareness should be made, usage should be stated, and its ethics should always be considered.

Different AI services have been established, whereas ChatGPT (Open AI) is well-known. This thesis used ChatGPT (Version 3.5, Open AI) to create scripts to detect and track the nauplii and copepodids from the experiments conducted. At the point this master is written, Chat GPT is not able to make advanced scripts on its own without explicit instructions. Even though making the script took considerably less time than it would have taken if AI had not been used as a supportive tool, it still required analytical thinking, knowledge of OpenCV, python coding, and mathematical understanding. Each function suggested by ChatGPT was carefully analysed and understood before letting it be a part of the total scripts. This ensured correct implementations of functions, limited the possibility of

computational errors, and ensured that the scripts were well understood before letting them be a part of the data collection process.

2.4.2 OpenCV

OpenCV is a powerful library in Python that processes image data (Bradski, 2000). The library is open-source and includes hundreds of functions to help researchers detect and track objects (Bradski, 2000). Since its publication in 1999, it has been used in various disciplines ranging from engineering to entertainment (Culjak *et al.*, 2012). OpenCV has previously been used in research on sea lice as well, e.g., by Kvæstad *et al.* (2020), which used it to detect and track copepodids of salmon lice in response to light stimuli.

2.4.3 Scripts

To detect and track the moving larvae, two main scripts were developed as part of this master's thesis. Simplified pseudocodes for these scripts are provided below. Fig. 2.5 provides a visualisation of the detection and tracking.

Script 1: Motion Detection.
Input: Each folder having the pictures obtained from each experiment
Output: AVI video file showing detected motion as white, dilated dots at a black background in 120 fps.
Duration: Approximately 15 minutes per 10 000 images

Algorithm 1: Preprocess Frames

- Adjusting the brightness and contrast of each frame to enhance visibility**.**
- Applying gaussian blur to each frame to reduce noise**.**
- Return each pre-processed frame for subsequent processing.

Algorithm 2: Motion Detection

- Using pixel values (indicating the brightness of the object) to sort out objects of interest from the pre-processed frames. Objects above pixel value of 200 are set to completely white (250), while objects below are set to completely black (0). This make sure objects lightened up by the IR-lights are detected, while darker spots are not.
- A white circular mask is given to objects that are detected moving between frames.
- To avoid objects standing still for multiple frames from not be detected (and not marked with a white mask), already applied white masks are given a decay rate of 0.99.
- White masks are dilated so that detected objects gets a larger circular white mask, making tracking easier in the following script (Script 2)

Algorithm 3: Process images

- After going through the two algorithms above, image frames are put together to a specified frame rate of 120 fps. The dimensions of the AVI video are kept like the dimensions of the images.

Script 2: Motion Tracking
Input: AVI video obtained from Script 1
Output: CSV-file including xy-coordinates of tracked motion across all frames where the tracked object is visible
Duration: Approximately 5 minutes for a 2-minute video

Algorithm 1: Motion tracking

- The findCounters-function provided in CV2 is used to track each white circular mask across all frames in the AVI-video (ouput from Script 1). A threshold size is set to ensure that small particles (below the pixel size of dilated larvae) are not tracked.
- Each object is given a specific ID, keeping the same ID for each objects thought the analysis until the object (the circular mask) disappears**.**
- The first appearance frame of each ID (tracked object) is stored in a list**.**
- The xy-coordinates of each object ID in each frame are stored in a list

Algorithm 2: Making of CSV-files

- Two csv files are generated, one having the y-coordinates, and another having the x-coordinates, for each object in each frame.
- The first row in the csv files is assigned to each tracked object IDs.
- The columns represent each frame, housing either the x- or y-coordinates.
- The list containing the first appearance frame of each ID decides at which column number the assignment of coordinates should start, ensuring that coordinates are placed according to the correct frame number.
- The frames where the object is not tracked, is given the value "0", indicating no detection in that frame.

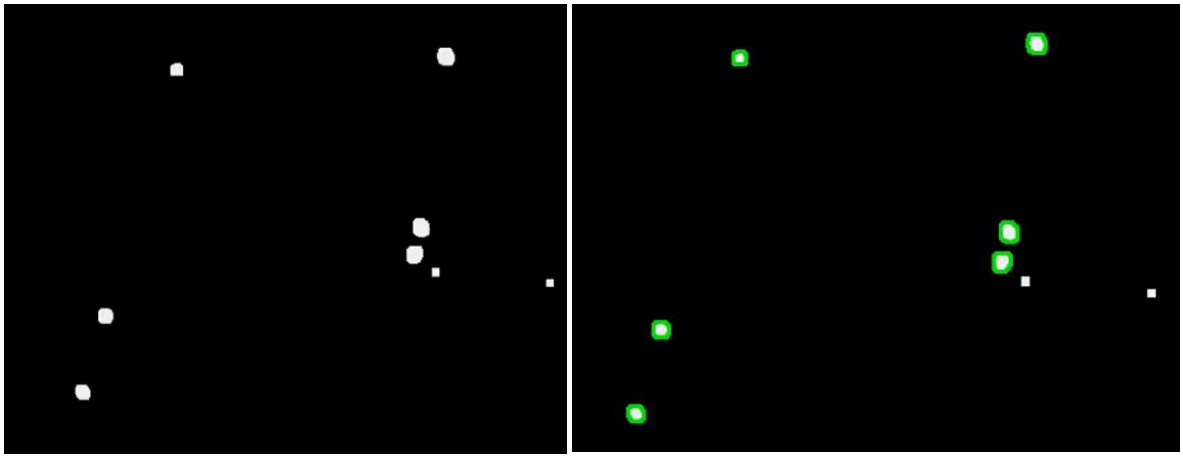

Figure 2.5: *Left: Example of the dilated white circular masks added to moving objects in script 1. The picture is taken from the output video in a zoomed-in position in the aquarium. Right: The dilated white circular mask is tracked in script 2. The picture illustrates white objects above a given size that are tracked, represented by green tracking lines around the objects. Small particles are not tracked and does not have green tracking lines around them.*

2.4.4 Track selection

Not all tracked objects were larvae. Some larger water drops, air bubbles and dust particles were also tracked. Hence, it was necessary to exclude these before further analysis. The following criteria were established for the inclusion or exclusion of detected and tracked objects:

1. The object had to be continuously tracked (having coordinates for all frames) for a minimum of 3000 frames (25 seconds) in dark condition and in the following light condition on both sides of frame number of which the light was turned on. Hence, Object ID 7, 8 and 9 (Fig. 2.6-A) are examples of tracks that were removed following this criterion. Only some objects that were not larvae were tracked for this long, so the next criterion was easy to follow.
2. The object had to exhibit a jump-and-sink pattern in the y-direction (vertical direction in the aquarium) or show some sort of movement other than in straight lines. Objects moving in completely straight lines or showing the absence of the jump-and-skink response (Fig. 2.6-A), were controlled for by visual inspection of movement in y-direction against time, x-direction against time, and x against y. In cases where this was not enough, visual inspection of the raw video (images turned into a video with no other processing) were conducted. If they turned out not to be larvae, they were removed from the analysis. Object ID 10 is an example of a track coming from an air bubble inside the aquarium slowly drifting upwards the aquarium wall (Fig. 2.6-A). This exclusion process minimized the risk of water droplets, air bubbles, or larger dust particles from being included in further analysis (Fig. 2.6-B).

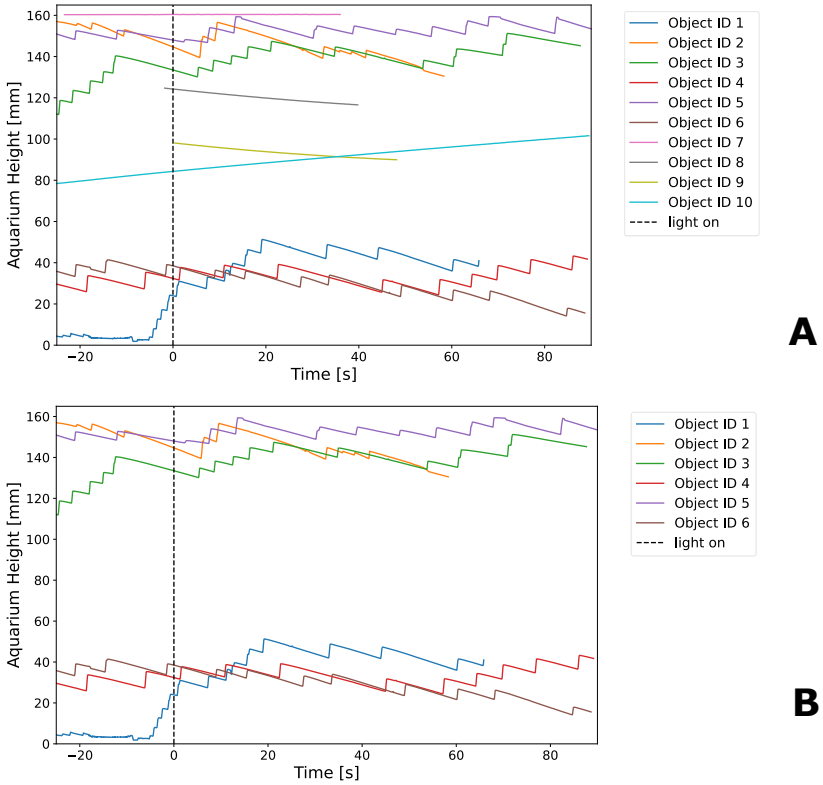

***Figure 2.6**: Example of exclusion of objects. (A) Tracks from one specific experiment before exclusion process (B) Exclusion preformed. Only valid tracks included in the analysis.*

The tracking of individual larvae became challenging when they moved towards either 1) the side walls of the aquarium, 2) the bottom plate of the aquarium, and 3) the top of the aquarium. Hence, larvae moving straight up to the top of the aquarium after he onset of light, are likely missed from the analysis. An alternative to only using continuously traceable individuals for data material would be to assume missed tracks as a maximum response. However, given the circumstances that larvae also disappeared when moving into the walls and in the bottom of the aquarium, this would be too simplistic assumption. An alternative method would be to manually consider each track based on disappearance. Given the scope of this master thesis, however, this would be too time-consuming. Hence, only tracks visible for the given amount of time mentioned here were included.

2.5 Processing of coordinates and calculations

The light was turned on at a different frame number in each experiment. This was due to the manual process of clicking run at a script outside the experiment room after 30 seconds, using a timer (Integrated timer in iPhone 5S, Apple). The exact light-on frame varied around frame number 3600 (30 seconds). Thus, the light on frame in each experiment was identified by scrolling through the pictures after frame number 3600 to see at which frame the light turned on through the reflection in the aluminium foil. This precision ensured accurate calculations of means and speeds between dark and light conditions among the tracked objects in all experiments.

To visualise the differences in positioning in the different light treatment groups through figures showing movement against or away from the light source, movement was plotted from a starting position frame. The starting position frame was the frame number corresponding to 25 seconds before the light-on-frame. All coordinates corresponding to larvae positioning after this starting position frame, where subtracted from the coordinate of the starting position frame. Hence, the starting point for each track become y=0. What is called 'mean deviation' in this thesis, is the difference in position from this starting position frame.

The contour tracking and the subsequent coordinates extraction were done from each object's centre points. As the larvae moved around and were visible to various degrees through the experiments, this sometimes resulted in larger differences in y and x-coordinates because of rapid changes in tracked centre points. Hence, individual tracks were smoothed out by plotting the movements based on a running mean of 20 frames. Speed was calculated using Euclidean distance, accounting for both x-and y-coordinates. The running mean of 20 frames was used to do this. The means corresponding to the vertical positioning from each individual tracked larvae were calculated from three periods:

- Dark Period of 25 seconds
- First Light Period (FLP) of 25 seconds
- Total Light Period (TLP) of 90 seconds (FLP + additional 65 seconds)

The FLP provided an adequate and comparable measure relative to the dark mean baseline, set based on the 25 seconds before the light was turned on. It also provided the possibility to analyse the response quickly after the onset of light. In addition, as one inclusion criterion was that the track had to be visible after light onset for a minimum of 25 seconds, the FLP includes all the visible tracks. Conversely, in the TLP, the tracks stop at the given frame number where the track was lost. Thus, The TLP ensured utilisation of the data, as it allowed for including longer tracks, even though many of these gradually disappeared throughout the TLP.

2.6 Statistics

2.6.1 Experimental design

The experimental design used in this study is a three-factor randomised complete block (RCB) design, randomly assigning all light combinations within each of the three replicates. Two batches of 15 larvae in each made up one replicate. To minimise the possibility of overexposure, a total of 9 runs with different light combinations were performed per batch. Compared to the completely randomised design without blocks, the RCB design prevents the same light combination to be used on the same group of larvae and reducing the risk of effect from cofounding factors of both biological and experimental character.

2.6.2 Statistical tests

The statistical software Minitab (Version 21.4.2.0, Minitab, LLC) was used to conduct statistical tests and graphical representations. Statistical analysis was carried out to analyse vertical positioning, average speed, and maximum speed in different light conditions for both copepodids and nauplii.

Paired t-tests were conducted to analyse the differences between means in dark and light conditions. The Holm–Bonferroni method was used to minimize the risk of Type I error.

Mixed effect models were used to analyse the response to different light treatments within the light condition, not taking the dark period into account. The fixed factors were waveband, intensity, and pulsation. In addition, all two-ways and three-ways combinations of these factors were accounted for. Tukey`s HSD was used to conduct Post Hoc Analysis to compare differences between different levels of factors from the mixed effect model.

Mixed models are appropriate in situations where repeated measurements are taken on the same individual or group over time (Detry & Ma, 2016). In addition, a mixed model can be used to control variability across groups (Detry & Ma, 2016). As the study included replicates, and because repeated measurements were conducted on the same 15 individuals over a longer time, a mixed effect model was chosen, with run order and replicate as random factors. Run order was the order of the experiment within each batch (1-9). As it was given 8 minutes of dark between each run, it could be discussed if the run orders indeed were independent from each other, and thus not necessarily having run order as a random factor. However, as no pilot study was conducted concerning larvae acclimatization time indicating that 8 minutes was enough, they were not assumed independent. If larva were more active in the first runs, and less active in the last runs, a mixed effect model would catch this difference and report its significance.

For the analysis concerning vertical positioning due to different light treatments, the response variables were chosen to be the mean of the tracked larvae in FLP and TLP. To analyse the difference between average and maximum speed, a total of four response variables were used in each its own mixed model: average and maximum speed in FLP and TLP.

2.6.3 Control of model assumptions

Residuals are the difference between observed data and the model's predicted data (Walpole et al., 2016). The mixed effect model is indeed a model from the data, which will differ from the exact observations, making error terms. There is one error term per track

as one track is extracted from one experiment. These error terms are assumed to be 1) normally distributed and 2) independent with 3) constant variance and 4) zero mean (Walpole et al., 2016). If these assumptions do not hold, other tests, such as nonparametric tests, could be a better choice. All assumptions were controlled for each of the mixed effect models performed in this thesis before concluding them valid and including them. Residual plots from all mixed effect models included are to be found in Appendix B (nauplius) and C (copepodid).

3 Results

3.1 Nauplius

A total of 377 nauplii met the criteria of continuous tracking in the First Light Period (FLP); 25 seconds in dark condition, followed by 25 seconds of light stimuli. A total of 54 experiments with 15 nauplii in each resulted in an average of 7.0 nauplii tracks per experiment and 20.9 tracks per light treatment group. The number of tracked nauplii decreased throughout the following 65 seconds of light stimuli, giving nauplii tracks visible for varying numbers of seconds in the Total Light Period (TLP); First Light Period, plus additional 65 seconds in light stimuli.

3.1.1 Differences in vertical positioning between dark and light condition

3.1.1.1 Comparison of vertical positioning withing each light treatment

In FLP, the average vertical position difference between dark and light condition ranged from -12.7 mm in B-H-P0 to +1.96 mm in R-L-P0 (Table 3.1). In TLP, the range was from -20.9 mm in B-H-P0 to +4.97 mm in R-L-P0 (Table 3.1). Most of the light treatments led to an average vertical positioning further away from the light source compared to the position in dark period (Fig. 3.1 and Fig. 3.2). This applied to almost all light treatments, except low-intensity constant red light (+1.96 mm in FLP and + 4.97 mm in TLP) and high-intensity red light with pulsation P1 (+0.80 mm in FLP and +0.76 mm in TLP). Hence, low-intensity constant red light led to the largest positive difference in vertical position compared to the dark positioning. However, the average vertical positioning in this light treatment was not significantly different from the average vertical positioning in the dark period ($p=0.052$ in FLP and $p=0.016$ in TLP, paired-test, significant levels adjusted with Holm-Bonferroni method).

Low-intensity light generally resulted in vertical positioning more like the vertical positioning in dark condition than high-intensity light (Fig. 3.1 and Fig. 3.2). In turn, high-intensity light led mostly to a vertical positioning further away from the light compared to both the dark conditions and the treatments with low-intensity light (Fig. 3.1). This was most prominent in light stimuli with high-intensity constant green light, where the average vertical position in the total light period was –19.1 mm and significantly different from the average vertical positioning in the dark period ($p<0.001$ in TLP, paired-test, significant levels adjusted with Holm-Bonferroni method) (Table 3.1)

Furthermore, high-intensity blue light with pulsation levels P0 (B-H-P0) and P2 (B-H-P2) caused a significant difference in the average vertical positioning of nauplii compared to the positioning in dark conditions ($p<0.001$, paired t-test, significant levels adjusted with Holm-Bonferroni method) (Table 3.2). This was the case for both light periods (FLP and TLP). B-H-P0 and B-H-P1 caused an average positioning difference of -20.9 mm and -13.3 mm, respectively. The only low intensity light condition that cause a significant difference from the dark period, was low intensity blue light with pulsation level P2 ($p<0.001$). Here, the vertical positioning in light condition differed -5.54 mm (FLP) and -12.1 mm (TLP) from the dark period (Table 3.1)

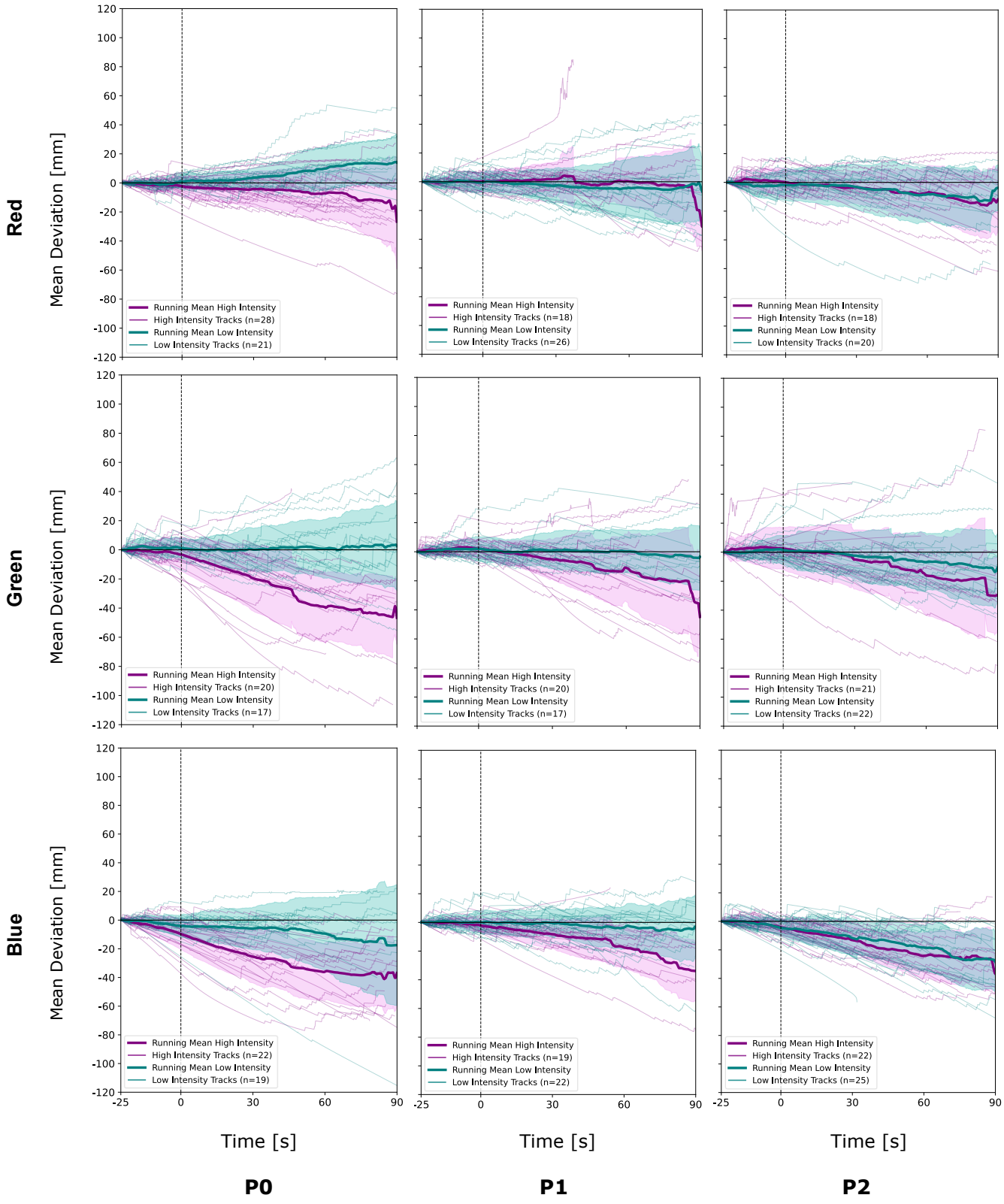

Figure 3.1: *Valid nauplius tracks (n=377) from all light treatment groups (18) plotted in a 3x3 matrix. Wavebands and pulsations make up the matrix. High and low intensity is distinguished by separate colours. Mean deviation (black line at x=0) represents vertical movement either away from (represented by negative y-values) or towards the light source (represented by positive y-values). Weaker colours around running means represent standard deviations in the running mean of similar colour.*

Table 3.1: *Overview of results from paired t-tests of average positioning in dark condition vs. light condition for nauplii and some associated descriptive statistics for each light treatment group. Mean dark position in aquarium obtained from 25 seconds before the onset of light, and ranges from 0 (aquarium bottom) to 160 (aquarium top) [mm]. Position difference in light periods reported as deviations from average position in dark period [mm]. Positive values indicate positioning closer to the light source relative to the dark period. Significant p-values (unadjusted, α=0.05) are written in bold. Adjusted significant p-values (Holm–Bonferroni method) are marked *.*

			First Light Period			*Total Light Period*		
Light treatment	N	Position (Dark)	Position Difference	T-value	p-value	Position Difference	T-value	p-value
R-L-P0	21	97.4	1.96	2.06	0.052	4.97	2.64	**0.016**
R-L-P1	26	92.6	-1.00	-0.84	>0.1	-2.53	-1.12	>0.1
R-L-P2	20	115.3	-0.24	-0.02	>0.1	-2.85	-1.04	>0.1
R-H-P0	28	101.8	-2.51	-2.28	**0.031**	-4.02	-1.96	0.060
R-H-P1	18	103.3	0.80	0.55	>0.1	0.76	0.33	>0.1
R-H-P2	20	115.3	-3.00	-2.42	**0.027**	-6.69	-2.62	**0.018**
G-L-P0	17	87.2	-1.49	-1.09	>0.1	-0.23	-0.10	>0.1
G-L-P1	17	85.8	-0.66	-0.50	>0.1	-1.89	-1.47	>0.1
G-L-P2	22	102.1	-0.59	-0.60	>0.1	-3.25	-1.08	>0.1
G-H-P0	20	78.0	-8.82	-3.44	**0.003**	-19.1	-4.31	**<0.001***
G-H-P1	20	77.4	-2.89	-2.23	**0.038**	-9.12	-2.60	**0.018**
G-H-P2	21	86.7	-2.53	-1.32	>0.1	-6.95	-1.98	0.062
B-L-P0	19	66.8	-2.96	-1.64	>0.1	-4.09	-1.19	>0.1
B-L-P1	22	108.3	-0.63	-0.64	>0.1	-1.85	-1.00	>0.1
B-L-P2	25	80.9	-5.54	-4.09	**<0.001***	-12.1	-5.31	**<0.001***
B-H-P0	22	87.7	-12.7	-6.49	**<0.001***	-20.9	-6.72	**<0.001***
B-H-P1	19	62.1	-4.17	-3.20	**0.005**	-8.28	-3.13	**0.006**
B-H-P2	22	82.5	-7.00	-6.25	**<0.001***	-13.3	-5.82	**<0.001***

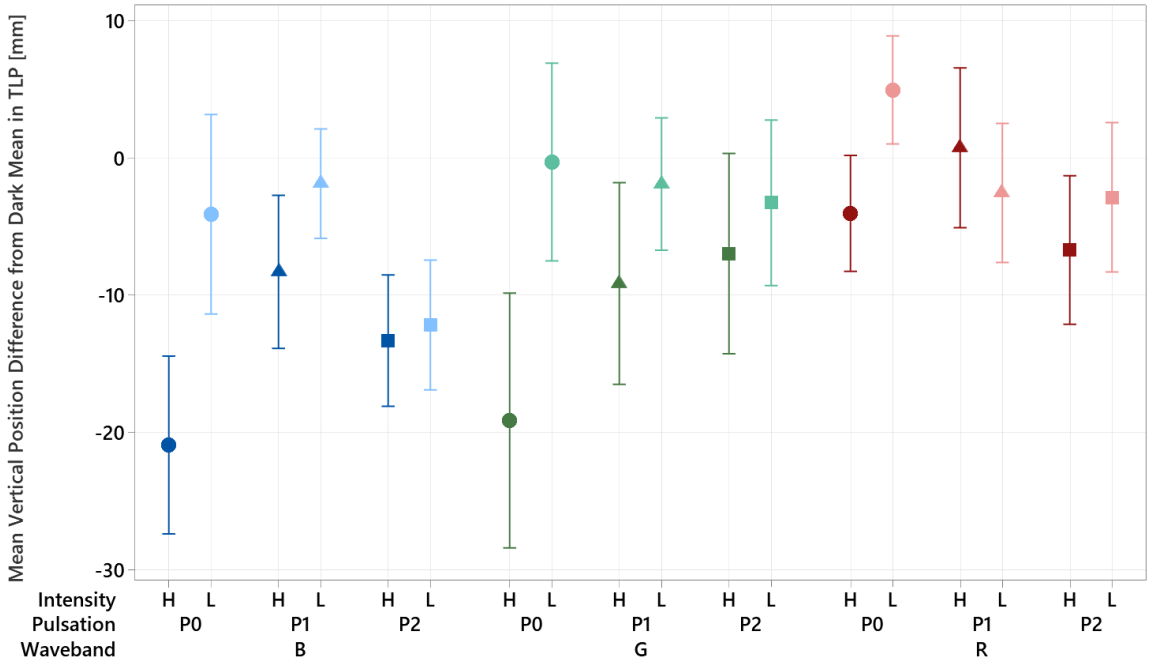

Figure 3.2: *Average vertical position difference (y-axis) between Total Light Period (TLP) and dark position among nauplii. Negative position difference indicates position further away from the light compared to the dark position. The x-axis displays 18 different light treatments. Annotations: B: blue; G: green; R: red; H: High; L: Low; P0: Constant light; P1: 0.5 sec light, 3 sec dark; P2: 2 sec light, 3 sec dark. Each mean is calculated based on all valid tracks corresponding to each light combination. Whiskers around the mean represent the 95% confidence interval for each mean.*

3.1.1.2 Visual analysis of general behaviour before and after the onset of light

Nauplii larvae exhibited various movement patterns. In some experiments, no individuals showed positive phototactic response (Fig. 3.3-A). In other experiments, nauplii moved both upwards (ID 3) and downwards (ID 4) after the onset of light (Fig. 3.3-B). Some stayed at the bottom (ID 1, Fig. 3.3-B) or on the surface (ID 4, Fig.3.3-C) of the aquarium during the entire experiment. Others moved around more (ID 4, Fig. 3.3-A). Hence, the positioning of individual nauplii varied within each experiment. Nauplii reaching the aquarium bottom through passive sinking, such as ID 1 (Fig. 3.3-B), expressed a strong jumping response followed by sinking behaviour. Nauplii that moved up towards the light, such as ID 2 and ID 4 (Fig. 3.3-B), exhibited smaller and more frequent jumps, represented by rapidly oscillating patterns. Some nauplii moving downwards expressed the same periodic movement pattern, such as ID 3 (Fig. 3.3-B). However, sinking nauplii were often characterised by a pattern of extended sinking periods including smaller jumps in between, such as ID 1 and ID 2 (Fig. 3.3-A).

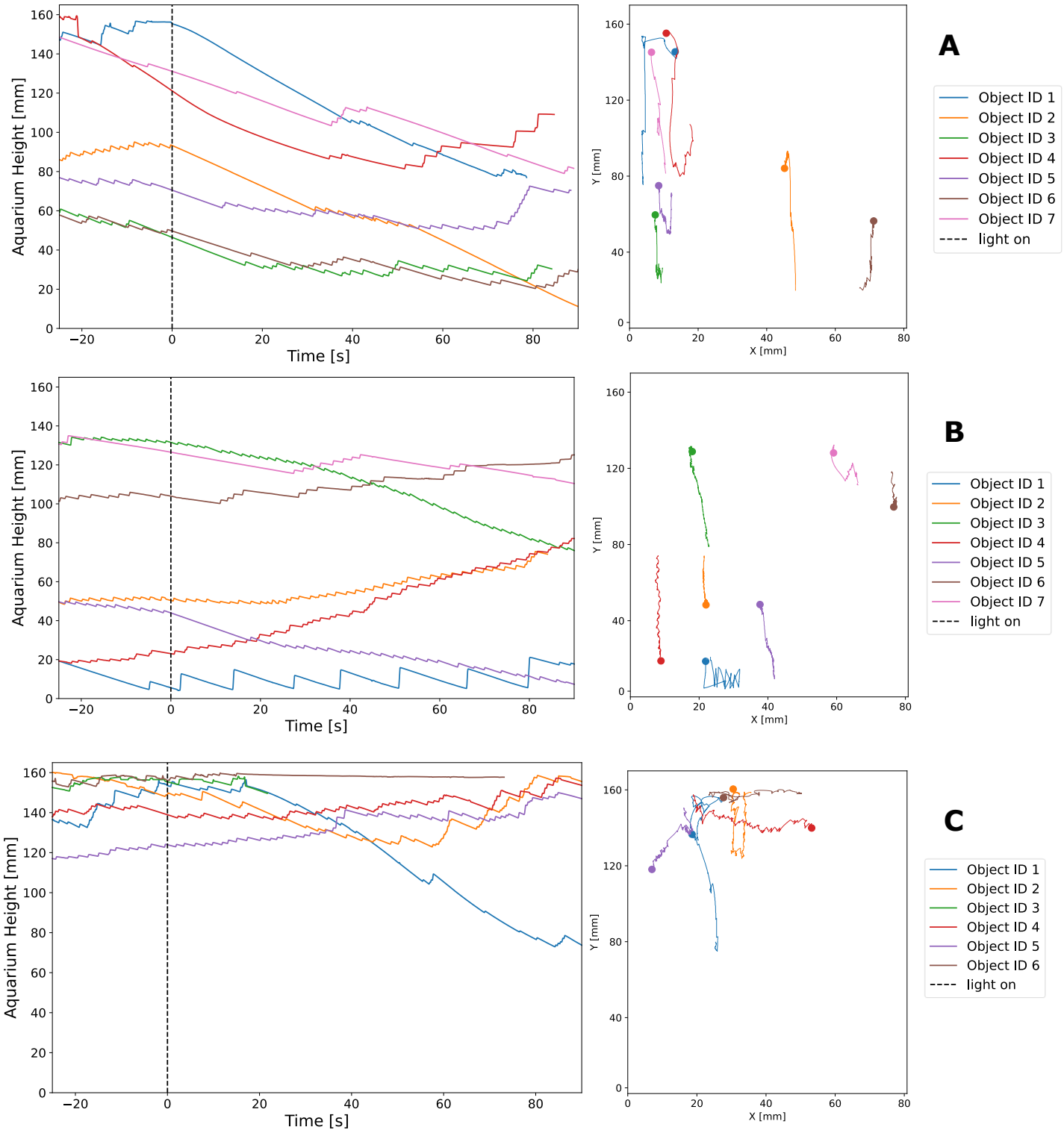

Figure 3.3: *Individual tracks from selected experiments (one replicate) of different light treatments: A) B-H-P0, B) G-L-P0, C) B-L-P1. Left: Tracks from copepodids plotted from y-coordinates, showing movement either up or down in the aquarium. Vertical dotted line represents the onset of light stimulus. Right: Tracks from copepodids plotted with both x- and y-coordinates, showing movement in 2D. Plotted dots represents start position for each nauplii. Object IDs are assigned to each track within the selected experiments through distinct colour coding, giving similar colours for each track in the plots to the left and right.*

3.1.2 Predictors of nauplii light response in terms of vertical positioning

In the following section, results from mixed effect models regarding vertical positioning within the light periods are presented. These results are obtained from comparing light response within the different light treatments, where the averages are derived from their response from the onset of light until the end of given light period (FLP or TLP).

Intensity was a significant predictor for the average vertical position of nauplii in light condition ($p<0.001$, $F=20.61$ in FLP and $p<0.001$, $F= 26.35$ in TLP, mixed effect model, replicate and run order as random factors; Appendix B.1-B.2). High-intensity light led to a significant difference in average vertical position compared to low-intensity light, in which nauplii in low-intensity light were positioned closer to the light source (Fig. 3.4). Hence, in high-intensity light, nauplii were positioned further away from the light source. A comparison of individual tracks from R-L-P0 and G-H-P0 (all replicates), reveals an almost reversed movement pattern (Fig. 3.5). While most nauplii in R-L-P0 exhibited movement up and down in the same position, or slightly towards the light source, most of them sank in G-H-PO (Fig. 3.5).

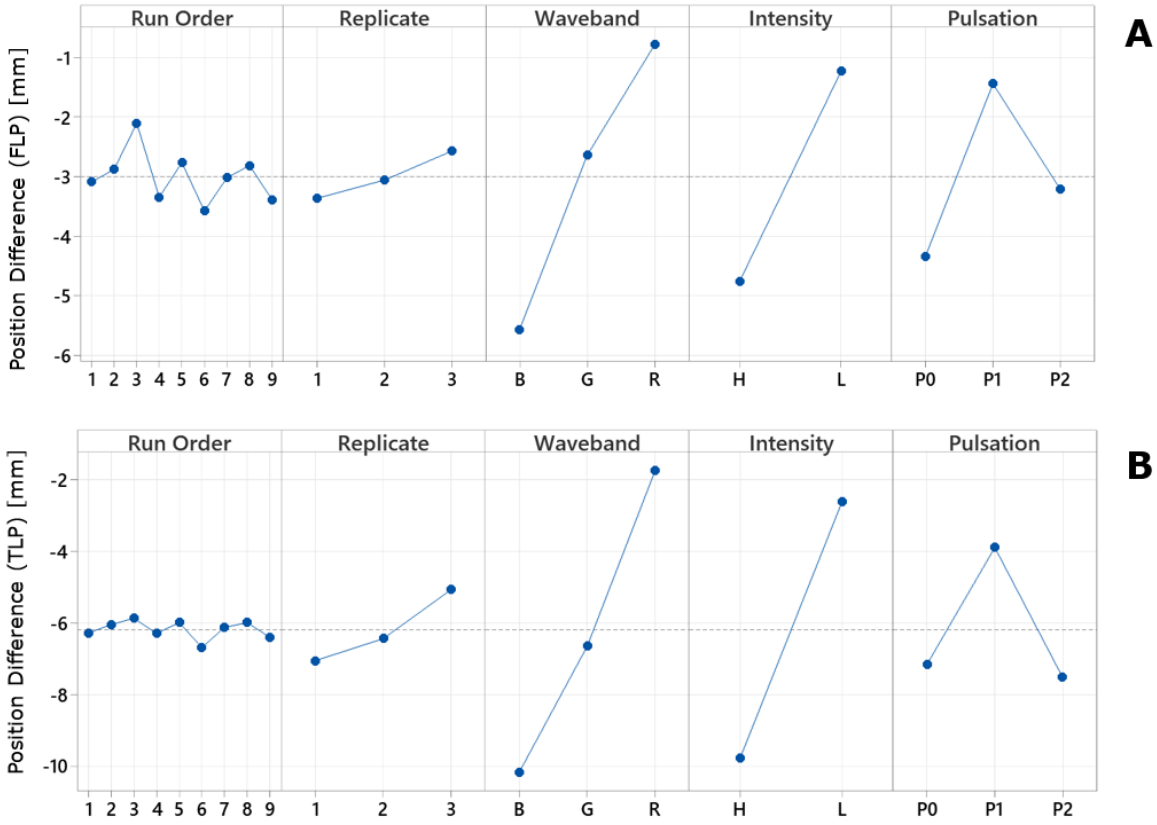

Figure 3.4*: Main effect plots for main and random factors that are parts of the mixed effect model from A) The First Light Period (FLP) and the B) Total Light Period (TLP). Position difference [mm] (y-axis) is the average positioning either down (negative values) or up (positive values) relative to the position at the onset of light. Note the difference in the scale of the y-axis in (A) and (B).*

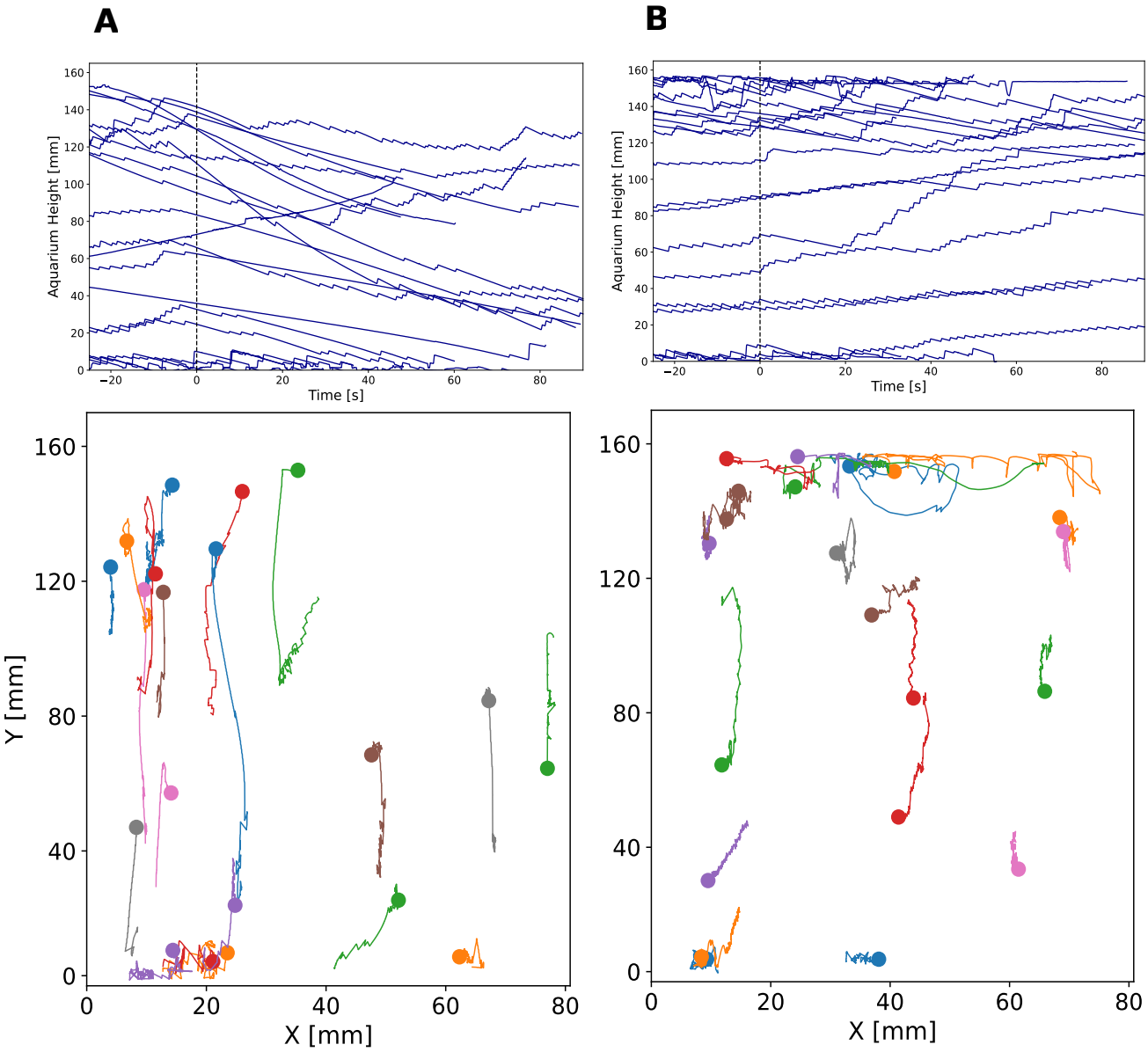

Figure 3.5: *All valid nauplii tracks from the three replicates from light treatment group (A) G-H-P0 (n=20) (B) R-L-PO (n=21). Top: Tracks plotted from y-coordinates, showing movement either up or down in the aquarium. Vertical dotted line represents the onset of light stimulus. Bottom: Same tracks as above, plotted with both x- and y-coordinates, showing movement in 2D. Plotted dots represents start position for each nauplii. Colours added for easier distinguishment between different tracks.*

Waveband was another significant predictor for the average vertical position of nauplii in light conditions ($p<0.001$, $F=13.16$ in FLP and $p<0.001$, $F=12.69$ in TLP). Even though all wavebands led to an average position further away from the light source than the position at the onset of the light (Figure 3.4), some of them led to less decline than others.

FLP: Post hoc test revealed a significant difference in vertical position obtained in red light and blue light ($p<0.001$, Tukey's Pairwise Comparison), and in green light and blue light ($p=0.012$, Tukey's Pairwise Comparison). Both red and green light kept the nauplii closer to the light than blue light (Fig. 3.4-A).

TLP: Post hoc test revealed a significant difference in red light and blue light ($p<0.001$, $T=5.01$, Tukey's Pairwise Comparison), and in red light and green light ($p=0.017$). Nauplii in blue and green light treatments had vertical positions significantly different from the vertical position in red light, in both cases causing a position closer to the light source compared to blue and green light (Fig. 3.4-B).

Pulsation was also a significant predictor for the average position of nauplii in the First Light Period ($p=0.008$, $F=4.97$), but not in the Total Light Period ($p=0.062$, $F=2.81$). P0 and P1 caused significantly different vertical positions ($p=0.006$, Tukey's Pairwise Comparison). Here, constant light (P0) caused more decline than P1 (Fig. 3.4-A)

Intensity*Pulsation was a significant factor interaction in nauplii light response ($p=0.004$, $F=5.60$ in FLP and $p=0.001$, $F=7.63$ in TLP).

FLP: Low-intensity light at all pulsation levels was significantly different from high-intensity constant light ($p<0.001$, Tukey's Pairwise Comparison). In addition, high-intensity light with P1 was significantly difference from high-intensity light with P0 ($p<0.001$). In all cases, the high-intensity constant light led to nauplii positioning further away from the light source.

TLP: As in FLP, Low-intensity light at all pulsation levels was significantly different from high-intensity constant light ($p<0.007$, Tukey's Pairwise Comparison). Furthermore, high-intensity light with P1 was significantly different from high-intensity light with P0 ($p=0.005$). In addition, low-intensity constant light was significantly different from the high-intensity light with pulsation P2 ($p=0.004$). In all cases, high-intensity constant light kept the nauplii further away from the light source than the low-intensity treatments (Fig. 3.5). High-intensity P2-light also caused vertical position further away from the light compared to the low-intensity constant light (Fig. 3.6)

Neither replicate nor run order were shown to be random factors significantly influencing the results (Appendix B.1-B.2). The three-way interaction Waveband*Intensity*Pulsation were not significant.

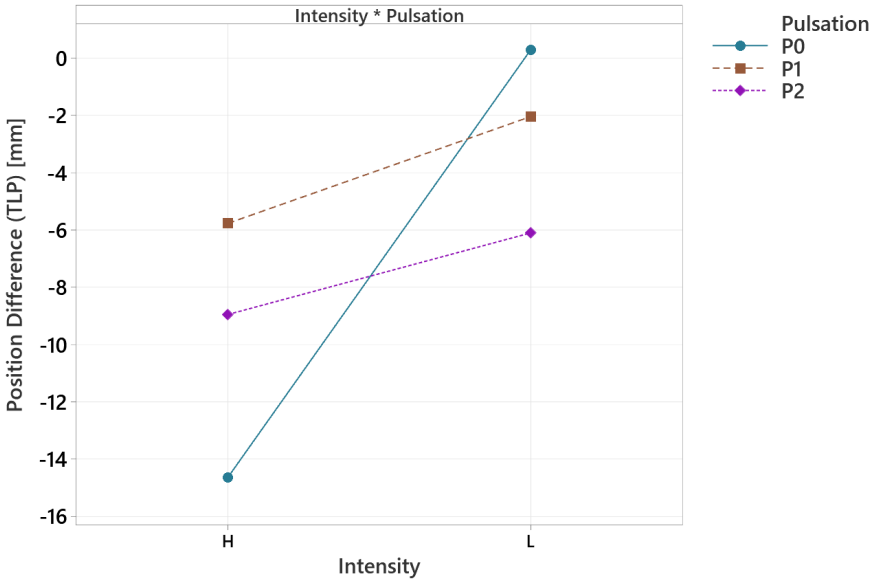

Figure 3.6: Interaction plot for Intensity*Pulsation. *Position difference [mm] (y-axis) is the average positioning either down (negative values) or up (positive values) relative to the position at the onset of light.* The coloured lines represent each pulsation level and show the levels interactions with the two levels of intensity (x-axis). Interaction plots represent the interaction between different factors at various levels (Walpole et al., 2016). Nonparallel lines show the tendency for interaction, while parallelism indicates the opposite, an absence of interaction between the factors (Walpole et al., 2016)

3.1.3 Descriptive statistics: Maximum and Average Speed

The average maximum speed in the dark condition was 16.0 mm/s (SD 11-3). The average maximum speed in light conditions was 14.6 mm/s (SD 11.5) in the FLP and 20.2 mm/s (SD 12.5) in the TLP. The maximum speed among all nauplius larvae occurred in light condition with a speed measuring 67.0 mm/s in the FLP. Maximum speed in dark conditions was 67.8 mm/s. Nauplii positioned closer to the bottom of the aquarium in both dark and light conditions, showed high maximum speeds (Fig. 3.7-A). The same did nauplii with average positioned in the upper part of the aquarium during light conditions, also having a bit higher vertical positioning compared to the dark period.

The average speed in dark conditions was 1.28 mm/s (SD 0.60). The average speed in light conditions was 1.20 mm/s (SD 0.56) in the FLP and 1.24 in the TLP (SD 0.51). The fastest average speed among all nauplius larvae was measured in the FLP, having nauplius moving 4.98 mm/s. Nauplii with the highest average speeds were positioned in the upper part of the aquarium, in the same location as nauplii with high maximum speeds (Fig. 3.7-B).

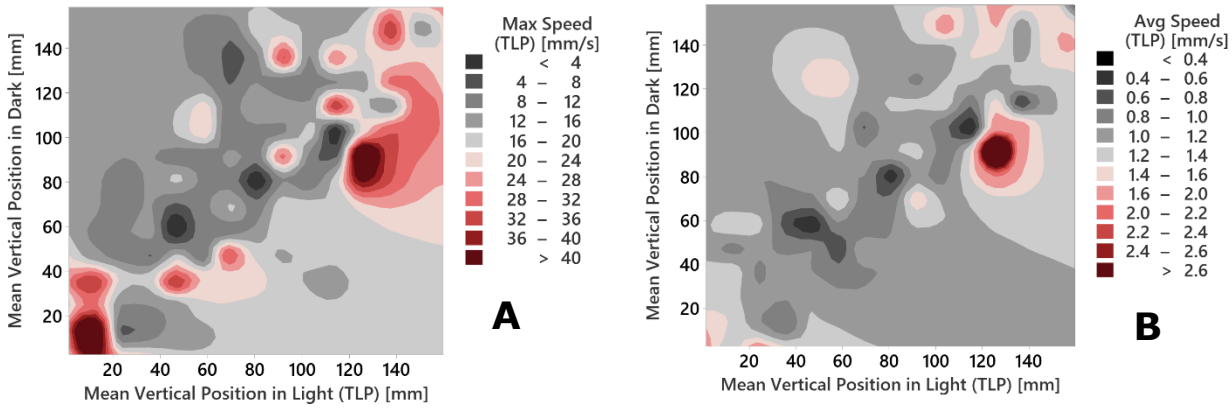

Figure 3.7: *Counter plots based on (A) maximum speed [mm/s] in the Total Light Period (TLP) and (B) Average speed in TLP. The speeds are connected to the mean vertical position in the dark (x-axis) and the mean vertical position in the TLP. Red colours indicate higher speeds in closeness to these areas compared to grey colours, which indicate slower speeds.*

3.1.4 Predictors of nauplii light response in terms of speed

The intensity was the only significant predictor and was so in predicting both average (in the FLP) and maximum speed (in both FLP and TLP). None of the other factors were significant, and neither were combinations of factors (Appendix B.3-B.6).

The intensity was a significant factor of average nauplii movement speed in the First Light Period ($p=0.017$, $F=5.85$, mixed effect model, run order and replicate as random factors, Appendix B.3). The average speeds in high-intensity light (1.13 mm/s) were significantly slower than in low-intensity light (1.27 mm/s) (Fig. 3.8-A). Furthermore, intensity was a significant predictor of maximum speed in both the FLP ($p=0.006$, $F=7.72$, Appendix B.5) and in the TLP ($P=0.016$, Appendix B.6). Here, maximum speeds were significantly slower in high-intensity light treatments compared to high-intensity (Fig. 3.8-B and -C).

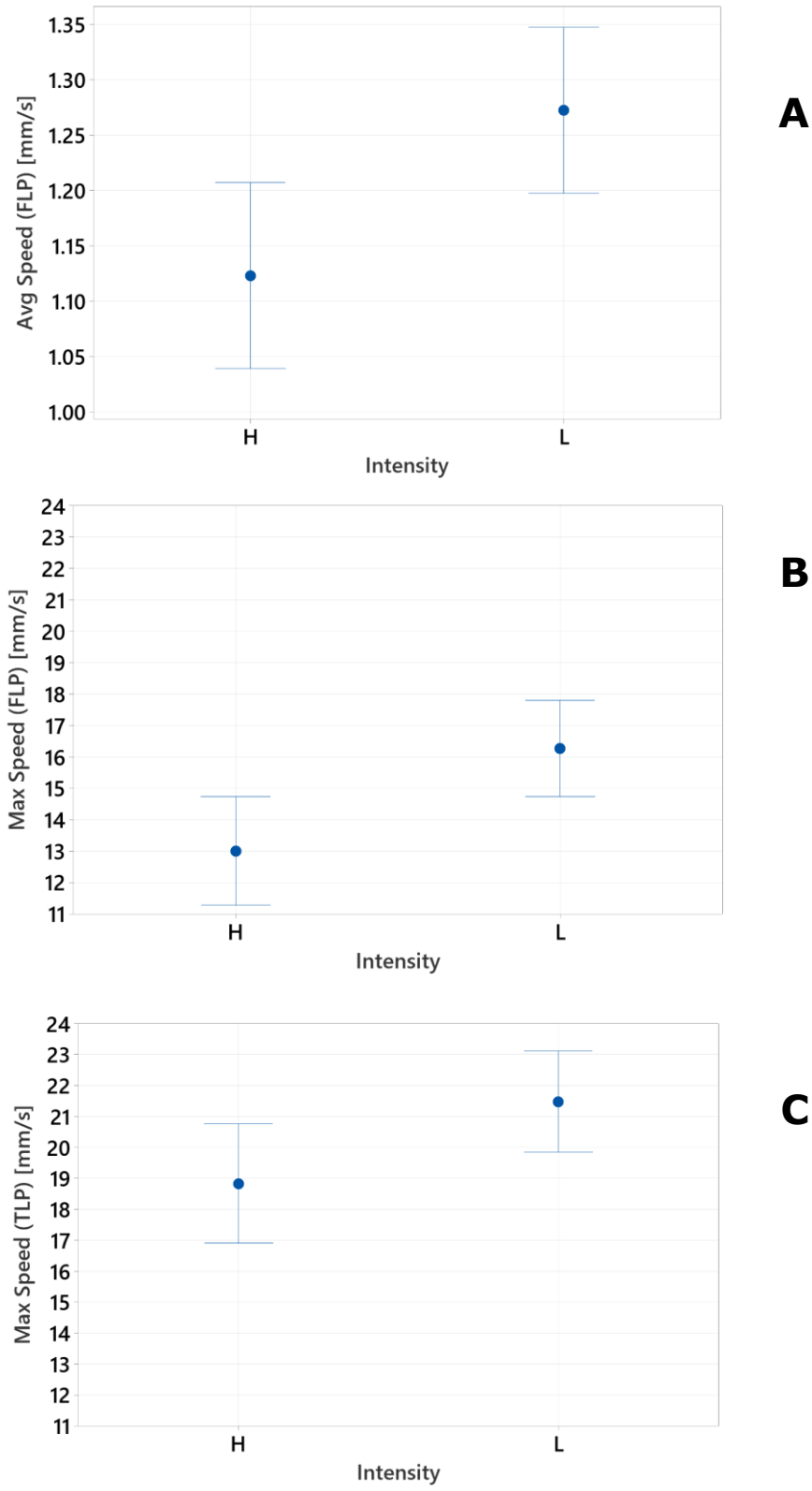

Figure 3.8: *Mean of (A) Average speed in FLP, (B) Maximum speed in FLP, (C) Maximum speed in TLP. The y-axis represents speeds in mm/s, while the x-axis represents High (H) and Low (L) intensity. Each mean is calculated based on all valid tracks within the given factor level. Whiskers around the mean represent the 95% confidence interval for each mean.*

3.2 Copepodid

A total of 308 copepodids met the criteria of continuous tracking in the First Light Period (FLP); 25 seconds in dark condition, followed by 25 seconds of light stimuli. A total of 54 experiments with 15 copepodids in each resulted in an average of 5.7 copepodid tracks per experiment and 17.1 tracks per light treatment group. The number of tracked copepodids decreased throughout the following 65 seconds of light stimuli, giving copepodid tracks visible for varying numbers of seconds in the Total Light Period (TLP); First Light Period, plus additional 65 seconds in light stimuli (90 seconds of light stimuli in total).

3.2.1 Differences in vertical positioning between dark and light condition

3.2.1.1 Comparison of vertical positioning withing each light treatment

No significant difference in vertical positioning between dark and light condition was found for any of the individual light treatment groups (Paired t-tests, adjusted significant level with Holm–Bonferroni method, Table 3.2). In FLP, the average vertical position difference between dark and light condition ranged from -5.33 mm in B-H-P2 to +8.38 mm in R-L-P2 (Table 3.2). In TLP, the range was from -10.1 mm in B-H-P2 to +11.5 mm in R-L-P2 (Table 3.2).

In TLP, low-intensity light consistently kept the copepodids closer to the light source compared with high-intensity light of similar wavebands and pulsation levels (Fig. 3.9 and Fig. 3.10). Although not significant, nearly all low-intensity light treatments, except B-L-P1 (-1.07 mm), G-L-P1 (-3.98 mm) and G-L-P2 (- 3.07 mm), led to an average positioning closer to the light source after the onset of light (Table 3.2). This is clear from the positive response in the average vertical position with time in most of the low-intensity light treatments (Fig. 3.10). Conversely, all high-intensity light treatments, except R-H-P0 (+ 1.50 mm in TLP), led to average positions further away from the light (Table 3.2).

In FLP, the light treatments generally led to the same response as in the TLP, with slightly differences. The vertical positions were generally closer to the dark mean compared to TLP, giving less differences than in TLP (Table 3.2).

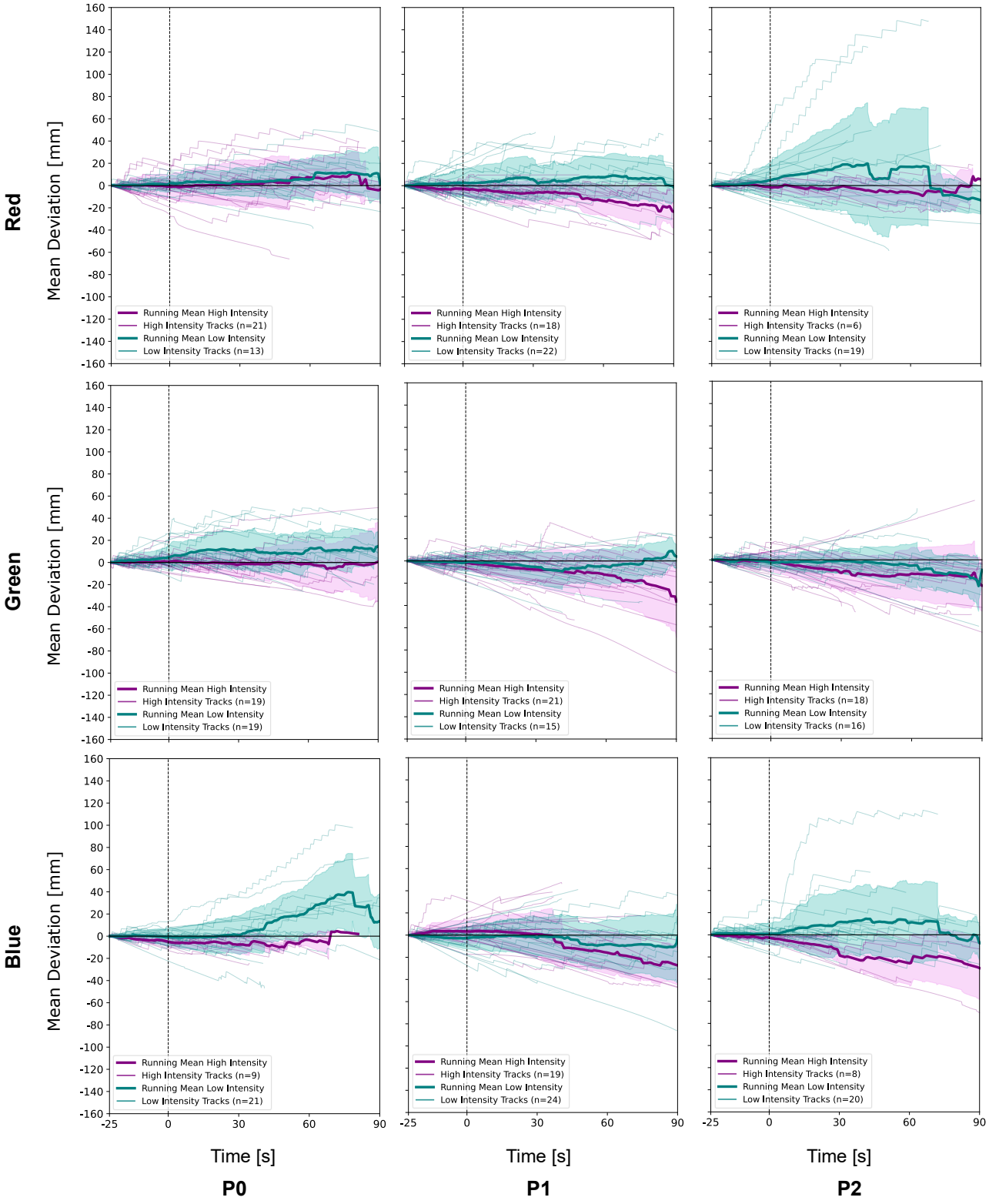

Fig. 3.9: *Valid copepodid tracks (n=308) from all light treatment groups (18) plotted in a 3x3 matrix. Wavebands and pulsations make up the matrix. High and low intensity is distinguished by colures in the plots. Mean deviation (black line at x=0) represents vertical movement either away from (represented by negative y-values) or towards the light source (represented by positive y-values). Weaker colours around the running means represents standard deviations connected to the running mean of similar colour.*

Table 3.2: *Overview of results from paired t-test of average positioning in dark condition vs. light condition for copepodids and some associated descriptive statistics for each light treatment group. Mean dark position in aquarium obtained from 25 seconds before the onset of light, and ranges from 0 (aquarium bottom) to 160 (aquarium top) [mm]. Position difference in light periods reported as deviations from average position in the aquarium in dark period [mm]. Positive values indicate positioning closer to the light source relative to the dark period. Significant p-values (unadjusted, α=0.05) are written in bold. Significant p-values after adjusted significant level (Holm–Bonferroni method) are marked * (none).*

			First Light Period			*Total Light Period*		
Light treatment	N	Position (Dark)	Position Difference	T-value	p-value	Position Difference	T-value	p-value
R-L-P0	13	101.9	2.08	1.18	>0.1	3.73	1.19	>0.1
R-L-P1	22	90.1	2.64	1.22	>0.1	5.15	1.91	0.070
R-L-P2	19	89.5	8.38	1.60	>0.1	11.5	1.54	>0.1
R-H-P0	21	97.00	0.18	0.14	>0.1	1.50	0.49	>0.1
R-H-P1	18	108.7	-2.87	-2.29	0.035	-5.86	-3.08	**0.007**
R-H-P2	6	52.2	-1.90	-1.02	>0.1	-3.31	-0.99	>0.1
G-L-P0	19	115.3	7.10	2.71	**0.014**	8.49	2.58	**0.019**
G-L-P1	15	103.0	-1.32	-0.70	>0.1	-3.98	-1.47	>0.1
G-L-P2	16	90.0	-1.31	-0.96	>0.1	-3.07	-1.07	>0.1
G-H-P0	19	142.33	-0.36	-0.36	>0.1	-1.28	-0.59	>0.1
G-H-P1	21	119.73	-3.55	-2.09	0.050	-8.18	-2.62	**0.016**
G-H-P2	18	87.5	-4.52	-2.21	**0.041**	-9.27	-2.77	**0.013**
B-L-P0	21	109.4	-0.61	-0.22	>0.1	4.40	-1.20	>0.1
B-L-P1	24	84.1	0.38	0.35	>0.1	-1.07	0.25	>0.1
B-L-P2	20	83.0	4.26	1.10	>0.1	5.91	1.10	>0.1
B-H-P0	9	80.1	-3.25	-1.99	0.082	-3.23	-1.89	0.096
B-H-P1	19	113.70	-0.07	-0.03	>0.1	-4.68	-1.21	>0.1
B-H-P2	8	64.7	-5.33	-2.78	**0.027**	-10.1	-2.37	0.050

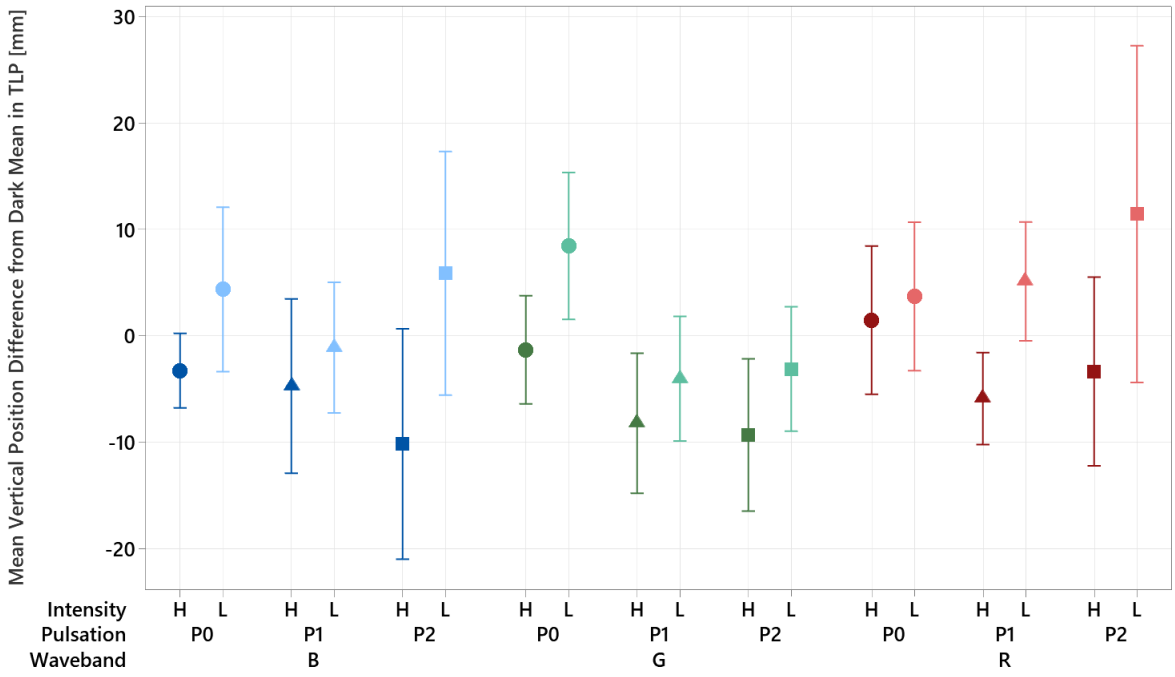

Figure 3.10: *Average vertical position difference (y-axis) between Total Light Period (TLP) and dark position among copepodids. Negative position difference indicates position further away from the light compared to the dark position. The x-axis displays 18 different light treatments. Annotations: B: blue; G: green; R: red; H: High; L: Low; P0: Constant light; P1: 0.5 sec light, 3 sec dark; P2: 2 sec light, 3 sec dark. Each mean is calculated based on all valid tracks corresponding to each light combination. Whiskers around the mean represent the 95% confidence interval for each mean.*

3.2.1.2 Visual analysis of general behaviour before and after the onset of light

Several individual copepodids exhibited what appears to be positive phototactic response against the light source when light was switched on. Such tracks are visible in several of the light treatment groups as positive movement in y-direction (Fig. 3.11). B-L-P0, B-L-P2 and R-L-P2 are examples of light treatments groups where individual copepodids moved more than 10 centimetres in the direction of the light source (Fig. 3.11 A-C). Some of these copepodids, as ID 1 (Fig. 3.11 C), started their movement in direction of the light source already in the dark condition, and continued their paths upwards in the light condition. Others accelerated against the light source with a jump-sink pattern, almost immediately at the onset of light (Fig. 3.11 A). ID 1 and 2 (Fig. 3.11 A) are examples of copepodids that seem to display such positive phototaxis. The jump-sink patterns varied from small jumps and sinks that drove the copepodids slowly upwards (Fig. 3.11-B, ID2), to larger jumps where the jump distance was considerably greater than the sinking distance (Fig. 3.11-A, ID1).

Numerous copepodids exhibited minor difference between the dark and light conditions. Many of them, as ID 3 (Fig. 3.11 B) and ID 7 (Fig. 3.11 A) were slowly descending in y-position with time, passively sinking. Some of these exhibited small jumps, before continuing sinking. Others, as ID 2 and ID 3 (Fig. 3.11 C), were in the relatively same position in both dark and light conditions. A continuous jump-sink pattern kept them in the same position.

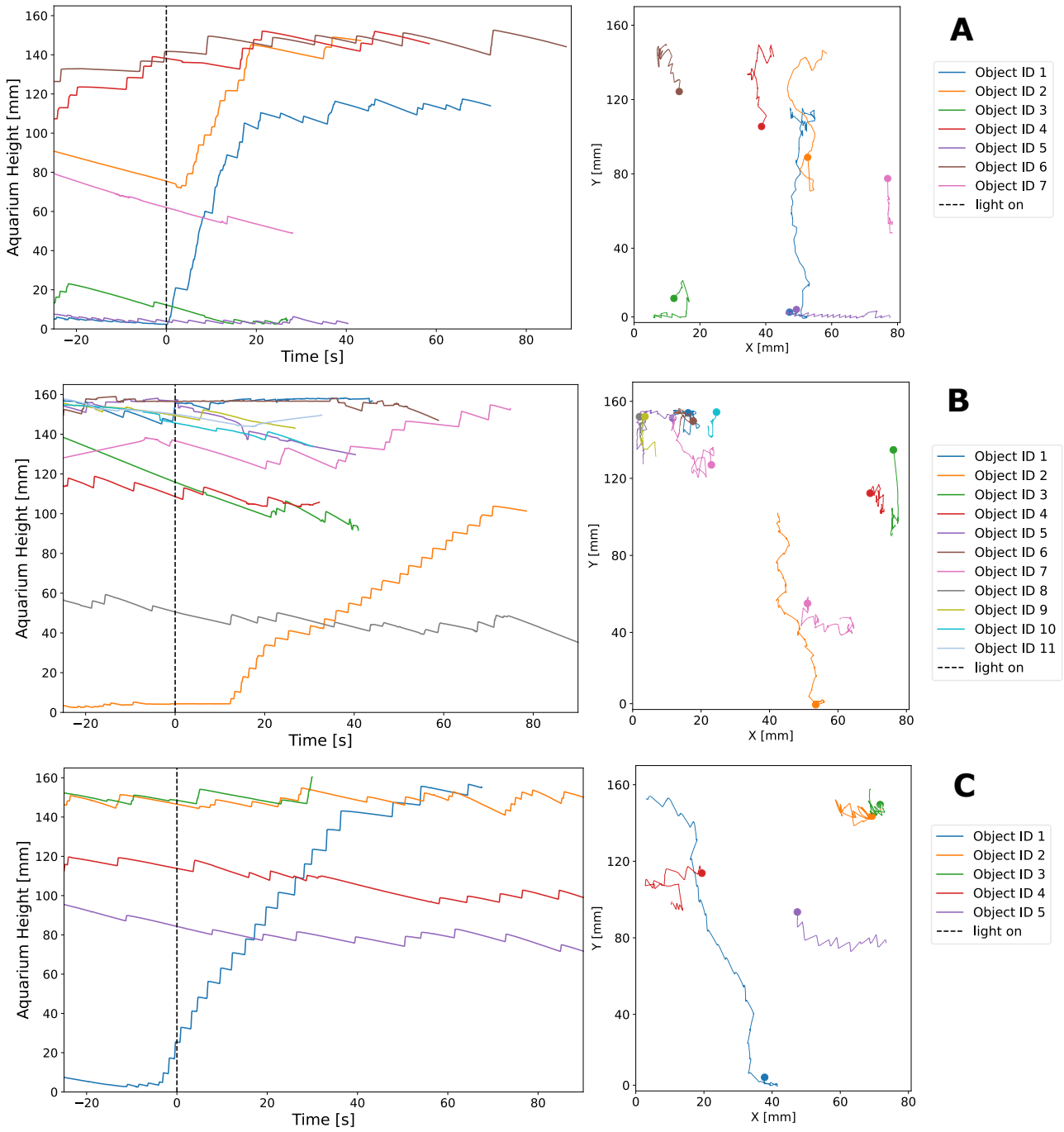

Figure 3.11: *Individual copepodid tracks from selected experiments of different light treatments: A) B-L-P2, B) B-L-P0, C) R-L-P2. Left: Tracks from copepodids plotted from y-coordinates, showing movement either up or down in the aquarium. Vertical dotted line represents the onset of light stimulus. Right: Tracks from copepodids plotted with both x- and y-coordinates, showing movement in 2D. Plotted dots represents start position for each nauplii. Object IDs are assigned to each track within the selected experiments through distinct colour coding, giving similar colours for each track in the plots to the left and right.*

3.2.2 Predictors of copepodid light response in terms of vertical positioning

In the following section, results from mixed effect models regarding vertical positioning within the light periods are presented. These results are obtained from comparing light response within the different light treatments, where the averages are derived from their response from the onset of light until the end of given light period (FLP or TLP).

Intensity was a significant predictor for the average vertical position of copepodids in light condition ($p=0.001$, $F=11.18$ in FLP and $p<0.001$, $F= 13.12$ in TLP, mixed effect model, replicate and run order as random factors; Appendix C.1-C.2). High-intensity light made the copepodids move further away from the light than low-intensity light (Fig. 3.12). Neither waveband nor pulsation were found to be significant predictors of copepodid light response ($p>0.1$). Indicated by high p-values, neither the 2-way nor the 3-way interaction factors were significant ($p>0.3$).

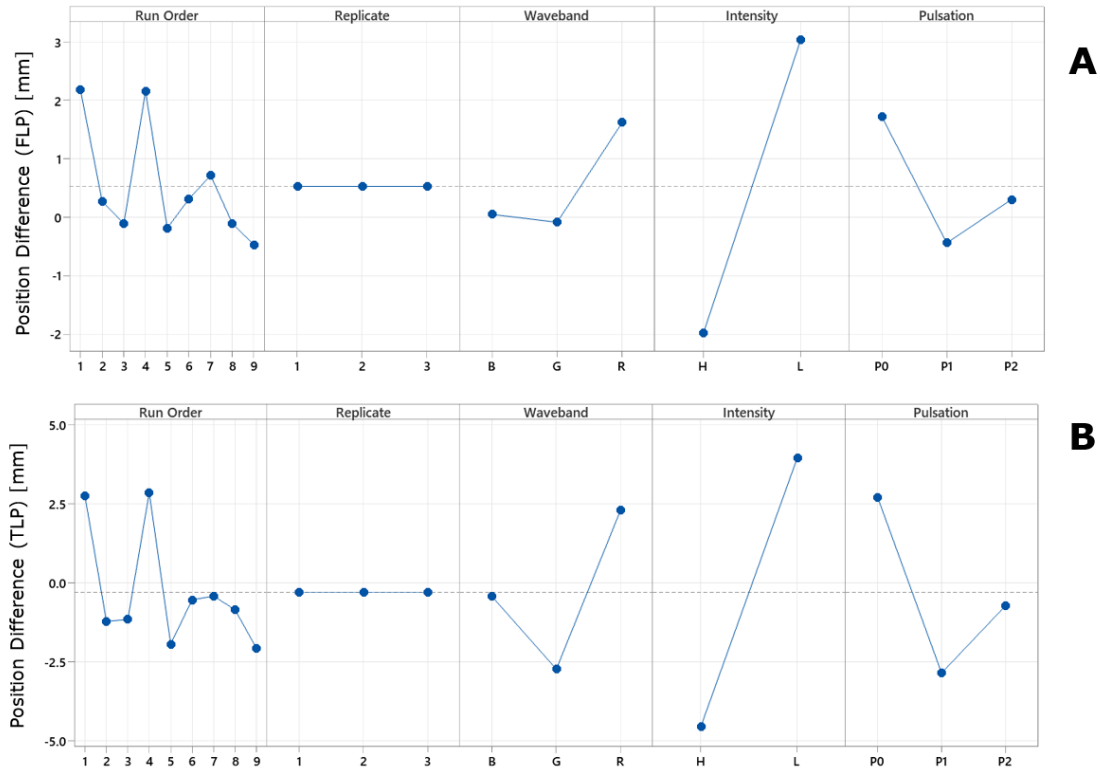

***Figure 3.12**: Main effect plots for main and random factors that are parts of the mixed effect model from A) The First Light Period (FLP) and the B) Total Light Period (TLP). Position difference [mm] (y-axis) is the average positioning either down (negative values) or up (positive values) relative to the position at the onset of light. Note the difference in the scale of the y-axis in (A) and (B).*

3.2.3 Descriptive statistics: Maximum and Average Speed

The average maximum speed in the dark condition was 19.2 mm/s (SD 9.96). The average maximum speed in light conditions was 17.6 mm/s (SD 10.1) in the FLP and 21.5 mm/s (SD 9.92) in the TLP. The maximum speed among all copepodids occurred in the dark period, measuring 55.83 mm/s. The maximum speed in the light condition occurred in light treatment R-L-P2 in replicate two during the TLP, measuring 53.33 mm/s. Maximum speed in FLP was in the same experiment for the same copepodid, measuring 44.75 mm/s (Fig.

3.13-A). Track 1 (Fig. 3.13-A) belongs to the copepodid measured to have the fastest speed (movement in Y-direction visible as Track 1 in Fig. 3.11-C).

Based on copepodid movement speeds from all light treatment groups, the average speed in dark condition and in the FLP was similar: 1.19mm/s (SD 0.54) and 1.19 mm/s (SD 0.64), respectively. The average speed in the TLP was 1.18 mm/s (SD 0.54). The highest average speed in dark condition was measured to 3.95 mm/s. In the light condition, the fastest average speed was obtained in light treatment R-L-P2 during the FLP, measuring 4.65 mm/s. The fastest average speed in TLP was 4.1 mm/s, also in light treatment R-L-P2. Several copepodids were crawling at the aquarium bottom during both dark and light conditions, influencing maximum and average speed. Track 1 (Fig. 3.13-B) is an example of this observation. The copepodid belonging to this track were crawling around at the aquarium bottom in the dark period giving slower average and maximum speeds compared to the light condition, where the copepodid moved upwards shortly after the onset of the light.

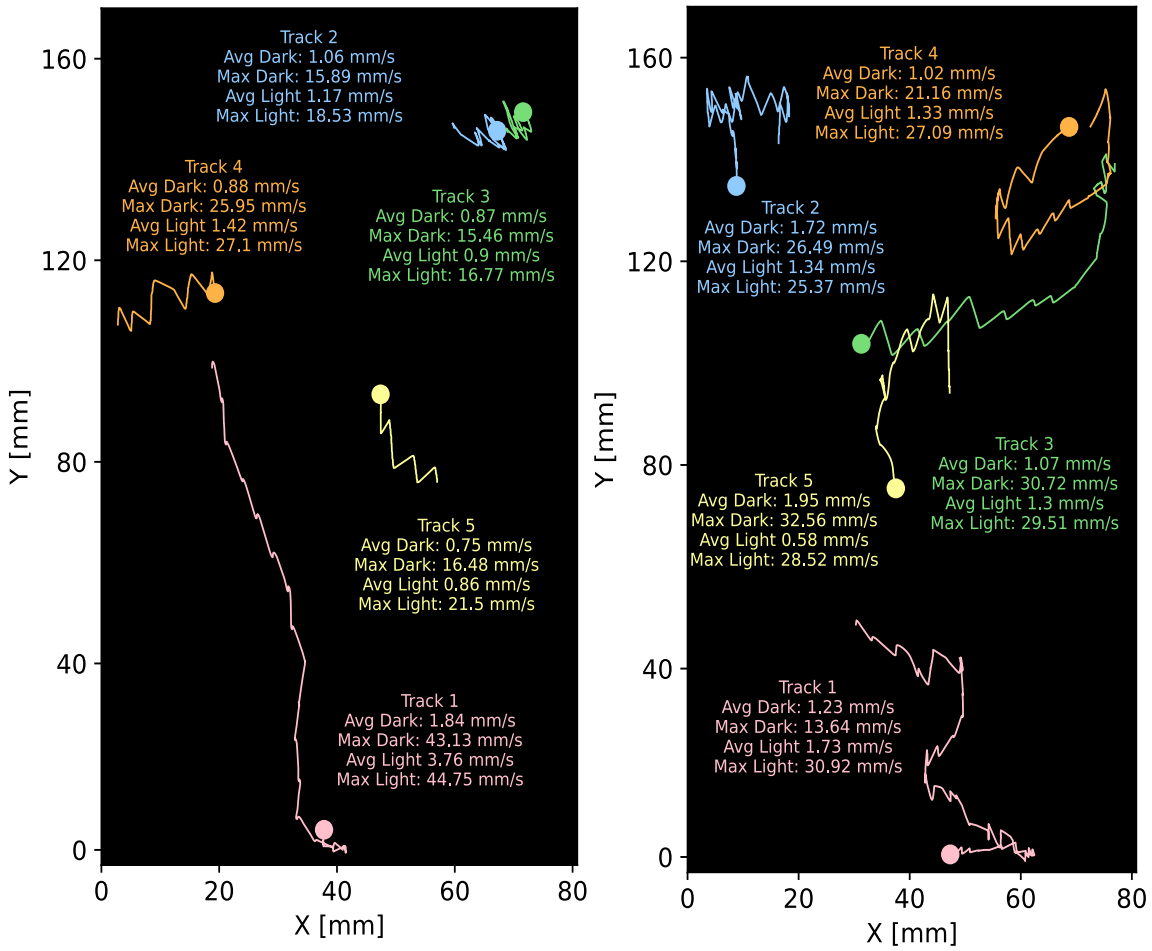

Figure 3.13: *Tracked copepodids in xy space (in the aquarium). A) Copepodid tracks from light treatment R-L-P2 in replicate 2. B) Copepodid tracks from light treatment R-L-P1 in replicate three. The y- and x-axis represent the aquarium dimensions, where the y-axis represents the aquarium height, and the x-axis represents the width. Each track is coloured to make distinguishing between the different tracks easier. Average and maximum speed in dark and light conditions are added to illustrate differences among individual tracks. Coloured circles represent the start of the tracks.*

3.2.4 Predictors of copepodid light response in terms of speed

Pulsation was a significant factor in predicting maximum speeds in the TLP (p=0.013, mixed effect model, replicate and run order as random factors, Appendix C.6). The Post Hoc analysis reveals that the difference between P2 and P1 are significant (p=0.023, Tukey's Pairwise Comparison). Pulsation level P2 gives a significantly higher speed than pulsation level P1 (Fig. 3.14). P0, constant light, was not found significantly different from the others. No other factors were significant predictors of average nor maximum speed. Neither replicate nor run order were shown to be random factors significantly influencing the results in any of the models.

The interaction effect **waveband*pulsation** was found significant in predicting average speeds in light conditions (p=0.040 (FLP) and p=0.013 (TLP), mixed effect model, replicate and run order as random factors, Appendix C.3-C.4). Pulsating blue light (P2) stood out in giving the highest average speed (Fig. 3.8). In contrast, in green and red light, the average speeds in experiments with pulsation level P2 are slower. Constant light is little affected by the different wavebands (Fig. 3.15). Pulsation level P1 gives higher average speeds in the red light, compared to the blue and green. Even though the variance analysis indicated significance, the post hoc analysis revealed no significant difference between any specific combinations of wavebands and pulsations (Tukey Pairwise Comparisons, p>0.01).

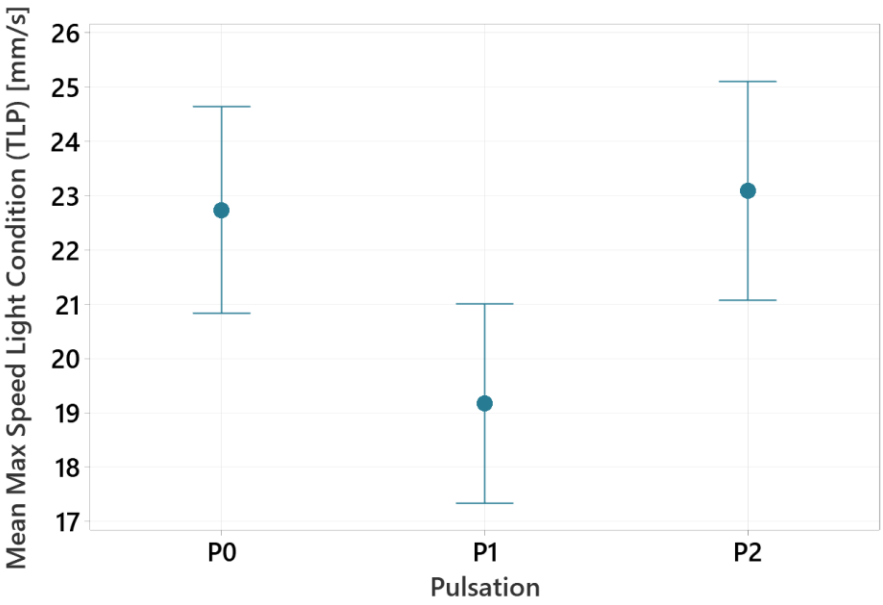

Figure 3.14: *Mean of maximum speeds obtained in light condition (TLP: Total Light Period) from experiments with different levels of pulsation. The y-axis represents speeds in mm/s, while the x-axis represents the three levels of pulsations light. Annotations; P0: Constant light; P1: 0.5 sec light, 3 sec dark; P2: 2 sec light, 3 sec dark. Each mean is calculated based on all valid tracks corresponding to each light combination. Whiskers around the mean represent the 95% confidence interval for each mean.*

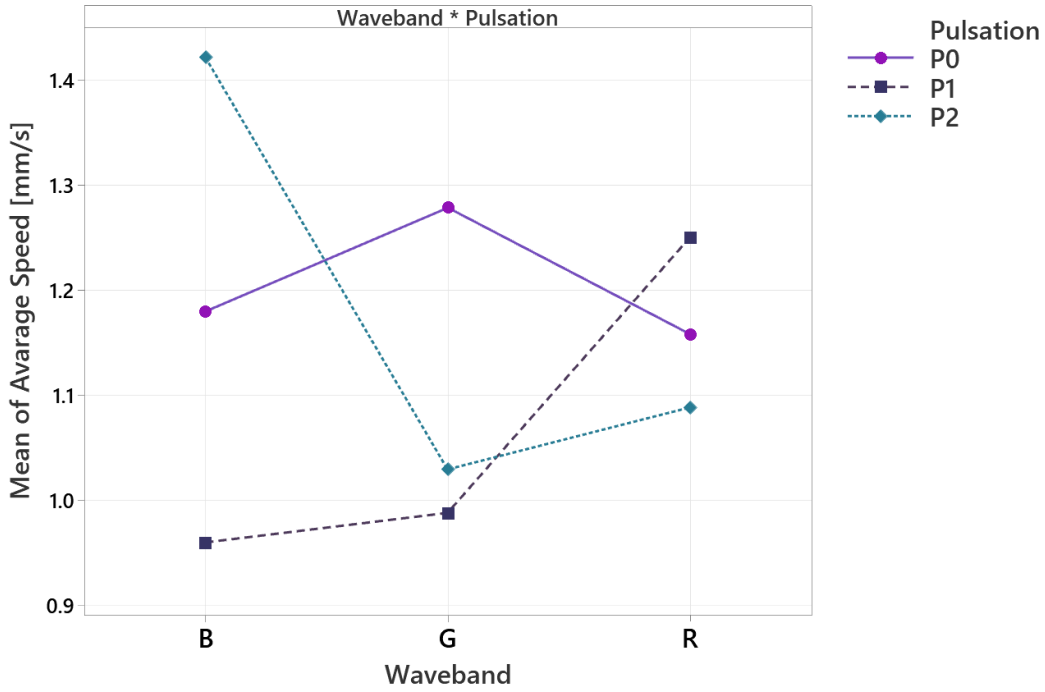

Figure 3.15: *Interaction plot for Waveband*Pulsation on the mean of average speed [mm/s] response (y-axis). The coloured lines represent each pulsation level and show the levels interactions with the levels of wavebands (x-axis).*

4 Discussion

4.1 General behaviour: Movement patterns and movement speeds

Both copepodids and nauplii of *Caligus elongatus* showed different types of movements and jump-and-sink patterns. Some of them gathered at the top of the aquarium with continuous jumps, which prevented them from sinking. Others moved around with varying sizes of jumps, ranging from small continuous jumps that moved them slowly upwards to larger, more powerful jumps. The sinking movements were also variable. Some slowly sank throughout the whole experiment. Others had longer or shorter periods of sinking, followed by small jumps, before continuing periods of decline. This applied to both copepodids and nauplii. Pike *et al.* (1993) found a gradual decrease in activity throughout the development stage of Nauplius II. The nauplius stages are often divided into Nauplius I and Nauplius II, but perceiving individuals within these stages to behave similarly should be done with caution. In fact, several morphological and behavioural internal changes occur within each stage (Pike *et al.,* 1993). Pike *et al.,* (1993), studying the development of *C. elongatus* from hatching to copepodid, decided to divide each stage into an early-, mid- and late stage. Larvae of Nauplius II were most active in the early and mid-phase, in which they were shown to exhibit positive phototaxis (Pike *et al.,* 1993). Towards the late phase, the activity decreased before converting to copepodid through moulting (Pike *et al.,* 1993). Hence, even though Nauplius II is in a specific development stage, there could also be individual differences between nauplii II based on their development within this stage. This could help explaining the observed differences in movement patterns among nauplii, possibly influenced by differences in activity levels.

Many copepodids aggregated on the bottom of the aquarium. Many of these were slowly crawling around at the bottom in both light and dark conditions, a behaviour not observed among the nauplii. In addition, a "looping" movement behaviour was observed among several of the copepodids, a movement previously observed in copepodids of *L. salmonis* as well (R. Genna, unpublished data in Bailey *et al.,* 2006). One of the developments differentiating copepodids from the previous nauplii stage is the development of swimming legs, making them faster and more mobile than the previous nauplius stages (Pike *et al.,* 1993). However, several copepodids were observed staying at the bottom, slowly jumping, or crawling around. During the experiments, several copepodids were also observed crawling alongside the walls of the aquarium. These observations illustrate that copepodids of *C. elongatus* can use these swimming legs to attach to, and walk around on, different surfaces. This aligns with the copepodid stage being the infection stage where the larvae fasten to a host (Piasecki, 1996). Another explanation for the observed differences in movement pattern of the copepodids could be exhaustion, making them passively sink to the bottom. However, looking at copepodids of *Lepeophtheirus salmonis,* which have been reported to be able to move with an average speed of 5.5 mm/s for 30 meters without habituating (a total of 90 minutes) (Fields *et al.,* 2018), this hypothesis needs stronger support. Furthermore, the fact that the experiments were conducted in controlled experimental can have influenced the results, making them different for what would been observed in nature. In nature, water masses are large, influenced by currents. The limited amount of space and the absence of drift in the water in the experimental setup can induce abnormal behaviour, explaining why both copepodids and nauplii exhibited different activity levels and absence of positive phototactic response among several of the larvae.

The maximum speed among all nauplii (67.82 mm/s) was found to be larger than the maximum speed among all copepodids (55.83 mm/s). However, the average maximum

speed was highest among copepodids than nauplii. Generally, more nauplii were visible in the aquarium, giving valid tracks (n=377), as they constantly moved around in the water column, with less crawling on the aquarium bottom as more common among the copepodids (n=308). Instead, nauplii reaching the aquarium bottom exhibited powerful jumps at high speeds. In fact, the highest speeds were found in nauplii jumping off the bottom of the aquarium. Compared to the copepodids, nauplii have not developed swimming legs (Pike *et al.,* 1993). Instead, they have appendages, allowing them to move by broad sweeping movement, making them rapid swimmers (Pike *et al.,* 1993). This, in combination with the fact that many of the copepodids were crawling around, many of which were less active than several of the nauplii, could explain why the highest maximum speed was observed among nauplii. In addition, the powerful jumps observed among nauplii directly when they hit the aquarium bottom, can indicate some sort of avoidance behaviour to surfaces. The larvae do not attach to host fish before reaching the copepodid stage (Piasecki, 1996). Instead of being adapted to host finding success, the larvae of nauplius II could benefit from maximum survival and dispersal in the water column. As avoidance behaviour to surfaces keeps the nauplii in the water column, this could help explain this observation. Nauplii of *C. elongatus* has been documented sitting on the mucus layer of salmon and being found in the upper layer of the water column close to cage sites (Hogans & Trudeau, 1989b). As poor swimmers, nauplii can rapidly be driven away from cage sites by currents, hence losing the proximity to the host fish. Hogans & Trudeau (1985b) hypothesised that this could be an adaptation keeping the nauplii closer to the host fish before moulting into the infectious stage as the copepodid. The avoidance behaviour of surfaces observed here does not align with this. Of course, this can be explained by the fact that the aquarium bottom does not resemble the mucus of fish, possibly exhibiting wrong tactile cues.

The maximum speed among copepodids was found to be 55.83 mm/s (in dark condition). In contrast with the possible predator avoidance in the nauplius II stage, the copepodid is in the infective stage, adapted to attach itself to host fish (Piasecki, 1996). With the maximum speed reported above, a copepodid would have to be 25-30 mm within a fish of 50 centimetres swimming at a speed of two times its body length to reach its body surface. Hogans and Trudeau (1989b) found that copepodids of *C. elongatus* within 10 centimetres of the host fish (*Salmo salar*) directly swam to the fish independent of light stimuli and the direction of the light. When further away than 10 cm, phototactic behaviour reoccurred (Hogans & Trudeau, 1989b). To reach a fast-moving fish from 10 cm, the maximum speed of 55.83 mm/s found in this thesis, is not enough for the copepodid to reach the host. This indicates adaptation not only to fish actively swimming at high speeds, but also to more stationary fish, assuring that the *copepodids* have enough time to reach host fish from longer distances using chemical cues. This aligns with fact that *C. elongatus* has been found to infect over 80 different fish species (Kabata, 1979) ranging from faster moving pelagic fish (e.g., *S. salar*) to more stationary fish as plaice (e.g., *Pleuronectes platessa* and *Limanda limanda)* and Gobiidae (Øines et al., 2006; Heuch et al., 2007).

4.2 Responses to light

4.2.1 Vertical positioning in dark and light condition

No significant difference in mean vertical positioning of copepodids between dark and light condition was found in any of the light treatments. No differences between light and dark

means exceeded 12 mm. This observation does not support previous studies reporting *C. elongatus* as positively phototactic (Hogans & Trudeau, 1989b; MacKinnon, 1993). In fact, their positioning in dark and light conditions are nearly identical. Szetey *et al.* (2021) obtained somewhat the same results for copepodids of *L. salmonis.* They found the copepodids to swim against the surface independent of the onset of light, suggesting aggregations of copepodids on the water surface at both day and night (Szetey *et al.,* 2021). Among the possible explanations for this, they hypothesise that the evolution of the copepodids of *L. salmonis*, in line with the highly increased aquaculture industry, might have changed how they respond to light since the Diel Vertical Migration patterns of *L. salmonis* were tested in the 90s (Szetey *et al.,* 2021). As the findings of Hogans and Trudeau (1989b) and MacKinnon (1993) regarding positive phototaxis of *C. elongatus* is of similar age, going nearly 30 years back in time, the findings in this thesis reveal that more research of is needed before concluding on the phototaxis of copepodids of *C. elongatus*.

Significant difference in mean vertical positioning between dark and light condition was found in nauplii in light treatment G-H-P0, B-H-P0, B-H-P2, and B-L-P2. All these light treatments led to a position further away from the light source, compared to their position in dark condition. Thus, no light treatments led to a positive phototactic response, but some led to negative phototactic response. This result differs from those by Hogans & Trudeau (1985b), who observed nauplii of *C. elongatus* to be positively phototactic, although with a less developed phototaxis ability than the copepodid. Given that copepodids are adapted to locate host fish, whereas it could be advantageous for nauplii to avoid predators, it would not be unexpected for nauplii to exhibit a negative phototactic response and, consequently, an opposite movement pattern. Generally, however, no phototaxis were observed when comparing the dark and light conditions among either nauplii or copepodids. The differences in activity level within each developmental stage of *C. elongatus* (Pike *et al.,* 1993), as detailed in the above section, can have influenced the larvae's response to light, and help explain this observation. Szetey *et al.* (2021) proposed the same explanation for the nauplii of S. salmonis they found to aggregation closer to the bottom, in line with the fact that lice are unable to swim during moulting.

Another explanation for the different results between this and previous studies on the phototaxis of *C. elongatus* (Hogans & Trudeau, 1989b; MacKinnon, 1993) can be genetic differences, which were also proposed by Szetey *et al.* (2021) as being the reason for the lack of phototactic response among copepodids of *L. salmonis*. Øines and Heuch (2005) used molecular methods (examination of fragments of mitochondrial COI) on parasitic copepods sampled from wild fish south in Norway (Arendal). They found two genotypes of *C. elongatus*, in which they argue that these genotypes "could very well be genetic evidence of sibling species of *C. elongatus*." Furthermore, they argue that this could explain the wide variety of hosts that *C. elongatus* parasitises (Kabata, 1979), as it might be two or more species. Difference between hosts might also influence their responses to light. Suppose the *C. elongatus* studied by Hogans and Trudeau (1989b) and Mackinnon (1993), both in Canada, was of another genotype than those used in this thesis. In that case, this might also be reflected in the observed differences in phototaxis. The larvae in this thesis were from 2. and 3. generation from Sørøya, Finnmark. All the collected lice from Sørøya in a study by Øines and Heuch (2007) were of genotype 1, in which they also saw distinct variations in the seasonal abundance of the two genotypes. This might suggest the occurrence of other environmental differences as well, such as behavioural responses to light. In March – June, there were considerably more genotype 1 lice than genotype 2 lice (Øines and Heuch, 2007). Following was an increase in genotype 2 from June to September-October and a decrease for genotype 1. Øines and Heuch (2007) proposed that

the observed large abundance of genotype 1 louse on lumpfish, which in March-April spawns in the kelp forest in the littoral zone, is an explanation for this observed seasonal patterns. Genotype 1 louse was also seen on other coastal fish species (Øines and Heuch, 2007). Heuch *et al.* (2007) found spawning lumpfish to be the most infected among the 4427 coastal fish investigated, with a prevalence of 61%. Lumpfish spawns at rocky bottom and in the kelp forest (Daborn & Gregory, 1983 in Heuch *et al.*, 2007), and Heuch *et al.* (2007) gillnetted them from 5 to 20 meters depth in March-April. Much red light is available in addition to green and blue light in the littoral sone and at the water at such low depths. If genotype 1 louse were to prefer and better adapted to parasitise lumpfish, it would benefit the host-attaching copepodids to stay in shallower areas. Based on this, two explanatory models could explain the observation of no positive phototaxis in this thesis: 1) The irradiance levels used stimulate such a coastal environment in which the larvae are within their preferred range of light, and 2) The irradiance levels where too low to stimulate such an environment, giving no positive phototactic response. Szetey *et al.* (2021) used 0.5 and 80 µmol photons $m^{-2}s^{-1}$ to represent dawn/tusk and daylight, respectively. The maximum E_{PAR} of 1.8×10^{-1} µmol photons $m^{-2}s^{-1}$ (high-intensity green light) used in this thesis, are lower than the E_{PAR} Szetey *et al.* (2021) used as lowest intensity. To better reflect the irradiance levels at shallower depths, the experiments conducted here could benefit from the usage of higher irradiance levels. In addition, the differences in shifts between the apparent distinct wavelengths during dawn and dusk might be significant for the phototaxis of copepods (Forward, 1988). Specific light conditions are only present during these periods, possibly being the point of the vertical migration (Forward, 1988). Such light conditions include not only the light of one specific colour but several parts of the spectrum with distinct intensities (Forward, 1988). Further experiments could benefit from having several colours simultaneously in addition to white light to better try to stimulate the distinct light conditions at twilight. In further studies, white light, including a mix of several colours, could be used to possibly better stimulate a coastal environment better.

The influence of other environmental factors, such as temperature, should also be considered. The water in the aquarium was maintained at 12 °C, a temperature that could favour moulting as it is closer to their reported optimum temperature of 14 °C (Hogans and Trudeau, 1989b). The larvae were transported from the hatchery to the laboratory to control the development stage, and this likely led to an increase in the water temperature in the weighing boat from 10 degrees in the hatchery water. Such a temperature increase could have induced temperature-based behavioural responses, potentially favouring those from light stimuli. This selection within different environmental cues, outperforming the effect of light stimuli, has been documented in larvae of *C. elongatus*, where copepodids within 10 cm of a host fish were observed swimming directly to the fish regardless of light coming from other directions (Hogans and Trudeau, 1989b). This highlights the need for future studies to include temperature as a fixed factor to control the effect of different environmental factors on phototactic behaviour.

One reason for not observing a phototactic response could be the aggregation of both nauplii and copepodites in the top part of the water column. The temperature of the aquarium water might have been an influencing factor in contributing to this. Revie et al. (2002) found a highly seasonal pattern in the infection rates of *C. elongatus* on farmed salmon in Scotland. Higher infection rates were found during summer (Revie *et al.,* 2002). Studying four farms in Scotland, McKenzie et al. (2004) found rapidly increasing numbers of *C. elongatus* from week 22, followed by a decline from week 40, again showing higher

abundance in summer months. Wootten et al. (1982) found a high abundance of *C. elongatus* in chalimus stages on farmed fish during October and early November. However, no following increase in C. elongatus in the adult stage was observed. This aligns with the observations of free-living chalimus stages of Caligidae species in plankton samples adjacent to aquaculture facilities (Maran et al., 2016). An explanation can be that chalimus and adult stages of C. elongatus choose host fishes due to different environmental factors, not only because of light conditions but of temperature as well. A higher abundance of louse on farmed fish during summer suggests aggregations of larvae in the upper part of the water column during higher temperatures. The aggregation of both nauplii and copepodites in the upper part of the water column during the experiment in both dark and light conditions might be because of the temperature of the water more than the onset of light.

The sinking response observed in many light treatments might also be due to temperature. Considering the possibility of the larva used being of genotype 1 and following Øines and Heuch (2007), which found no genotype 2 lice in northern areas but predominantly in areas influenced by the Norwegian coastal current, this might indicate adaptations to lower temperatures in genotype 1 lice. Because *C. elongatus* of genotype 1 was abundant in shallow areas from March to April (Heuch *et al.,* 2007), the surface water temperatures are not as high as the water used in the experiments in this thesis (around 12 ℃). Their abundance in northern areas with lower temperatures might explain the absence of phototactic behaviour observed in this thesis. Temperatures deeper in the water column are generally colder. Hence, the observed sinking behaviour might reflect their behaviour in higher temperatures more than their response to light. Again, this highlights the need for further investigation to understand better the interplay between different environmental factors in the phototactic behaviour of both nauplii and copepodids of *C. elongatus*.

It is essential to mention that the phototactic behaviour of a species observed in laboratory experiments does not comprehensively explain its migration pattern. Although positive phototactic responses have been observed in several studies regarding different species of copepods, such as *C. elongatus (*(Hogans & Trudeau, 1989b; MacKinnon, 1993) and *L. salmonis (*Wootten et al., 1982; Bron et al., 1993), such observations have not been observed *in situ (*Irish Department of The Marine, 1992, 1994 in Heutch et al., 1995*). Hetuch et al. (1995, p. 685) state that* "Forward (1988) suggested that the use of direct light produces artifactual information about phototactic behaviour in many zooplankton species." The experiments in this thesis were conducted in a laboratory, different from their natural habitat. Consideration of several factors is necessary to explain the migration pattern of a species. Hence, stimulating a natural migration environment in vitro is challenging, especially in small-scale laboratory experiments (Ringelberg, 1999). Several other factors are contributing to the directional movement in species, including pheromones released into the environment from fish (Bailey *et al.,* 2006; Ringelberg, 1999). A laboratory experiment cannot consider all potential parameters affecting light response (MacKinnon, 1993). For example, turbidity, the concentration of dissolved matter in the water, can affect the movement (Lampert, 1989). At the same time, noise is a significant factor affecting organisms' sensory systems regarding underwater vision and response to light (Lythgoe, 1988). Such noise can be light scattering, often caused by the water itself or other objects in the water. In this study, the aquarium surfaces are examples of material that could influence the results though light scattering. It should also be remembered that the experiments conducted in this thesis are done in a vertical setup. Gravity is a factor that can influence the movement pattern of copepodid larvae

(MacKinnon, 1993). MacKinnon (1993) adopted a horisontal experimental setup to minimise this influence. Possible, the negative buoyance of the larvae in addition to the gravity, might have influenced the results.

Furthermore, the arrangement of larvae might have influenced the results in cases when larvae cannot move anymore towards the light because they are already gathering in the top of the aquarium. Hence, a limitation of the method is the height of the aquarium, and that larvae that are already at the top of the aquarium cannot move any closer to the light. In addition, the fact that the climate room containing the hatchery had a light-dark cycle of 24:0 h could have led to abnormal behaviours of the larvae that were used, indicating the need for longer acclimation time than the 15 minutes given.

4.2.2 Reponses to different light treatments in terms of vertical positioning

When comparing different light treatments, the difference in mean vertical position between nauplii in high-intensity light vs. low-intensity light was highly significant. In high-intensity light, especially in the blue and green part of the spectrum, nauplii were positioned further away from the light source than in low-intensity light. The significant difference in positioning between high and low-intensity light suggests either no response to light (hence passively sinking as they are negatively buoyant), or an avoidance behaviour induced due to the high intensity of light. These observations align with the results of Szetey *et al.* (2021), who found nauplii of *L. salmonis* to respond strongly and ascend more rapidly to increasing light intensities. They did not find the copepodids to do the same and proposed the observed difference to light as life stage dependent. However, the results of this thesis showed that also the copepodids of *C. elongatus* responded by a significant decrease in vertical positioning in response to higher light intensity. Hence, this proposed explanation did not hold for *C. elongatus* in terms of different response to increased light intensity, although nauplii responded to high-intensity light by moving further away from the light source compared to the copepodids. Again, it should be noted that Szetey *et al.* (2021) used higher irradiance levels than in this thesis. In further studies, more levels of light intensities could be used to compare light intensities over smaller intervals.

The observed significant difference between low-and high-intensity light among both nauplii and copepodids is potentially explained in relation to temperature. Especially in high-light intensities, it would be beneficial for the larvae not to be too close to the surface to avoid potentially harmful radiation. For instance, larvae of *L. salmonis* are found in coastal waters where UV light is apparent (Heuch et al., 1995; Aarseth and Schram, 1999). Hylander et al. (2009) found the vertical migration of copepods weak in UV stress. Aarseth and Schram (1999) found copepods (*Calanus finmarchicus and L. salmonis)* to exhibit avoidance behaviour to UV light, suggesting they can distinguish between white light and UV light. However, no UV light was apparent in the experiments conducted in this thesis. Nevertheless, if the irradiance from the high-intensity light resembles an area with potentially harmful UV radiation, it could explain the observed difference in vertical positioning in the light condition. The high-intensity light in combination with the temperature might have stimulated warm surface water during daytime where UV light is apparent. Many organisms exhibit positive phototaxis to a given threshold of intensity before descending (negative phototaxis) when the light intensity becomes too high (Jékely, 2009) The combination of warmer water simulating a surface environment and the high-intensity light might have caused an interaction effect. Furthermore, among nauplii, the waveband was a significant predictor for vertical positioning, where positioning in green and red light, closest to the light, was significantly different from blue light, leading to

positioning further away. This might suggest avoidance behaviour to smaller wavelengths closer to the wavelengths of UV light. However, this becomes speculative as no interaction effect was observed for intensity*waveband.

Pulsation was a significant predictor for the average position of nauplii in the FLP, but not in the TLP. In the FLP, pulsation P2 led to a vertical position further away from the light source than P1. Many crustaceans have been suggested to being adapted to avoid shadows as a part of their predator avoidance (Forward, 1986). Pulsation might resemble shadows from predators swimming by. Forward (1986) found zoeae of the crab *Rhithropanopeus harrisii* to exhibit negative phototaxis in response to pulsating light. In the case where pulsations level P2 resemble such a shadow effect more than P1, this can explain the observed avoidance behaviour in P2 light.

Intensity*Pulsation was a significant factor interaction explaining nauplii light response. Here, constant high intensity light resulted in positions further away from the light source than constant low intensity light. Forward (1977) found species of Brachyura in the zoeae stage to normally exhibit positive phototaxis at high intensities, and *vice versa* in low intensity light. However, when sudden light intensity increased were induced, the same organisms exhibited sinking responses and become negative phototactic. The onset of constant light from dark condition to high-intensity in this thesis, might have stimulated such a shadow effect, helping in the explanation of the lowered vertical position among nauplii in constant high-intensity light. This aligns with the results of Flamarique et al (2000), which proposed that the naupliar visual system in nauplii of *L. salmonis* are well adapted to detection of shadows under a bright light field.

4.2.3 Reponses to different light treatments in terms of speed

For copepodids, pulsation was a significant predictor in determining maximum speed in light conditions. Here, pulsation level P2 gave a significantly higher maximum speed than P1. The longer blinking frequence in the P2 light might, in a better way than the P1 light, resemble schools of fish swimming by, hence inducing higher maximum speeds to get a higher possibility to get close to a host. The higher the maximum speeds, the more water can be covered and the higher the possibility of getting closer to a host fish. Flamarique *et al.* (2000) proposed the same argument for L. salmonis, observing actively swimming copepodids in response to flashes of light. In the case where pulsation P2 resembles schools of fish swimming, this might explain the significantly higher maximum speeds compared to P1, where the pulsation (0.5 sec on, 3 sec off) might be too slow to resemble potential hosts swimming by. The significant interaction effect of Waveband*Pulsation indicates an possible adaptation to schools of fish swimming at specific depths with different amounts of irradiance obtained from different wavelengths. However, as the post hoc analysis did not point to some specific combinations, this needs to be investigated further.

The intensity was the only significant predictor of nauplii speed and was so for both average speed (in the FLP) and maximum speed (in both FLP and TLP). High-intensity light led to significantly slower speeds. This aligns with the significant difference between high and low intensity in terms of vertical positioning, as detailed below. With high-intensity light giving positioning further from the above light source than low-intensity light, this indicates a sinking behaviour, also reflected by this significant difference in nauplii speed.

5 Conclusion

The primary goal of this thesis was to investigate behavioural responses to light stimuli in nauplii and copepodids of *Caligus elongatus* in controlled laboratory conditions, aiming to investigate differences in vertical positioning and the average and maximum speed in response to light.

Both copepodids and nauplii of *C. elongatus* showed diverse activity levels, vertical positioning, and jump-and-sink patterns. Some individuals exhibited what seemed to be positive phototactic behaviour through a rapid increase in the aquarium right after the onset of light. However, at the group level, no positive phototactic behavioural responses in either nauplii or copepodites in any of the light treatments were found to be significant. Hence, the results in this thesis do not support previous studies reporting that larvae of *C. elongatus* exhibit positive phototaxis. Instead, many copepodids aggregated on the bottom of the aquarium or the water surface during both dark and light periods. Proposed explanations for this are the influence of temperature, genetic variations, low irradiance levels, and the difficulties in stimulating a natural environment in laboratory conditions. In addition, the difference in activity levels observed within the same development stages could have influenced the results.

High-intensity light led to a descent in the water column compared to low-intensity light for both development stages. The proposed explanation was avoidance behaviour to avoid predation (for nauplii) and potentially harmful radiation. Again, temperature could have influenced the vertical positioning in cases where there is an interaction effect between different light treatments and the temperature. In addition, pulsation and the interaction effect of intensity*pulsation were found to be significant predictors on nauplii vertical positioning, in which pulsation level P2 led to positioning further away from the light source. The same was observed for pulsation level P0 (constant) in high-intensity light. The proposed explanation for both observations is that the pulsation and the immediate onset of high-intensity constant light, imitated shadows from potential predators and induces avoidance behaviour among nauplii.

The maximum speed among all nauplii (67.82 mm/s) was higher than the maximum speed among all copepodids (55.83 mm/s). However, the average maximum speed was higher among copepodids than nauplii. High-intensity light caused significantly slower average and maximum speed. This aligns with the fact that high-intensity light gave positioning further down in the water column, having sinking larvae. For copepodids, pulsation was a significant predictor in determining maximum speed in light conditions. Pulsation level P2 led to a significantly higher maximum speed compared to P1. The proposed explanation for this is that P2 resembles schools of fish swimming by explaining the higher speed as a part of the host-finding mechanism.

The above findings suggest that more research is needed on the phototaxis of larvae of *C. elongatus*. The results highlight the need for further research to fully understand the implications of light stimuli on the behaviour of nauplii and copepodids of *C. elongatus*. In further research, experiments with higher levels of irradiance could be used to better stimulate the ocean environment at shallower depths. Temperature should be considered as a potential influencing factor.

References

Bailey, R. J. E., Birkett, M. A., Ingvarsdóttir, A., Mordue, A. J., Mordue, W., O'Shea, B., . . . Wadhams, L. J. (2006). The role of semiochemicals in host location and non-host avoidance by salmon louse (Lepeophtheirus salmonis) copepodids. *Canadian journal of fisheries and aquatic sciences, 63*(2), 448-456. doi:10.1139/f05-231

Bandara, K., Varpe, Ø., Wijewardene, L., Tverberg, V., & Eiane, K. (2021). Two hundred years of zooplankton vertical migration research. *Biol Rev Camb Philos Soc, 96*(4), 1547-1589. doi:10.1111/brv.12715

Barrett, L. T., Oppedal, F., Robinson, N., & Dempster, T. (2020). Prevention not cure: a review of methods to avoid sea lice infestations in salmon aquaculture. *Reviews in aquaculture, 12*(4), 2527-2543. doi:10.1111/raq.12456

Baylor, E. R. (1959). Infra-Red Observation and Cinematography of Microcrustacea. *Limnology and oceanography, 4*(4), 498-499. doi:10.4319/lo.1959.4.4.0498

Berge, J., Cottier, F., Last, K. S., Varpe, Ø., Leu, E., Søreide, J., . . . Nygård, H. (2009). Diel vertical migration of Arctic zooplankton during the polar night. *Biology letters, 5*(1), 69-72.

Bhardwaj, A., Kishore, S., & Pandey, D. K. (2022). Artificial Intelligence in Biological Sciences. *Life (Basel), 12*(9). doi:10.3390/life12091430

Bjørn, P. A., & Finstad, B. (1998). The development of salmon lice (Lepeophtheirus salmonis) on artificially infected post smolts of sea trout (Salmo trutta). *Canadian journal of zoology, 76*(5), 970-977. doi:10.1139/cjz-76-5-970

Bjørnstad, L. F., & Solstad, M. A. (2019). *Undersøkelse av lysrespons og svømmeadferd hos lakselus (Lepeophtheirus salmonis) ved hjelp av deteksjon og sporing.* (Masters thesis). NTNU, Trondheim, Norway.

Boxaspen, K. (2006). A review of the biology and genetics of sea lice. *ICES journal of marine science, 63*(7), 1304-1316. doi:10.1016/j.icesjms.2006.04.017

Bradski, G. (2000). *The Opencv Library* (Vol. 25).

Brandal, P., Egidins, E., & Romslo, I. (1976). *Host blood: a major food component for the parasitic copepod Lepeophtheirus salmonis Kroyeri, 1838 (Crustacea: Caligidae)*.

Bron, J. E., Frisch, D., Goetze, E., Johnson, S. C., Lee, C. E., & Wyngaard, G. A. (2011). Observing copepods through a genomic lens. *Frontiers in zoology, 8*(1), 1-15.

Bron, J. E., Sommerville, C., & Rae, G. H. (1993). *Aspects of the behaviour of copepodid larvae of the salmon louse Lepeophtheirus salmonis (Kroyer, 1837)*. Chichester (United Kingdom): Chichester (United Kingdom): Ellis Horwood Limited.

Båtnes, A. S., Miljeteig, C., Berge, J., Greenacre, M., & Johnsen, G. (2015). Quantifying the light sensitivity of Calanus spp. during the polar night: potential for orchestrated migrations conducted by ambient light from the sun, moon, or aurora borealis? *Polar biology, 38*(1), 51-65. doi:10.1007/s00300-013-1415-4

Clarke, G. L. (1971). *Light conditions in the sea in relation to the diurnal vertical migrations of animal.* Paper presented at the Proceedings of the International symposium on biological sound scattering in the ocean. Washington, DC: Maury Center Ocean Science.

Cohen, J. H., & Forward Jr, R. B. (2002). Spectral sensitivity of vertically migrating marine copepods. *The Biological Bulletin, 203*(3), 307-314.

Costello, M. J. (1993). *Review of methods to control sea lice (Caligidae: Crustacea) infestations on salmon (Salmo salar) farms*. Chichester (United Kingdom): Chichester (United Kingdom): Ellis Horwood Limited.

Costello, M. J. (2006). Ecology of sea lice parasitic on farmed and wild fish. *Trends Parasitol, 22*(10), 475-483. doi:10.1016/j.pt.2006.08.006

Cottier, F. R., Tarling, G. A., Wold, A., & Falk-Petersen, S. (2006). Unsynchronised and synchronised vertical migration of zooplankton in a high Arctic fjord. *Limnology and oceanography, 51*(6), 2586-2599. doi:10.4319/lo.2006.51.6.2586

Cronin, T. W. (1986). Optical design and evolutionary adaptation in crustacean compound eyes. *Journal of Crustacean Biology, 6*(1), 1-23.

Cronin, T. W., & Jinks, R. N. (2001). Ontogeny of Vision in Marine Crustaceans. *Integr. Comp. Biol, 41*(5), 1098-1107. doi:10.1093/icb/41.5.1098
Culjak, I., Abram, D., Pribanic, T., Džapo, H., & Cifrek, M. (2012). *A brief introduction to OpenCV*.
Detry, M. A., & Ma, Y. (2016). Analyzing Repeated Measurements Using Mixed Models. *Jama, 315*(4), 407-408. doi:10.1001/jama.2015.19394
Elofsson, R. (2006). The frontal eyes of crustaceans. *Arthropod Structure & Development, 35*(4), 275-291. doi:https://doi.org/10.1016/j.asd.2006.08.004
Fields, D. M., Skiftesvik, A. B., & Browman, H. I. (2018). Behavioural responses of infective-stage copepodids of the salmon louse (Lepeophtheirus salmonis, Copepoda:Caligidae) to host-related sensory cues. *J Fish Dis, 41*(6), 875-884. doi:10.1111/jfd.12690
Flamarique, I. N., Browman, H. I., Bélanger, M., & Boxaspen, K. (2000). Ontogenetic Changes in Visual Sensitivity of The Parasitic Salmon Louse Lepeophtheirus Salmonis. *Journal of Experimental Biology, 203*(11), 1659-1669. doi:10.1242/jeb.203.11.1649
Forward, R. (1988). Diel vertical migration: zooplankton photobiology and behaviour. *Oceanogr. Mar. Biol. Annu. Rev, 26*(36), 1-393.
Forward, R. B. (1976). Light and Diurnal Vertical Migration: Photobehavior and Photophysiology of Plankton. (pp. 157-209). Boston, MA: Boston, MA: Springer US.
Forward, R. B. (1977). Occurrence of a shadow response among brachyuran larvae. *Marine Biology, 39*(4), 331-341. doi:10.1007/BF00391936
Frangoulis, C., Christou, E., & Hecq, J. H. (2005). Comparison of Marine Copepod Outfluxes: Nature, Rate, Fate and Role in the Carbon and Nitrogen Cycles. *Advances in marine biology, 47*, 253-309. doi:10.1016/S0065-2881(04)47004-7
Furberg, M. H. (2022). *Sammenlikning av mekanisk og termisk avlusning: Klekkesuksess og larveutvikling fra eggstrenger med vurdering av smittepotensial hos lakselus (Lepeophtheirus salmonis).* (Masters thesis). NTNU, Trondheim, Norway.
Gravil, H. R. (1996). *Studies on the biology and ecology of the free swimming larval stages of Lepeophtheirus Salmonis (Kroyer, 1838) and Caligus Elongatus Nordmann, 1832 (Copepoda: Caligidae).* (PHD-Thesis). University of Stirling, Retrieved from http://hdl.handle.net/1893/2380
Grefsrud , E. S., Andersen , L. B., Grøsvik , Karlsen , L. B. Ø., Kvamme Bjørn Olav, Hansen , P. K., . . . Solberg, M. F. (2023). *Risikorapport norsk fiskeoppdrett 2023 — Produksjonsdødelighet hos oppdrettsfisk og miljøeffekter av norsk fiskeoppdrett*. Retrieved from
Hartnoll, R. G. (2001). Growth in Crustacea - Twenty years on. *Hydrobiologia, 449*(1-3), 111-122. doi:10.1023/A:1017597104367
Hassoun, S., Jefferson, F., Shi, X., Stucky, B., Wang, J., & Rosa, E. (2021). Artificial Intelligence for Biology. *Integrative and Comparative Biology, 61*. doi:10.1093/icb/icab188
Hays, G., Proctor, C., John, A., & Warner, A. (1994). Interspecific differences in the diel vertical migration of marine copepods: the implications of size, color, and morphology. *Limnology and oceanography, 39*(7), 1621-1629.
Hays, G. C. (2003). A review of the adaptive significance and ecosystem consequences of zooplankton diel vertical migrations. *Hydrobiologia, 503*(1-3), 163-170. doi:10.1023/B:HYDR.0000008476.23617.b0
Hayward, C. J., Aiken, H. M., & Nowak, B. F. (2008). An epizootic of Caligus chiastos on farmed southern bluefin tuna Thunnus maccoyii off South Australia. *Dis Aquat Organ, 79*(1), 57-63. doi:10.3354/dao01890
Hemmingsen, W., MacKenzie, K., Sagerup, K., Remen, M., Bloch-Hansen, K., & Dagbjartarson Imsland, A. K. (2020). Caligus elongatus and other sea lice of the genus Caligus as parasites of farmed salmonids: A review. *Aquaculture, 522*, 735160. doi:10.1016/j.aquaculture.2020.735160
Heuch, P. A., Parsons, A., & Boxaspen, K. (1995). Diel vertical migration: A possible host-finding mechanism in salmon louse (Lepeophtheirus salmonis) copepodids?

Canadian journal of fisheries and aquatic sciences, 52(4), 681-689. doi:10.1139/f95-069
Heuch, P. A., & Schram, T. A. (1999). Crustacea (krepsdyr). In T. Poppe, Ø. Bergh, & D. Keeping (Eds.), *Fiskehelse og fiskesykdommer* (pp. 219-228). Oslo: Universitetsforl.

Heuch, P. A., Øines, Ø., Knutsen, J. A., & Schram, T. A. (2007). Infection of wild fishes by the parasitic copepod Caligus elongatus on the south east coast of Norway. *Diseases of aquatic organisms, 77*(2), 149-158.
Hogans, W., & Trudeau, D. J. (1989a). Caligus elongatus (Copepoda: Caligoida) from Atlantic salmon (Salmo salar) cultured in marine waters of the Lower Bay of Fundy. *Canadian journal of zoology, 67*(4), 1080-1082.
Hogans, W., & Trudeau, D. J. (1989b). Preliminary Studies on the Biology of Sea Lice, Caligus elongatus, Caligus curtus and Lepeophtheirus salmonis (Copepoda:Caligoida) Parasitic on Cage-Cultured Salmonids in the Lower Bay of Fundy. *Canadian Technical Report of Fisheries and Aquatic Sciences, 1715*.
Honsberg, C. B., & Bowden, S. G. (2019). Photovoltaics Education Website (Chapter 2: Properties of Sunlight) Retrieved from www.pveducation.org

Humes, A. G. (1994). How many copepods? *Hydrobiologia, 292-293*(1), 1-7. doi:10.1007/BF00229916

Hylander, S., Larsson, N., & Hansson, L.-A. (2009). Zooplankton vertical migration and plasticity of pigmentation arising from simultaneous UV and predation threats. *Limnology and oceanography, 54*(2), 483-491. doi:https://doi.org/10.4319/lo.2009.54.2.0483
Iversen, A., Hermansen, Ø., Nystøyl, R., & Hess, E. J. (2017). *Kostnadsutvikling i lakseoppdrett – med fokus på fôr- og lusekostnader*. Retrieved from https://nofima.brage.unit.no/nofima-xmlui/handle/11250/2481501
Jékely, G. (2009). Evolution of phototaxis. *Philosophical Transactions of the Royal Society B: Biological Sciences, 364*(1531), 2795-2808.
Jonasz, M., & Fournier, G. (2007). *Light Scattering by Particles in Water: Theoretical and Experimental Foundations* (1st ed. ed.). San Diego: San Diego: Elsevier Science & Technology.
Kabata, Z. (1972). Developmental Stages of Caligus clemensi (Copepoda: Caligidae). *Journal of the Fisheries Research Board of Canada, 29*(11), 1571-1593. doi:10.1139/f72-245
Kabata, Z. (1979). *Parasitic Copepoda of British fishes* (Vol. 152). London: British Museum.
Kirk, J. T. O. (2011). *Light and photosynthesis in aquatic ecosystems* (3.utg. ed.). Cambridge: Cambridge University Press.
Kvæstad, B., Nordtug, T., & Hagemann, A. (2020). A machine vision system for tracking population behavior of zooplankton in small-scale experiments: a case study on salmon lice (Lepeophtheirus salmonis Krøyer, 1838) copepodite population responses to different light stimuli. *Biology open, 9*(6), bio050724.
Lampert, W. (1989). The Adaptive Significance of Diel Vertical Migration of Zooplankton. *Functional ecology, 3*(1), 21-27. doi:10.2307/2389671
Land, M. F., & Nilsson, D.-E. (2012). *Animal eyes* (2nd ed. ed.). Oxford: Oxford University Press.
Lythgoe, J. N. (1988). Light and Vision in the Aquatic Environment In J. Atema, R. R. Fay, A. N. Popper, & W. N. Tavolga (Eds.), *Sensory Biology of Aquatic Animals* (pp. 57-82). New York, NY: Springer-Verlag.
MacKinnon, B. M. (1993). Response of the Copepodid Larvae of Caligus elongatus to Light, and the Ultrastructure of the Eyes. *Canadian journal of fisheries and aquatic sciences, 50*(4), 793-799. doi:10.1139/f93-092
Maran, B. A. V., Suárez-Morales, E., Ohtsuka, S., Soh, H. Y., & Hwang, U. W. (2016). On the occurrence of caligids (Copepoda: Siphonostomatoida) in the marine

plankton: A review and checklist. *Zootaxa, 4174*(1), 437-447. doi:10.11646/zootaxa.4174.1.27
McKenzie, E., Gettinby, G., McCart, K., & Revie, C. W. (2004). Time-series models of sea lice Caligus elongatus (Nordmann) abundance on Atlantic salmon Salmo salar L. in Loch Sunart, Scotland. *Aquaculture research, 35*(8), 764-772.
Meld. St. 16. (2014-2015). *Forutsigbarhet og miljømessig bærekraftig vekst i norsk lakse- og ørretoppdrett*
Menzel, R. (1979). Spectral Sensitivity and Color Vision in Invertebrates. In H. Autrum (Ed.), *Comparative Physiology and Evolution of Vision in Invertebrates: A: Invertebrate Photoreceptors* (pp. 503-580). Berlin, Heidelberg: Springer Berlin Heidelberg.
Miljeteig, C., Olsen, A. J., Båtnes, A. S., Altin, D., Nordtug, T., Alver, M. O., . . . Jenssen, B. M. (2014). Sex and life stage dependent phototactic response of the marine copepod Calanus finmarchicus (Copepoda: Calanoida). *Journal of experimental marine biology and ecology, 451*, 16-24.
Norwegian Scientific Advisory Committee for Atlantic Salmon (2023). *Status of wild Atlantic salmon in Norway 2023* Retrieved from https://www.vitenskapsradet.no/Portals/vitenskapsradet/Status%20of%20wild%20Atlantic%20salmon%20in%20Norway%202023.pdf
Overton, K., Dempster, T., Oppedal, F., Kristiansen, T. S., Gismervik, K., & Stien, L. H. (2018). Salmon lice treatments and salmon mortality in Norwegian aquaculture: a review. *Reviews in aquaculture, 11*(4), 1398-1417. doi:10.1111/raq.12299
Piasecki, W. (1996). The developmental stages of Caligus elongatus von Nordmann, 1832 (Copepoda: Caligidae). *Revue canadienne de zoologie, 74*(8), 1459-1478. doi:10.1139/z96-161
Piasecki, W., & MacKinnon, B. (1993). Changes in structure of the frontal filament in sequential developmental stages of Caligus elongatus von Nordmann, 1832 (Crustacea, Copepoda, Siphonostomatoida). *Canadian journal of zoology, 71*(5), 889-895.
Piasecki, W., & MacKinnon, B. M. (1995). Life cycle of a sea louse, Caligus e/ongatus von Nordmann, 1832 (Copepoda, Siphonostomatoida, Caligidae) *Can. J. Zoo, 73*, 74-82.
Piasecki, W., & MacKinnon, B. M. (1995). Life cycle of a sea louse, Caligus elongatus von Nordmann, 1832 (Copepoda, Siphonostomatoida, Caligidae). *Canadian journal of zoology, 73*(1), 74-82. doi:10.1139/z95-009
Piasecki, W., Venmathi Maran, B. A., & Ohtsuka, S. (2023). Are We Ready to Get Rid of the Terms "Chalimus" and "Preadult" in the Caligid (Crustacea: Copepoda: Caligidae) Life Cycle Nomenclature? *Pathogens, 12*(3), 460. doi:10.3390/pathogens12030460
Pike, A. W., Mordue, A. J., & Ritchie, G. (1993). The development of Caligus elongatus Nordmann from hatching to copepodid in relation to temperature. In G. A. Boxshall & D. Defaye (Eds.), *Pathogens Of Wild And Farmed Fish : Sea Lice* (pp. 51-60). Chichester (United Kingdom): Chichester (United Kingdom): Ellis Horwood Limited.
Pike, A. W., & Wadsworth, S. L. (1999). Sealice on salmonids: their biology and control. *Adv Parasitol, 44*, 233-337. doi:10.1016/s0065-308x(08)60233-x
Revie, C. W., Gettinby, G., Treasurer, J., & Rae, G. (2002). The epidemiology of the sea lice, Caligus elongatus Nordmann, in marine aquaculture of Atlantic salmon, Salmo salar L., in Scotland. *Journal of Fish Diseases, 25*(7), 391-399.
Ringelberg, J. (1999). The photobehaviour of Daphnia spp. as a model to explain diel vertical migration in zooplankton. *Biological reviews of the Cambridge Philosophical Society, 74*(4), 397-423. doi:10.1111/j.1469-185X.1999.tb00036.x
Schram, T. A. (2004). Practical identification of pelagic sea lice larvae. *Journal of the Marine Biological Association of the United Kingdom, 84*(1), 103-110.
Sommerset I, Wiik-Nielsen J, Moldal T, Oliveira VHS, Svendsen JC, Haukaas A, & Brun E. (2024). Fiskehelserapporten 2023. *Veterinærinstituttets rapportserie, 8a/2024*

Steck, M., Theam, K. C., & Porter, M. L. (2023). The Cornucopia of Copepod Eyes: The Evolution of Extreme Visual System Novelty. *Distributed Vision: From Simple Sensors to Sophisticated Combination Eyes*, 223-266.
Stomp, M. (2008). *Colourful coexistence: a new solution to the plankton paradox.* (PHD). Universiteit van Amsterdam Amsterdam,
Szetey, A., Wright, D. W., Oppedal, F., & Dempster, T. (2021). Salmon lice nauplii and copepodids display different vertical migration patterns in response to light. *Aquaculture Environment Interactions, 13*, 121-131. doi:10.3354/AEI00396
The Norwegian Directorate of Fisheries. (2023a). *Atlantic salmon, rainbow trout and trout - Grow out production*. Retrieved from: https://www.fiskeridir.no/Akvakultur/Tall-og-analyse/Akvakulturstatistikk-tidsserier/Laks-regnbueoerret-og-oerret/Matfiskproduksjon
The Norwegian Directorate of Fisheries. (2023b). *Use of cleanerfish 1998-2022*. Retrieved from: https://www.fiskeridir.no/English/Aquaculture/Statistics/Cleanerfish-Lumpfish-and-Wrasse
Thorstad, E. B., & Finstad, B. (2018). *Impacts of salmon lice emanating from salmon farms on wild Atlantic salmon and sea trout*. Retrieved from https://brage.nina.no/nina-xmlui/handle/11250/2475746
Torrissen, O., Jones, S., Asche, F., Guttormsen, A., Skilbrei, O. T., Nilsen, F., . . . Jackson, D. (2013). Salmon lice - impact on wild salmonids and salmon aquaculture. *J Fish Dis, 36*(3), 171-194. doi:10.1111/jfd.12061
Vatn, J. A. Å. (2019). *Metode for kartlegging av den fototaktiske svømmeresponsen til Lepeophtheirus salmonis.* (Masters thesis). NMBU, Oslo, Norway.
Verasztó, C., Gühmann, M., Jia, H., Rajan, V. B. V., Bezares-Calderón, L. A., Pineiro-Lopez, C., . . . Yokoyama, S. (2018). Ciliary and rhabdomeric photoreceptor-cell circuits form a spectral depth gauge in marine zooplankton. *Elife, 7*, e36440.
Walpole, R. E. (2016). *Probability & statistics for engineers and scientists* (9th ed. ed.). Harlow: Pearson Education.
Walter, T. C., & Boxshall, G. (2024). Wold of Copepods Database. Retrieved from https://www.marinespecies.org/copepoda
Wootten, R., Smith, J. W., & Needham, E. (1982). Aspects of the biology of the parasitic copepods Lepeophtheirus salmonis and Caligus elongatus on farmed salmonids, and their treatment. *Proceedings of the Royal Society of Edinburgh, Section B: Biological Sciences, 81*(3), 185-197.
Young, H. D., Freedman, R. A., & Ford, A. L. (2015). *Sears and Zemansky's university physics : with modern physics : Volume two* (14th. ed., Scandinavian ed., Global ed. ed.). Harlow, England: Pearson.
Øines, Ø., & Heuch, P. A. (2005). Identification of sea louse species of the genus Caligus using mtDNA. *Journal of the Marine Biological Association of the United Kingdom, 85*(1), 73-79. doi:10.1017/S0025315405010854h
Øines, Ø., & Heuch, P. A. (2007). Caligus elongatus Nordmann genotypes on wild and farmed fish. *Journal of Fish Diseases, 30*(2), 81-91. doi:https://doi.org/10.1111/j.1365-2761.2007.00783.x
Øines, Ø., Simonsen, J. H., Knutsen, J. A., & Heuch, P. A. (2006). Host preference of adult Caligus elongatus Nordmann in the laboratory and its implications for Atlantic cod aquaculture. *J Fish Dis, 29*(3), 167-174. doi:10.1111/j.1365-2761.2006.00702.x
Aarseth, K. A., & Schram, T. A. (1999). Wavelength-specific behaviour in Lepeophtheirus salmonis and Calanus finmarchicus to ultraviolet and visible light in laboratory experiments (Crustacea: Copepoda). *Marine ecology. Progress series (Halstenbek), 186*, 211-217. doi:10.3354/meps186211

Appendices

Appendix A: Randomisation of experiments

Appendix A.1: Nauplius

Randomisation - Nauplius Stage

Replicate 1				Replicate 2				Replicate 3			
Experiment number	Colour	Intensity	Pulsation	Experiment number	Colour	Intensity	Pulsation	Experiment number	Colour	Intensity	Pulsation
Batch 1				Batch 3				Batch 5			
1	R	L	P0	19	B	H	P2	37	G	L	P0
2	R	H	P1	20	B	L	P0	38	B	L	P1
3	R	H	P0	21	G	L	P2	39	R	H	P1
4	G	H	P0	22	G	H	P1	40	R	H	P0
5	R	H	P2	23	R	H	P0	41	R	L	P1
6	G	L	P2	24	R	H	P2	42	G	H	P1
7	G	L	P1	25	G	H	P2	43	G	L	P1
8	B	H	P2	26	B	H	P1	44	R	H	P2
9	B	H	P0	27	G	H	P0	45	B	H	P2
Batch 2				Batch 4				Batch 6			
10	R	L	P2	28	B	L	P1	46	R	L	P2
11	G	L	P0	29	B	H	P0	47	G	L	P2
12	G	H	P1	30	R	L	P2	48	B	L	P2
13	B	L	P1	31	R	L	P1	49	G	H	P0
14	B	L	P0	32	B	L	P2	50	B	H	P1
15	R	L	P1	33	G	L	P0	51	G	H	P2
16	B	H	P1	34	R	L	P0	52	R	L	P0
17	B	L	P2	35	R	H	P1	53	B	H	P0
18	G	H	P2	36	G	L	P1	54	B	L	P0

Appendix A.2: Copepodid

Randomisation – Copepodid Experiments

Replicate 1				Replicate 2				Replicate 3			
Experiment number	Waveband	Intensity	Pulsation	Experiment number	Waveband	Intensity	Pulsation	Experiment number	Waveband	Intensity	Pulsation
Batch 1				Batch 3				Batch 5			
1	G	H	P0	19	R	L	P0	37	B	L	P1
2	R	H	P1	20	B	H	P1	38	B	L	P0
3	B	L	P1	21	G	L	P2	39	G	H	P1
4	R	L	P0	22	B	L	P0	40	B	H	P1
5	G	L	P0	23	R	H	P2	41	B	H	P0
6	G	H	P1	24	B	H	P0	42	G	L	P1
7	B	H	P0	25	G	H	P2	43	G	H	P2
8	B	L	P0	26	R	L	P2	44	G	H	P0
9	B	H	P2	27	G	L	P1	45	R	L	P0
Batch 2				Batch 4				Batch 6			
10	G	L	P1	28	R	L	P1	46	R	.H	P0
11	R	H	P0	29	G	H	P1	47	R	L	P2
12	R	L	P2	30	B	L	P1	48	B	L	P2
13	B	L	P2	31	B	H	P2	49	R	H	P1
14	R	L	P1	32	R	H	P0	50	G	L	P2
15	G	H	P2	33	G	L	P0	51	R	L	P1
16	B	H	P1	34	R	H	P1	52	B	H	P2
17	G	L	P2	35	B	L	P2	53	R	H	P2
18	R	H	P2	36	G	H	P0	54	G	L	P0

Appendix B: Model Summaries Nauplius

Appendix B1: Model Summary Mean Deviation First Light Period (FLP)

Method

Variance estimation	Restricted maximum likelihood
DF for fixed effects	Kenward-Roger

Factor Information

Factor	Type	Levels	Values
Run Order	Random	9	1; 2; 3; 4; 5; 6; 7; 8; 9
Replicate	Random	3	1; 2; 3
Waveband	Fixed	3	B; G; R
Intensity	Fixed	2	H; L
Pulsation	Fixed	3	P0; P1; P2

Variance Components

Source	Var	% of Total	SE Var	Z-Value	P-Value
Replicate	0.347187	0.68%	0.741947	0.467940	0.320
Run Order	0.681877	1.34%	1.236940	0.551261	0.291
Error	49.691683	97.97%	3.759379	13.218058	0.000
Total	50.720747				

-2 Log likelihood = 2518.297033

Tests of Fixed Effects

Term	DF Num	DF Den	F-Value	P-Value
Waveband	2.00	143.80	13.16	0.000
Intensity	1.00	220.78	20.61	0.000
Pulsation	2.00	263.97	4.97	0.008
Waveband*Intensity	2.00	191.98	0.98	0.378
Waveband*Pulsation	4.00	241.35	2.24	0.065
Intensity*Pulsation	2.00	158.04	5.60	0.004
Waveband*Intensity*Pulsation	4.00	130.83	0.69	0.602

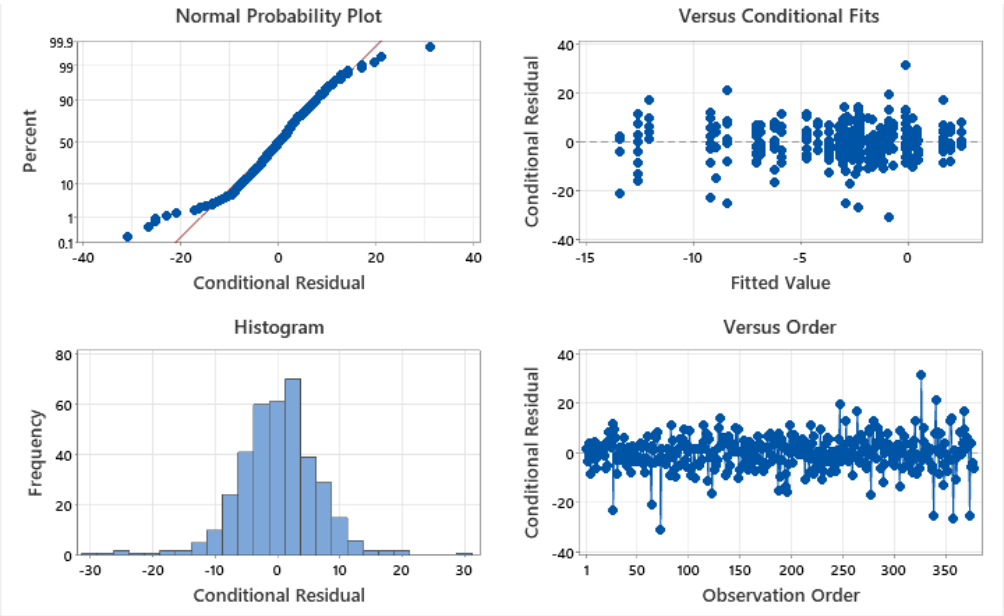

Appendix B2: Model Summary Mean Deviation Total Light Period (TLP)

Method

Variance estimation	Restricted maximum likelihood
DF for fixed effects	Kenward-Roger

Factor Information

Factor	Type	Levels	Values
Run Order	Random	9	1; 2; 3; 4; 5; 6; 7; 8; 9
Replicate	Random	3	1; 2; 3
Waveband	Fixed	3	B; G; R
Intensity	Fixed	2	H; L
Pulsation	Fixed	3	P0; P1; P2

Variance Components

Source	Var	% of Total	SE Var	Z-Value	P-Value
Replicate	1.803670	1.08%	3.108215	0.580291	0.281
Run Order	0.643928	0.39%	3.180973	0.202431	0.420
Error	163.868925	98.53%	12.392929	13.222777	0.000
Total	166.316523				

-2 Log likelihood = 2945.356137

Tests of Fixed Effects

Term	DF Num	DF Den	F-Value	P-Value
Waveband	2.00	102.67	12.69	0.000
Intensity	1.00	181.30	26.35	0.000
Pulsation	2.00	222.85	2.81	0.062
Waveband*Intensity	2.00	162.30	1.83	0.164
Waveband*Pulsation	4.00	205.25	2.41	0.050
Intensity*Pulsation	2.00	122.47	7.63	0.001
Waveband*Intensity*Pulsation	4.00	95.90	0.80	0.531

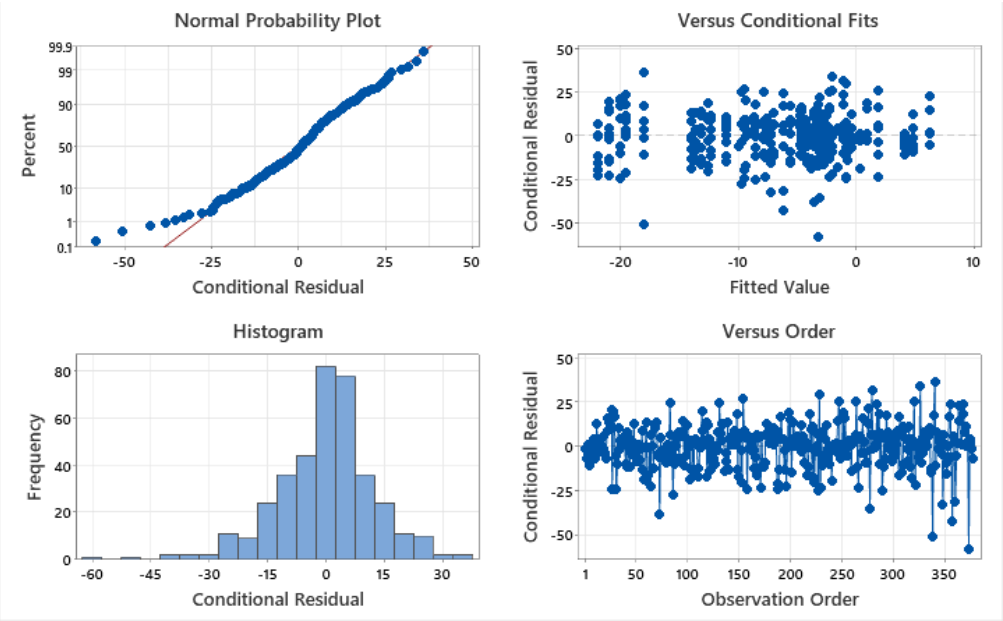

Appendix B3: Model Summary Average Speed First Light Period (FLP)

Method

Variance estimation	Restricted maximum likelihood
DF for fixed effects	Kenward-Roger

Factor Information

Factor	Type	Levels	Values
Run Order	Random	9	1; 2; 3; 4; 5; 6; 7; 8; 9
Replicate	Random	3	1; 2; 3
Waveband	Fixed	3	B; G; R
Intensity	Fixed	2	H; L
Pulsation	Fixed	3	P0; P1; P2

Variance Components

Source	Var	% of Total	SE Var	Z-Value	P-Value
Replicate	0.000000	0.00%	*	*	*
Run Order	0.000259	0.08%	0.005825	0.044380	0.482
Error	0.311030	99.92%	0.023498	13.236399	0.000
Total	0.311288				

-2 Log likelihood = 693.151069

Tests of Fixed Effects

Term	DF Num	DF Den	F-Value	P-Value
Waveband	2.00	81.77	0.09	0.916
Intensity	1.00	156.94	5.85	0.017
Pulsation	2.00	196.42	0.34	0.711
Waveband*Intensity	2.00	141.25	0.58	0.563
Waveband*Pulsation	4.00	182.35	0.77	0.547
Intensity*Pulsation	2.00	102.24	0.34	0.715
Waveband*Intensity*Pulsation	4.00	77.31	0.93	0.452

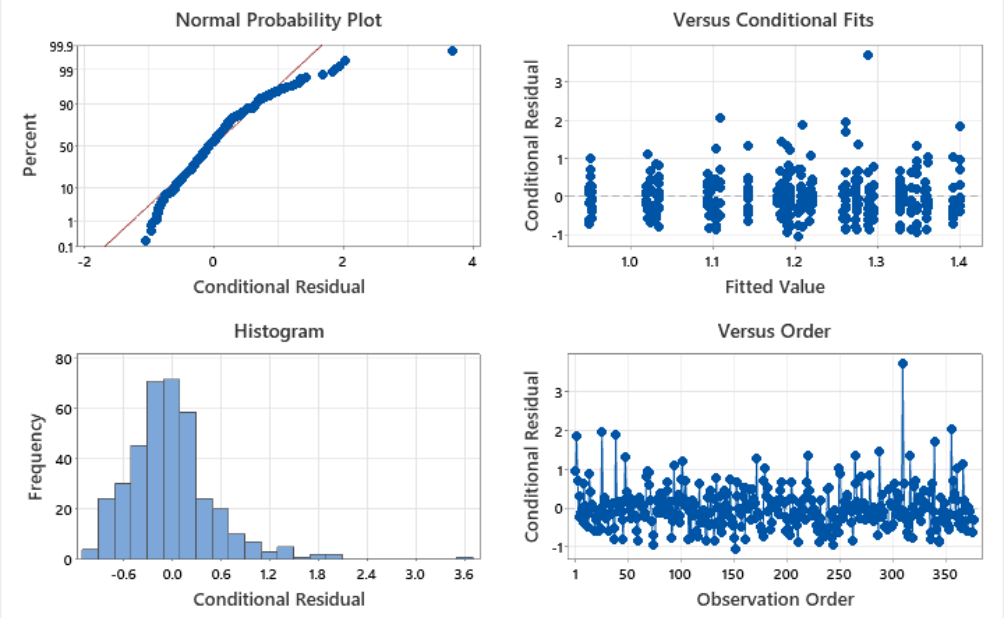

Appendix B4: Model Summary Average Speed Totalt Light Period (TLP)

Method

Variance estimation	Restricted maximum likelihood
DF for fixed effects	Kenward-Roger

Factor Information

Factor	Type	Levels	Values
Run Order	Random	9	1; 2; 3; 4; 5; 6; 7; 8; 9
Replicate	Random	3	1; 2; 3
Waveband	Fixed	3	B; G; R
Intensity	Fixed	2	H; L
Pulsation	Fixed	3	P0; P1; P2

Variance Components

Source	Var	% of Total	SE Var	Z-Value	P-Value
Replicate	0.000318	0.13%	0.002447	0.130045	0.448
Run Order	0.000000	0.00%	*	*	*
Error	0.252914	99.87%	0.018933	13.358142	0.000
Total	0.253232				

-2 Log likelihood = 618.995377

Tests of Fixed Effects

Term	DF Num	DF Den	F-Value	P-Value
Waveband	2.00	357.40	0.23	0.796
Intensity	1.00	358.38	3.33	0.069
Pulsation	2.00	358.14	0.15	0.857
Waveband*Intensity	2.00	358.29	0.55	0.580
Waveband*Pulsation	4.00	357.29	1.42	0.228
Intensity*Pulsation	2.00	357.60	1.97	0.141
Waveband*Intensity*Pulsation	4.00	358.20	2.21	0.067

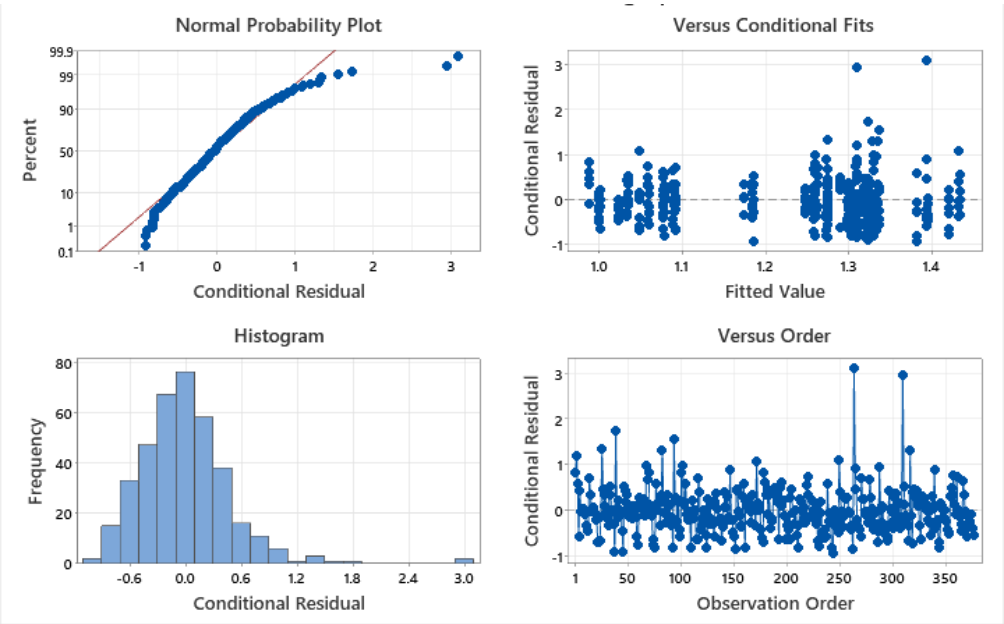

Appendix B5: Model Summary Maximum Speed First Light Period (FLP)

Method

Variance estimation	Restricted maximum likelihood
DF for fixed effects	Kenward-Roger

Factor Information

Factor	Type	Levels	Values
Run Order	Random	9	1; 2; 3; 4; 5; 6; 7; 8; 9
Replicate	Random	3	1; 2; 3
Waveband	Fixed	3	B; G; R
Intensity	Fixed	2	H; L
Pulsation	Fixed	3	P0; P1; P2

Variance Components

Source	Var	% of Total	SE Var	Z-Value	P-Value
Replicate	5.052891	3.74%	6.063699	0.833302	0.202
Run Order	1.807711	1.34%	3.318346	0.544763	0.293
Error	128.098482	94.92%	9.703448	13.201337	0.000
Total	134.959084				

-2 Log likelihood = 2860.609678

Tests of Fixed Effects

Term	DF Num	DF Den	F-Value	P-Value
Waveband	2.00	140.47	0.04	0.958
Intensity	1.00	217.30	7.72	0.006
Pulsation	2.00	261.15	0.55	0.579
Waveband*Intensity	2.00	188.36	0.21	0.812
Waveband*Pulsation	4.00	237.70	0.14	0.965
Intensity*Pulsation	2.00	153.82	0.95	0.388
Waveband*Intensity*Pulsation	4.00	127.04	0.29	0.887

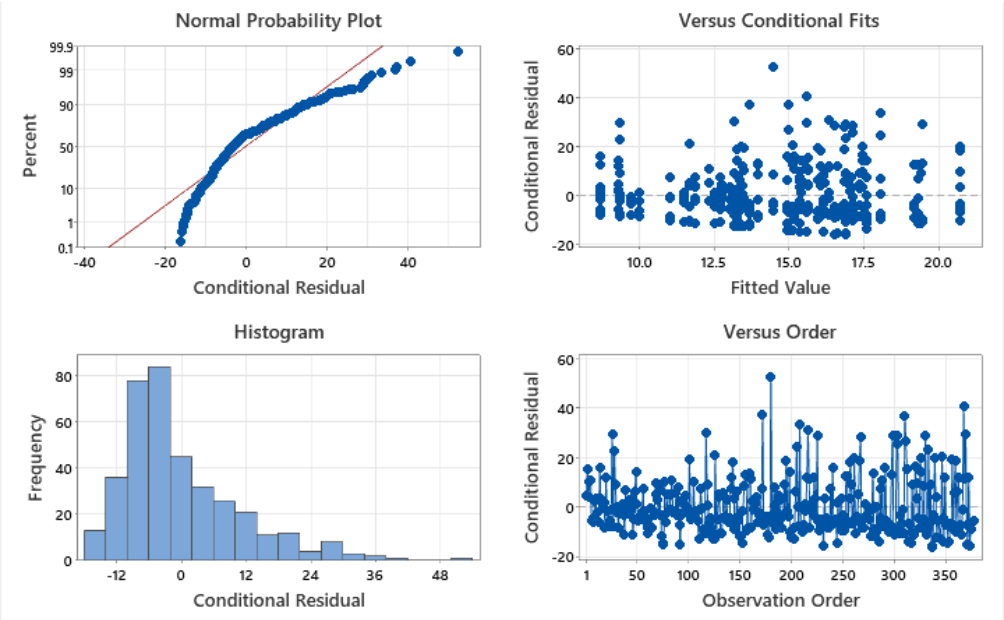

Appendix B6: Model Summary Maximum Speed Total Light Period (FLP)

Method

Variance estimation	Restricted maximum likelihood
DF for fixed effects	Kenward-Roger

Factor Information

Factor	Type	Levels	Values
Run Order	Random	9	1; 2; 3; 4; 5; 6; 7; 8; 9
Replicate	Random	3	1; 2; 3
Waveband	Fixed	3	B; G; R
Intensity	Fixed	2	H; L
Pulsation	Fixed	3	P0; P1; P2

Variance Components

Source	Var	% of Total	SE Var	Z-Value	P-Value
Replicate	9.681768	5.98%	10.863235	0.891242	0.186
Run Order	8.217949	5.08%	7.145032	1.150163	0.125
Error	143.955818	88.94%	10.911881	13.192576	0.000
Total	161.855534				

-2 Log likelihood = 2908.380370

Tests of Fixed Effects

Term	DF Num	DF Den	F-Value	P-Value
Waveband	2.00	267.51	1.04	0.354
Intensity	1.00	309.84	5.84	0.016
Pulsation	2.00	334.59	0.15	0.862
Waveband*Intensity	2.00	277.23	1.52	0.220
Waveband*Pulsation	4.00	315.58	0.26	0.902
Intensity*Pulsation	2.00	259.08	1.98	0.141
Waveband*Intensity*Pulsation	4.00	241.15	0.81	0.517

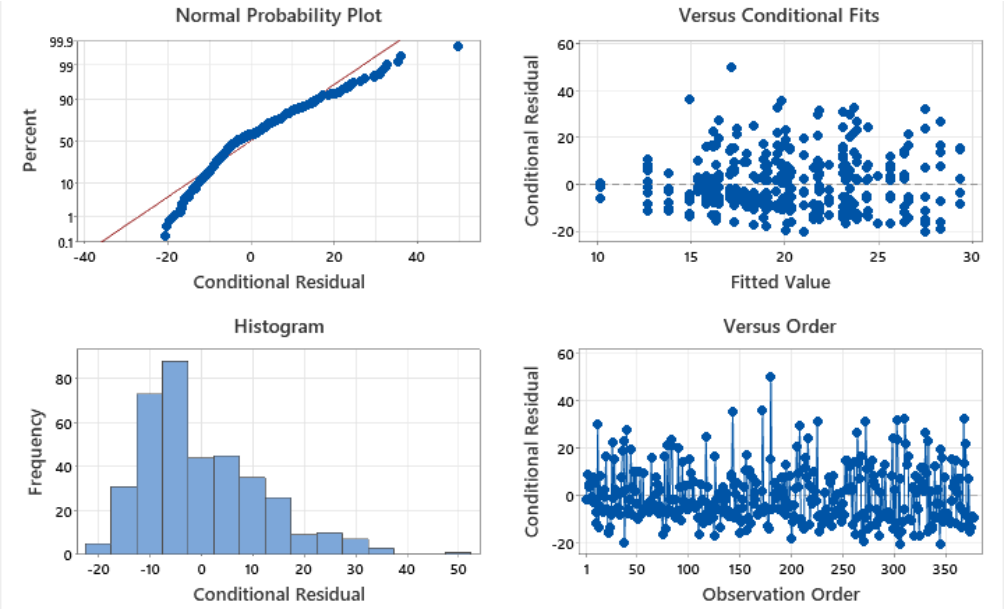

Appendix C: Model Summaries Copepodid

Appendix C1: Model Summary Mean Deviation First Light Period (FLP)

Method

Variance estimation	Restricted maximum likelihood
DF for fixed effects	Kenward-Roger

Factor Information

Factor	Type	Levels	Values
Run Order	Random	9	1; 2; 3; 4; 5; 6; 7; 8; 9
Replicate	Random	3	1; 2; 3
Waveband	Fixed	3	B; G; R
Intensity	Fixed	2	H; L
Pulsation	Fixed	3	P0; P1; P2

Variance Components

Source	Var	% of Total	SE Var	Z-Value	P-Value
Run Order	2.939315	2.98%	3.860781	0.761326	0.223
Replicate	0.000000	0.00%	*	*	*
Error	95.601585	97.02%	8.784066	10.883523	0.000
Total	98.540899				

-2 Log likelihood = 1885.846246

Tests of Fixed Effects

Term	DF Num	DF Den	F-Value	P-Value
Waveband	2.00	118.98	0.55	0.579
Intensity	1.00	163.38	11.18	0.001
Pulsation	2.00	170.88	0.84	0.434
Waveband*Intensity	2.00	225.11	0.05	0.948
Waveband*Pulsation	4.00	196.74	1.02	0.397
Intensity*Pulsation	2.00	63.79	0.51	0.601
Waveband*Intensity*Pulsation	4.00	164.95	1.18	0.319

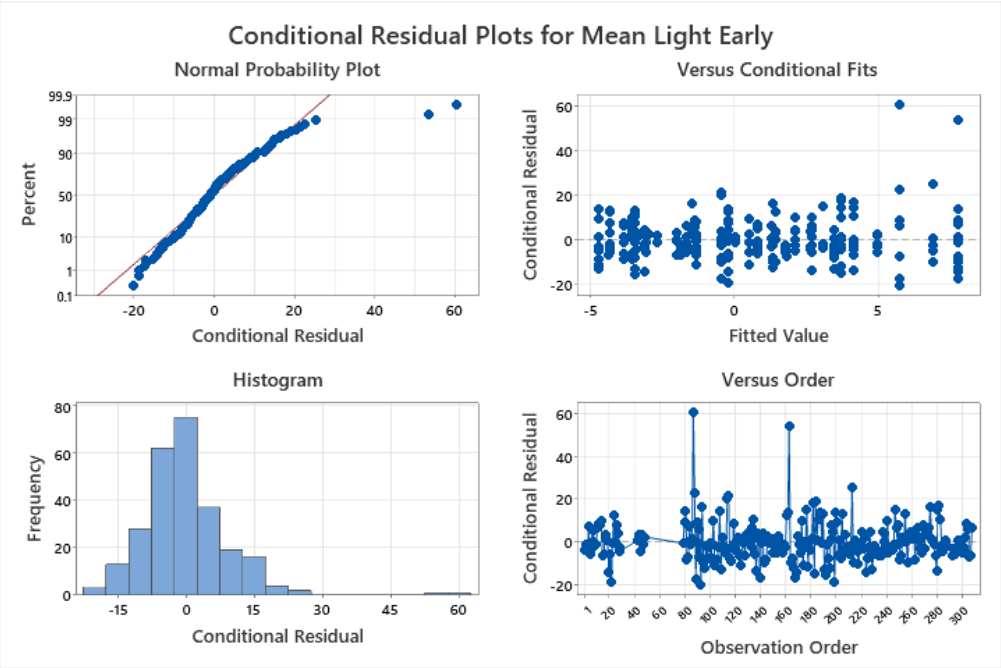

Appendix C2: Model Summary Mean Deviation Total Light Period (TLP)

Method

Variance estimation	Restricted maximum likelihood
DF for fixed effects	Kenward-Roger

Factor Information

Factor	Type	Levels	Values
Run Order	Random	9	1; 2; 3; 4; 5; 6; 7; 8; 9
Replicate	Random	3	1; 2; 3
Waveband	Fixed	3	B; G; R
Intensity	Fixed	2	H; L
Pulsation	Fixed	3	P0; P1; P2

Variance Components

Source	Var	% of Total	SE Var	Z-Value	P-Value
Run Order	8.803052	3.69%	9.935763	0.885997	0.188
Replicate	0.000000	0.00%	*	*	*
Error	229.698828	96.31%	21.096503	10.888005	0.000
Total	238.501880				

-2 Log likelihood = 2099.485160

Tests of Fixed Effects

Term	DF Num	DF Den	F-Value	P-Value
Waveband	2.00	130.03	1.59	0.207
Intensity	1.00	170.59	13.12	0.000
Pulsation	2.00	182.41	2.29	0.104
Waveband*Intensity	2.00	228.97	0.17	0.841
Waveband*Pulsation	4.00	203.66	0.76	0.555
Intensity*Pulsation	2.00	70.53	0.49	0.616
Waveband*Intensity*Pulsation	4.00	174.26	0.94	0.443

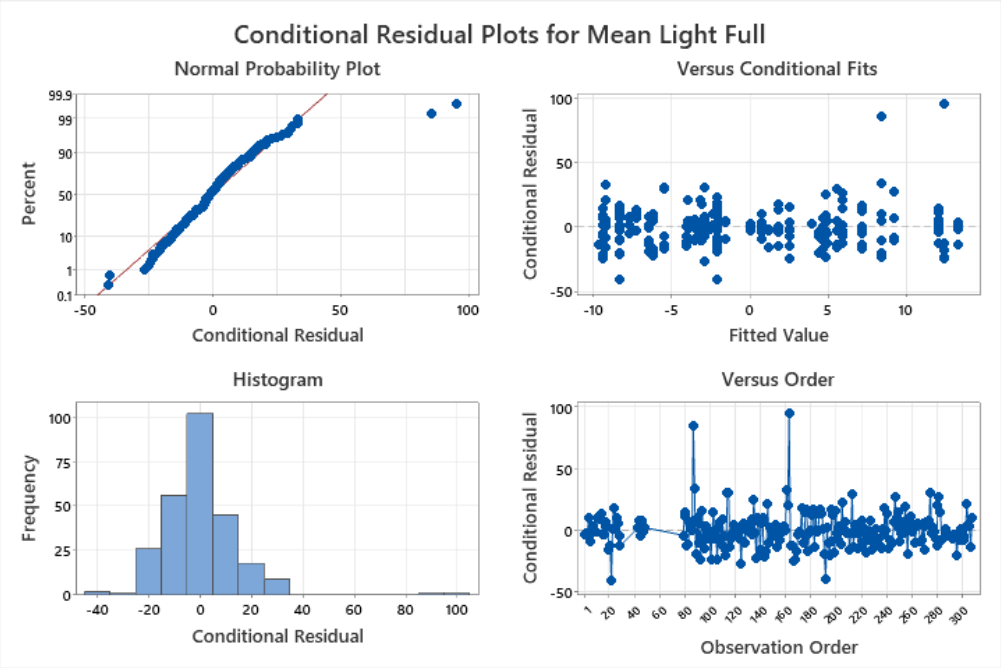

Appendix C3: Model Summary Average Speed First Light Period (FLP)

Method

Variance estimation	Restricted maximum likelihood
DF for fixed effects	Kenward-Roger

Factor Information

Factor	Type	Levels	Values
Run Order	Random	9	1; 2; 3; 4; 5; 6; 7; 8; 9
Replicate	Random	3	1; 2; 3
Waveband	Fixed	3	B; G; R
Intensity	Fixed	2	H; L
Pulsation	Fixed	3	P0; P1; P2

Variance Components

Source	Var	% of Total	SE Var	Z-Value	P-Value
Run Order	0.000000	0.00%	*	*	*
Replicate	0.000000	0.00%	*	*	*
Error	0.324678	100.00%	0.029455	11.022704	0.000
Total	0.324678				

-2 Log likelihood = 501.016655

Tests of Fixed Effects

Term	DF Num	DF Den	F-Value	P-Value
Waveband	2.00	243.00	0.35	0.705
Intensity	1.00	243.00	1.27	0.262
Pulsation	2.00	243.00	1.74	0.177
Waveband*Intensity	2.00	243.00	0.14	0.868
Waveband*Pulsation	4.00	243.00	2.56	0.040
Intensity*Pulsation	2.00	243.00	1.19	0.306
Waveband*Intensity*Pulsation	4.00	243.00	2.33	0.057

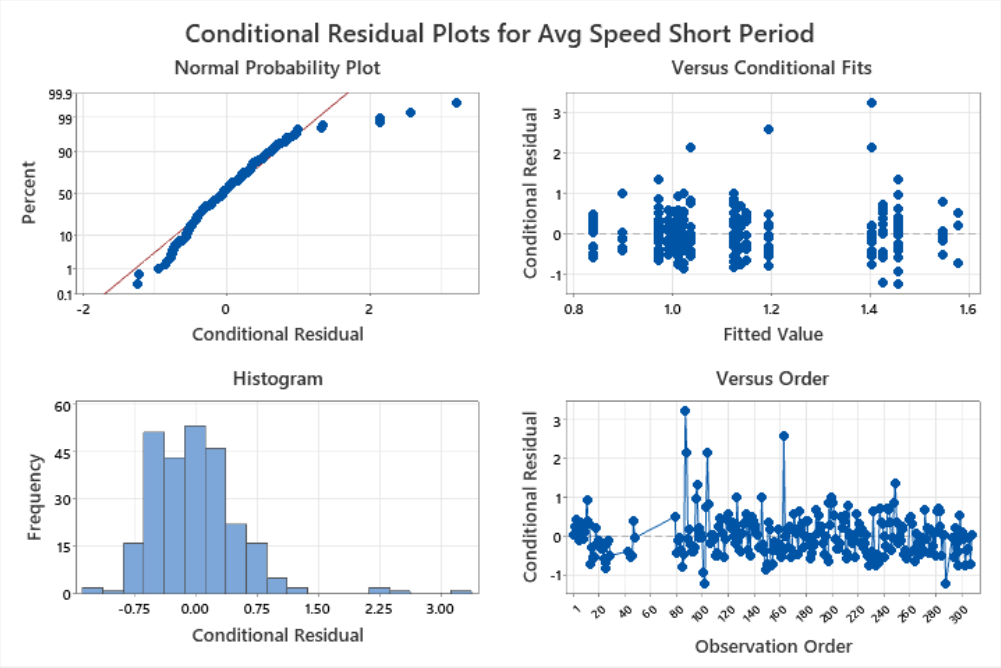

Appendix C4: Model Summary Average Speed Totalt Light Period (TLP)

Method

Variance estimation	Restricted maximum likelihood
DF for fixed effects	Kenward-Roger

Factor Information

Factor	Type	Levels	Values
Run Order	Random	9	1; 2; 3; 4; 5; 6; 7; 8; 9
Replicate	Random	3	1; 2; 3
Waveband	Fixed	3	B; G; R
Intensity	Fixed	2	H; L
Pulsation	Fixed	3	P0; P1; P2

Variance Components

Source	Var	% of Total	SE Var	Z-Value	P-Value
Run Order	0.000000	0.00%	*	*	*
Replicate	0.000000	0.00%	*	*	*
Error	0.216085	100.00%	0.019604	11.022704	0.000
Total	0.216085				

-2 Log likelihood = 402.076145

Tests of Fixed Effects

Term	DF Num	DF Den	F-Value	P-Value
Waveband	2.00	243.00	0.64	0.530
Intensity	1.00	243.00	0.00	0.974
Pulsation	2.00	243.00	2.02	0.135
Waveband*Intensity	2.00	243.00	0.20	0.817
Waveband*Pulsation	4.00	243.00	3.23	0.013
Intensity*Pulsation	2.00	243.00	2.11	0.123
Waveband*Intensity*Pulsation	4.00	243.00	2.27	0.062

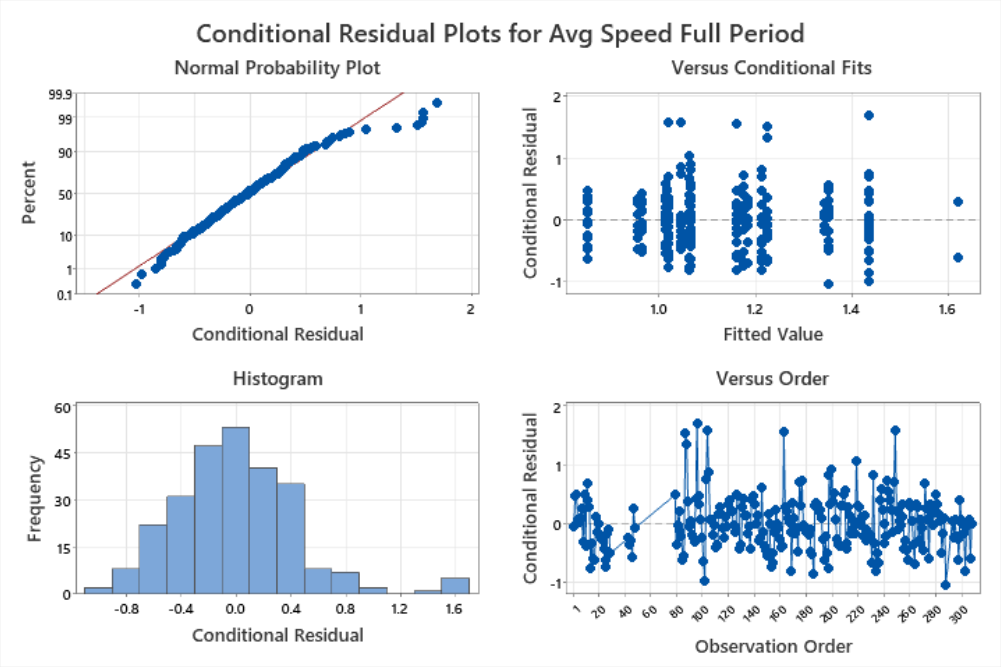

Appendix C5: Model Summary Maximum Speed First Light Period (FLP)

Method

Variance estimation	Restricted maximum likelihood
DF for fixed effects	Kenward-Roger

Factor Information

Factor	Type	Levels	Values
Run Order	Random	9	1; 2; 3; 4; 5; 6; 7; 8; 9
Replicate	Random	3	1; 2; 3
Waveband	Fixed	3	B; G; R
Intensity	Fixed	2	H; L
Pulsation	Fixed	3	P0; P1; P2

Variance Components

Source	Var	% of Total	SE Var	Z-Value	P-Value
Run Order	1.965929	1.98%	3.476883	0.565429	0.286
Replicate	0.000000	0.00%	*	*	*
Error	97.106552	98.02%	8.925355	10.879853	0.000
Total	99.072481				

-2 Log likelihood = 1888.667223

Tests of Fixed Effects

Term	DF Num	DF Den	F-Value	P-Value
Waveband	2.00	103.26	0.53	0.593
Intensity	1.00	153.45	1.62	0.205
Pulsation	2.00	152.28	2.95	0.055
Waveband*Intensity	2.00	217.93	2.18	0.116
Waveband*Pulsation	4.00	185.26	1.12	0.347
Intensity*Pulsation	2.00	55.62	0.23	0.799
Waveband*Intensity*Pulsation	4.00	150.78	1.43	0.227

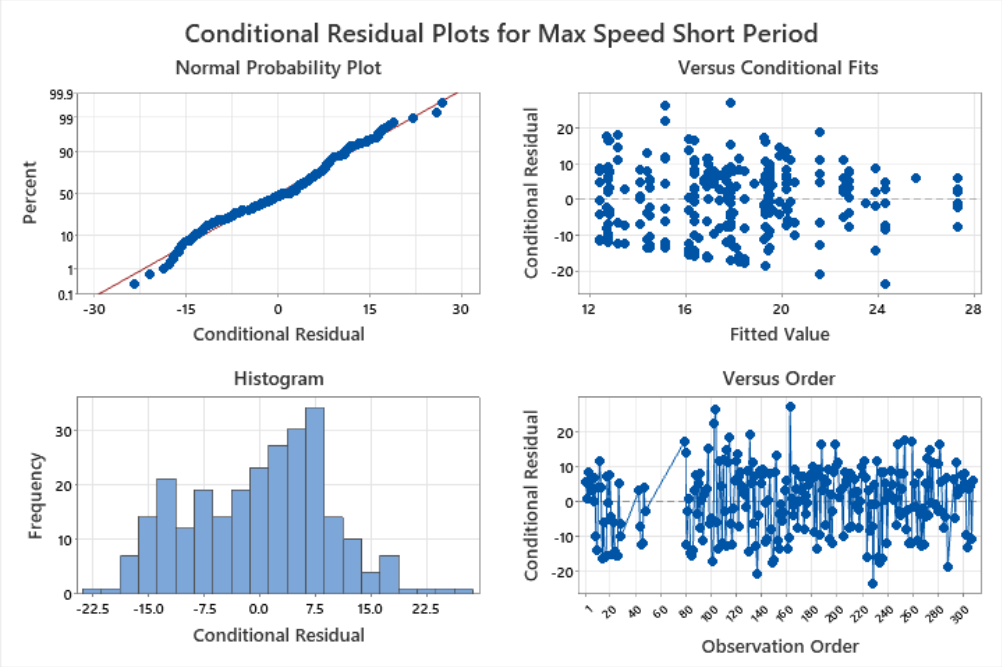

Appendix C6: Model Summary Maximum Speed Total Light Period (FLP)

Method

Variance estimation	Restricted maximum likelihood
DF for fixed effects	Kenward-Roger
Rows unused	47

Factor Information

Factor	Type	Levels	Values
Run Order	Random	9	1; 2; 3; 4; 5; 6; 7; 8; 9
Replicate	Random	3	1; 2; 3
Waveband	Fixed	3	B; G; R
Intensity	Fixed	2	H; L
Pulsation	Fixed	3	P0; P1; P2

Variance Components

Source	Var	% of Total	SE Var	Z-Value	P-Value
Run Order	3.440549	3.48%	4.136203	0.831813	0.203
Replicate	4.035727	4.08%	5.533719	0.729297	0.233
Error	91.448306	92.44%	8.449879	10.822439	0.000
Total	98.924581				

-2 Log likelihood = 1878.419525

Tests of Fixed Effects

Term	DF Num	DF Den	F-Value	P-Value
Waveband	2.00	115.40	0.87	0.421
Intensity	1.00	155.95	0.41	0.525
Pulsation	2.00	166.61	4.47	0.013
Waveband*Intensity	2.00	219.15	0.76	0.471
Waveband*Pulsation	4.00	198.46	1.16	0.331
Intensity*Pulsation	2.00	62.56	0.68	0.511
Waveband*Intensity*Pulsation	4.00	157.75	1.50	0.206

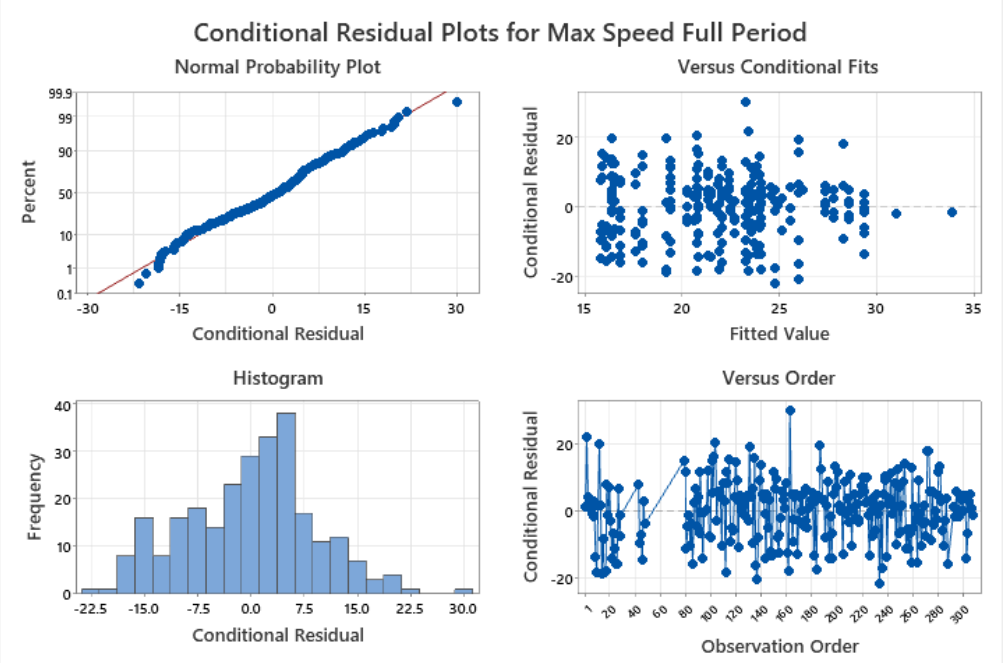

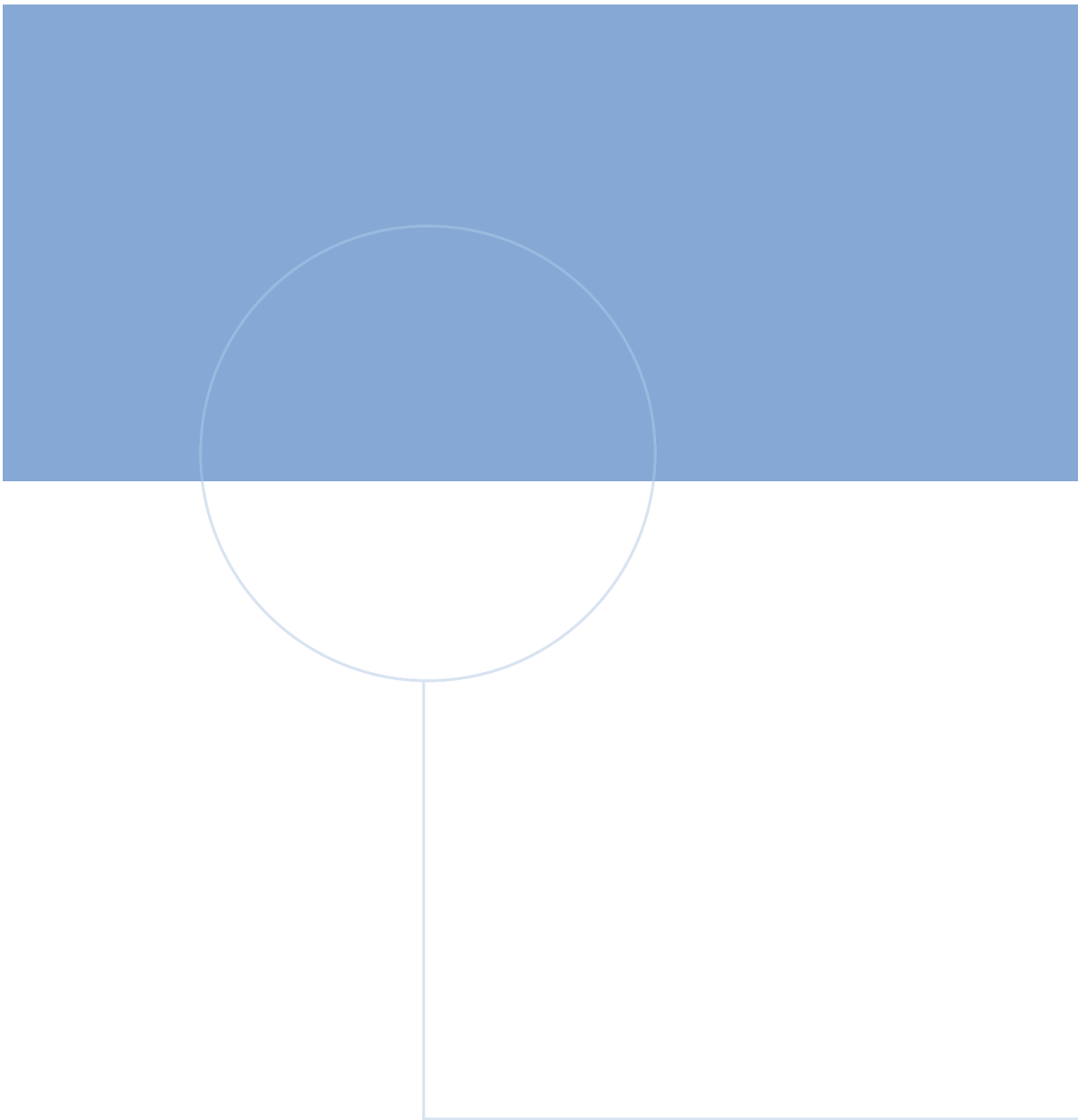

NTNU
Norwegian University of
Science and Technology

NTNU
Taskforce Salmon Lice